Durham E-Theses

Spectroscopic techniques at millimetric wavelengths

Brown, G.

How to cite:

Brown, G. (1967) *Spectroscopic techniques at millimetric wavelengths*, Durham theses, Durham University. Available at Durham E-Theses Online: http://etheses.dur.ac.uk/8536/

Spectroscopic Techniques at

Millimetric Wavelengths

by

G. Brown, B.Sc (Dunelm).

A thesis submitted in candidature for the degree of

Doctor of Philosophy

University of Durham

September, 1967.

Abstract

The design and construction of a complete microwave spectrometer operating at 35 Gc/s is described. The receiver is of the superheterodyne type with an intermediate frequency of 45 Mc/s; the local oscillator signal is derived by a novel method from the output of the monitor klystron. A superconducting magnet is used, capable of producing steady magnetic fields up to 42.6 kilo-oersteds.

A second spectrometer is described which uses the same magnet and cryogenic system as the other spectrometer but which has a completely different microwave section. This equipment has been used to measure spin-lattice relaxation times in ruby and sapphire at 35 Gc/s using a single reflex klystron producing a pulse power at the specimen of about 10 microwatts. The results are compared with those obtained by the standard pulse saturation method and are shown to agree within experimental error.

A third spectrometer operating at 70 Gc/s by harmonic generation from 35 Gc/s has been constructed and used to measure directly the relaxation times in the same specimens, using microwave pulses of less than 2 microwatts at

the specimen. The results are compared with those at 35 Gc/s

and a value for the frequency dependence of relaxation time in

this region is calculated. Preliminary experiments with a

superheterodyne receiver at 70 Gc/s are described; the complete

70 Gc/s superheterodyne spectrometer is powered from a single

35 Gc/s reflex klystron. A special case of subharmonic mixing

has been found to be more efficient with this system and suggestions

for improving the performance are given.

The uses of the microwave diode as

a low-level detector, mixer, modulator and harmonic generator are

described as they occur in the text.

Acknowledgments

Spectroscopic Techniques at Millimetric Wavelengths

Contents

Symbols used in the block diagrams

Att : Attenuator

BM : Balanced mixer

CRO : Cathode-ray oscilloscope

D : Diode detector

DA : Differential amplifier

DCA : Directly-coupled amplifier

E-H : E - H tuner

I : Isolator

IF : IF amplifier

K : Klystron, low-power reflex

L : Load, resistive

MD : Mixer diode

ML : Matched load

M T : Magic T

PG : Pulse generator

PK : Power klystron, pulsed

PS : Phase shifter

PWM : Pulse waveform monitor

S : Specimen

SG : Signal generator, RF

T : Taper

TCM : Transmission crystal modulator

TS : Trigger source, multivibrator

WM : Wavemeter, absorption

3dB : 3 dB directional coupler

6dB : 6 dB directional coupler

Chapter 1

Introduction

1.1 The development of microwave spectroscopy

Microwave spectroscopy began in 1934 with the classic experiments of Cleeton and Williams (1) on the absorption spectrum of ammonia. The wavelengths they used ranged between 1 and 4 cm, and their efforts are particularly noteworthy in view of the very limited techniques available to them at that time. To make their measurements "it became necessary to produce electromagnetic waves of shorter wavelength than had been produced before by vacuum tubes". To do this, they constructed small split-anode magnetrons with anode radii of less than 0.5 mm. With the ammonia gas held in a rubber bag, and microwave radiation focused on it with parabolic reflectors, Cleeton and Williams observed the inversion of the ammonia molecule.

Experimental workers were severely hampered by the lack of equipment available, and for this reason microwave spectroscopy lay dormant for many years. The much-needed research and development came during the Second World War when an intense effort was put into the development of radar. This opened up the field of microwave technology and, by the end of the war, microwave spectrometers of sufficient sensitivity could be assembled

and used. Bleaney and Penrose (2) were the first to publish,
following up the work of Cleeton and Williams, and Good (3)
followed with the discovery of hyperfine structure in the ammonia
spectrum.

Paramagnetic resonance experiments
were first reported by Zavoisky (4) in the USSR and by Cummerow
and Halliday (5) in America; Griffiths (6) observed ferromagnetic
resonance, while Bloch (7), and Bloch, Hansen and Packard (8)
founded nuclear magnetic resonance. Microwave spectroscopy had
begun, twelve years after the pioneer experiment had taken place.

1.2 Electron spin resonance

The phenomenon of electron spin
resonance depends upon the fact that an electron has charge, mass,
angular momentum and magnetic moment, and will thus interact with
its surroundings. The way in which it interacts can be used to
supply detailed information about the atom or ion of which it is
a part. For example, the experimentally determined data given by
electron spin resonance (ESR) on the transition group metal ions
is listed by Bowers and Owen (9) and by Orton (10). The ESR
spectrum can be used to identify an unknown transition metal ion
or a lattice defect, or to distinguish between two valence states

of the same ion. The chemist uses ESR as a method which can

identify chemical bonding in molecules and crystals. The systems

which can be studied by electron spin resonance can be broadly

classified as:

(a) transition elements;

(b) free radicals;

(c) conduction electrons;

(d) biological materials;

(e) semiconductors;

(f) irradiated substances.

At the present time biological materials and irradiated substances

are receiving most attention in electron spin resonance laboratories.

1.3 Techniques in electron spin resonance

In order to carry out a specific

experiment using ESR, three basic pieces of apparatus are

necessary: a source of microwave radiation; a specimen holder; a

microwave receiver. The source can be a klystron, magnetron or a

backward-wave oscillator, depending upon the frequency used and

the power required. The specimen holder can take a variety of forms

and will not be discussed here. The microwave receiver is usually

the most complex part of an ESR spectrometer because, in contrast

to optical emission spectroscopy, it is the absorption spectrum which is being studied, and since the absorption coefficients involved are very small, the receiver must be highly sensitive and very stable. The type of receiver depends largely upon the device used to detect the microwave radiation. Bolometers and thermistors are usually restricted to absolute measurements of CW power, their response times varying from 0.5 msec to about 12 sec (11). The commonest microwave power detector is the point-contact diode, and this can be used for all ESR work. Receivers employing point-contact diodes fall into three general classes: crystal-video; superheterodyne; synchrodyne. It is the receiver which largely dictates the accuracy and resolution of the overall microwave system, assuming that the individual components are of good quality.

If a steady magnetic field H_o is applied to a free electron, or to an atom having an unpaired electron, the magnetic moment vector of the electron will precess about the direction of H_o with an angular frequency ω which is proportional both to H_o and to the electronic magnetic moment. ω is the Larmor precession frequency and its value is given as:

$$\omega = \gamma H_o \quad ,$$

where γ is the gyromagnetic ratio. A sample containing many free electrons, or many unpaired spins, when subjected to a magnetic field H_o, would not show any detectable evidence of the Larmor precession. Each electron would be precessing at the same frequency but with completely random phase and there would be no "bulk precession" present. If a rotating magnetic field H_1 were introduced perpendicular to H_o and of frequency equal to ω, it would serve two purposes: (a) to establish a reference phase for the precessing electrons;

(b) to exert a secular torque on each electron, tending to tip its magnetic moment vector relative to H_o. Effect (b) produces an alteration of the energy of the electron and this change of energy is absorbed from that stored in the rotating field H_1. In practice H_1 is the microwave field and the Larmor precession, or electron spin resonance, becomes observable as an absorption of microwave power by the specimen under observation. This simple classical picture is now modified by the quantum theory: an atomic spin can only exist in one of a certain discrete set of allowed orientations (with respect to the direction of the field H_o) and energies. For example, the Cr^{3+} ion in ruby has four allowed orientations, leading to the four energy levels

for the Cr^{3+} ion. These four levels comprise the lowest orbital energy level of this ion, and are called paramagnetic, or Zeeman, levels.

The orientation of a spin vector (or a magnetic moment vector) disturbed by an applied radio-frequency (RF) field tends to revert to its original state, and the rate at which it does this is determined by the spin-lattice relaxation time, T_1. The processes by which energy exchange occurs between the electron spin system and the crystal lattice are complicated and obscure, but the effect that the magnitude of the spin-lattice relaxation time has on the suitability of a substance for maser operation (12) is very important, since it determines almost exclusively the pump power requirement. Consequently, much research has been carried out on ways of measuring T_1. Although the first measurements of T_1 were begun by Gorter (13) in 1936, the value of T_1 given by his non-resonant technique is an average over all the spin transitions in a given material. The maser is essentially dependent upon resonance for its operation and it is logical that a microwave resonant technique should be used to measure the spin-lattice relaxation time under conditions as close as possible to those of maser operation. In order to obtain maser

action it is necessary for the paramagnetic crystal to be at a
very low temperature, typically that of liquid helium, 4.2°K.
The reason for this is that the strength of maser action is
proportional to the population difference of the two signal levels.
The negative population difference under conditions of inversion
is of the same order as the positive population difference under
conditions of thermal equilibrium. The positive population
difference is determined by the Boltzmann ratio

$$N_i/N_j = \exp(- hf_{ij}/kT) \quad .$$

To keep this ratio as large as possible, T must be small; to
fulfil this condition, liquid helium temperatures are usually
used. It has been found that at temperatures less than about 20°K,
the spin-lattice relaxation time varies inversely with temperature,
and as a result the pump power requirement decreases with
decreasing temperature, for a given crystal.

The microwave spectrometer resembles
the maser in many aspects and it is the ideal instrument for
examining the properties of maser materials under physical
conditions almost identical to those of maser operation.

1.4 The measurement of relaxation time

There are six methods which have been described and widely used for the determination of spin-lattice relaxation time. These methods are outlined below with particular emphasis laid on: (a) the material;

(b) the measuring frequency;

(c) the power needed.

1.4.1 The CW saturation method

Eschenfelder and Weidner 1953: iron ammonium alum and chromium potassium alum; 9.3 Gc/s; 1 watt; (14).

The specimen is placed in a liquid helium-cooled cavity; the power absorbed in the specimen is measured as a function of the incident power by measuring the reflection coefficient looking into the cavity. This involves some complex calculations to evaluate Q_M, the absorption Q of the specimen, Q_L, the loaded cavity Q off magnetic resonance, and R, the reflection coefficient. The incident microwave power P_i is measured with a barretter bridge. It is shown that a plot of Q_M/Q_L against $P_i(1 - R)^2$ yields a straight line whose slope is proportional to TT_1, where T is the absolute temperature.

The biggest disadvantage of this method is the need to measure

the incident microwave power; it is not a relative power which

must be measured but an absolute power, and this leads to large

inaccuracy. This method has also been used by Portis (15; 16),

Redfield (17), Kipling, Smith, Vanier and Woonton (18), and by

Theobald (19).

1.4.2 The DC magnetisation method

Damon 1953: nickel ferrite; 9 Gc/s; 50 kW pulsed; (20).

Bloembergen and Wang 1953: manganese sulphate and nickel ferrite;

9 Gc/s; 50 kW pulsed; (21).

Feng and Bloembergen 1963: ruby; 9.3 and 24 Gc/s; 1 watt and

40 mW pulsed; (22).

The specimen is mounted in a cavity

and is saturated at magnetic resonance by a microwave pulse. This

changes the DC magnetisation of the specimen, and it is the

component of this magnetisation in the direction of the applied

magnetic field which is detected in a pickup coil mounted outside

the cavity. The induced voltage in this coil is proportional to

the time derivative of the DC magnetisation. This is fed to an

integrating amplifier, the output of which records the relaxation

behaviour of this component of the DC magnetisation. The technique

is simple in principle but requires quite sensitive and elaborate
equipment for handling the signals from the pickup coil. The
microwave system is very elementary.

1.4.3 The pulse saturation method

Davis, Strandberg and Kyhl 1958: lanthanum in gadolinium ethyl
sulphate, aluminium in ammonium chrome alum, and chromium in
aluminium oxide (ruby); 8.75 Gc/s; power not given - probably
about 1 watt; (23).

A standard, two-klystron
superheterodyne spectrometer is used with a monitor power of
about $10^{-3}\mu$W. The resonance is saturated by a pulse from the
magnetron, during which time the receiver is protected by a T-R
switch. The magnetron pulse equalises the populations of the two
spin levels being investigated and there is no absorption of
power from the monitor klystron. After the end of the pulse the
populations of the levels begin to revert to their thermal
equilibrium values, and as this occurs an increasing amount of
power is absorbed from the monitor klystron. The receiver picks
up this increasing absorption signal and it is recorded as a
function of time on a cathode-ray oscilloscope. By definition
(see section 1.3 and Chapter 5) the spin levels revert to their

undisturbed state in an exponential manner the time constant of which is the spin-lattice relaxation time, and it is this exponential which is recorded on the display. This has become the standard technique for measuring relaxation time; it is theoretically possible for this method to resolve any number of relaxation times which may be present (see Chapter 5). This technique has been used many times, principally by Bowers and Mims (24), Pace, Sampson and Thorp (25) and Manenkov and Prokhorov (26).

1.4.4   The inversion recovery method

Castle, Chester and Wagner 1960: potassium cobalticyanide; 9 Gc/s; 12 watts; (27).

In this method the spin populations are inverted by adiabatic rapid passage, and the recovery from this condition is monitored by a standard superheterodyne spectrometer. The technique for producing inversion is as follows. The DC magnetic field is held below the resonance value; auxiliary Helmholtz coils are used to sweep the magnetic field through resonance, first upwards and then downwards. A short saturating pulse of microwave power is applied to the system as it goes through resonance for the first time. As resonance is swept

through for the second time, the spectrometer receiver displays

an inverted resonance line. The intensity of this inverted line

depends upon how quickly the second sweep through the line follows

the first. If the interval is long enough, the line will be no

longer inverted and will appear as a normal absorption line,

regaining its maximum intensity after the spin-lattice relaxation

process has removed the effect of the inversion. Thus, if the

resonance is swept through repetitively after the inverting pulse

has been applied, the locus of the peak of the displayed line, as

it varies from its maximum inverted value through zero to maximum

absorption, gives the exponential recovery of the spin system

from which the value of T_1 can be found. Further measurements on

ruby using this technique have been reported by Thorp, Pace and

Sampson (28; 29).

1.4.5 The AC saturation method

Herve and Pescia 1960: paramagnetic coal (unspecified) and DPPH;

frequency unspecified; 100 watts; (30).

This is a variation on the method of

Damon (20), discussed in section 1.4.2. A 100% modulated microwave

field is used to saturate the resonance at frequencies variable

up to 30 Mc/s. The changes in the component of the magnetisation

in the direction of the DC magnetic field are detected by a small
pickup coil near the specimen. When the modulation frequency is
low compared with $1/T_1$ the power modulation produces a magnetisation
variation which is picked up by the coil. When the modulation
frequency is higher than $1/T_1$ the magnetisation can no longer
follow the power variation and the signal induced in the coil
decreases, This alteration in the induced signal with variation
of the modulating frequency enables T_1 to be measured. Further
details of this method have been given by Herve and Pescia (31),
Bassompierre and Pescia (32) and by Herve (33) but it is
interesting to note that in none of these papers is the working
frequency given.

1.4.6   The ultrasonic method

Dobrov and Browne 1963: ruby; (34).

This method is completely different
from any of the methods so far discussed. Instead of using
microwave electromagnetic waves as the energy source it uses
microwave acoustic energy at 9.3 Gc/s generated by quartz rods
bonded to the ruby specimen. The technique uses the spin-lattice
interaction in the opposite manner to the previous experiments.
The specimen is placed in a DC magnetic field and if acoustic

power is supplied to the specimen it will be absorbed if the frequency is correct. At resonance the coherent phonons, produced in the specimen by the transducers, have the correct energy to excite transitions of spins by virtue of the spin-lattice interaction (perhaps the term lattice-spin interaction is more useful here). In this manner an acoustic absorption spectrum for ruby as a function of magnetic field can be plotted and it shows the three allowed spin transitions of the four level chromium ion. From these ultrasonic absorption measurements values of T_1 can be derived.

Methods 1.4.1 to 1.4.5 have been used over a frequency range from 8.5 to 35 Gc/s but no work has been reported above this figure. This is because each method requires that the resonance should be saturated by the microwave power. At frequencies up to 35 Gc/s this is no problem; above this frequency, klystrons and backward-wave oscillators giving sufficient power output are very few and are extremely expensive, and for this reason traditional measurements of T_1 have not been made above 35 Gc/s. Values of the spin-lattice relaxation time at a frequency of 70 Gc/s have been inferred from the pulsed magnetic field measurements of Rimai, Bierig and Silverman (35) on

rare-earth ions, but no direct measurements have been made.

This brief synopsis on experimental methods is not intended to give a complete picture of work in electron spin resonance. Quite the opposite; it is intended to illustrate two facets only of an immense field of study - (a) the indispensable role played by electronics and microwave technology, and (b) the importance of relaxation time measurements in the study of maser materials, for it is these two subjects which form the basis of the present work described in the following chapters.

1.5 Outline of the present work

Chapters 2 and 4 describe the design of a complete microwave spectrometer operating at 35 Gc/s. It is intended for use in the measurement of spin-lattice relaxation times in paramagnetic materials by the pulse saturation technique (23). Superheterodyne detection is employed, the local oscillator signal being derived by a novel method. The design and operation of the superhet are described in detail. A superconducting solenoid is used because the cryogenic apparatus is used in another spectrometer operating at 70 Gc/s and described in chapters 6 and 7. A review of the principal types of microwave

receiver is given in Chapter 3, both as a general background and to assist in explaining the reasons for using superheterodyne detection for one measuring technique and crystal-video detection for another technique. The 35 Gc/s superhet principle (36) is adapted for use at 70 Gc/s and has raised some interesting points: these are discussed in Chapter 6. To make relaxation time measurements possible above 35 Gc/s, a technique has been evolved (37) to overcome the need for microwave saturating power and is explained in Chapter 5 and Chapter 7. Chapter 5 describes the use of the method at 35 Gc/s and shows it to have an accuracy equal to that of the pulse saturation method. Chapter 7 describes the use of the method at 70 Gc/s and gives what are believed to be the first direct measurements of spin-lattice relaxation times at this frequency in ruby and sapphire. Each chapter includes, where appropriate, suggestions for the improvement of existing apparatus and techniques, and ideas for further research work.

Chapter 2

The Spectrometer - 1. The Magnet Assembly and Cryostat.

This chapter deals with the cryogenic part of the spectrometer giving details of the overall design with accent on the reasons behind the choice of the individual pieces of apparatus.

2.1 The superconducting magnet

With a view to extending electron spin resonance experiments into the O-band region (70 Gc/s), a magnet was required which could produce at least 30 kilo-oersteds. To meet this requirement, a superconducting magnet made by International Research and Development Co. Ltd., was chosen. The magnet had a maximum field of 42.6 kOe at an energising current of 22 amps. Initial tests made by D.R. Mason in 1964, based on some observed paramagnetic resonance line widths, indicated that the field homogeneity was about 1 part in 10^5. The magnet is wound with a Niobium/Zirconium alloy having a critical temperature of about 8°K. The phenomenon of "training" has not been observed with this magnet, but it is a well-known property of most superconducting alloys including Nb/Zr (1). When the current through a superconducting wire in an external magnetic

field is increased for the first time the wire may pass into the normal state at a current well below the critical value. If the prodedure is repeated the transition takes place at a higher current, and only after a number of cycles is the final critical current reached. This is the usual description of training, and no satisfactory explanation of it has been given. The bore of the IRD magnet is 0.75 inch and even with Q-band waveguide in position there is ample room for the placing of an auxiliary modulating coil.

The question now arose as to the type of power supply required and whether or not a superconducting switch, to enable the use of the "persistent current", would be an advantage. The initial testing of the magnet had been carried out by wiring it in series with a Newport Instruments Type D electromagnet in use on an adjacent spectrometer. The way this was done is illustrated in figure 1. The arrangement worked extremely well and it was decided to use this method permanently. A safety diode, Westinghouse type S8AN70, was connected as shown in figure 1 to fulfil two specific purposes:

(a) When the magnet is normal, its resistance is about
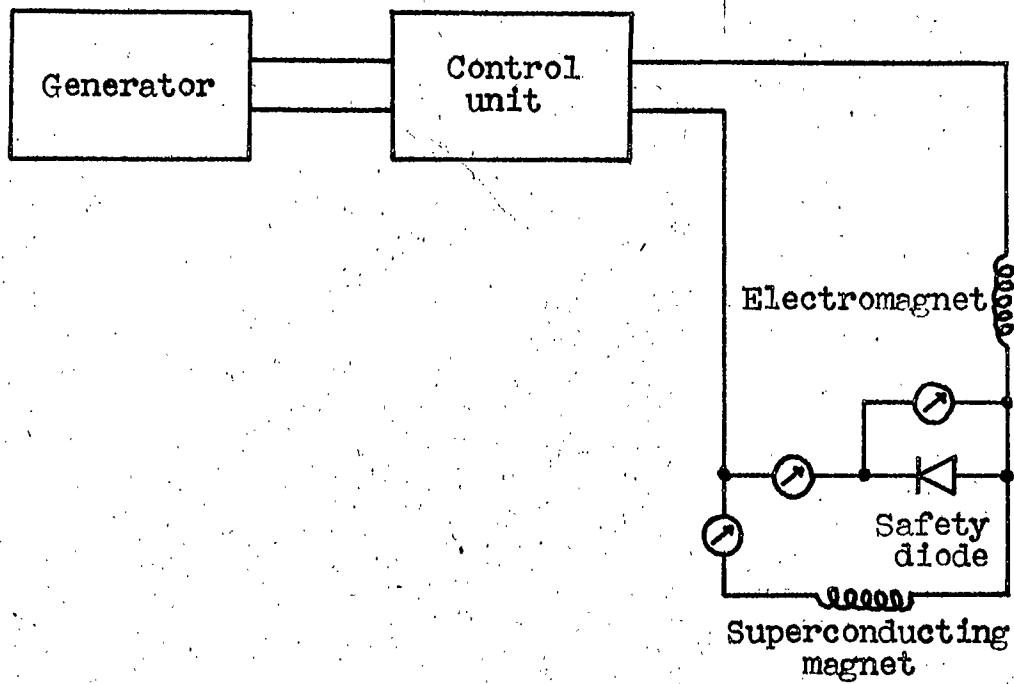
Figure 1.

Power supply for the superconducting magnet

1500 ohms. This resistance in series with the Newport electromagnet would cause the generator to run away because the feedback control voltage would be virtually removed. To provide a low-resistance path while the magnet is normal, the diode is connected as shown. The control unit is then unaware of the superconducting magnet being in circuit. When superconductivity occurs, current flows preferentially through the solenoid because its resistance vanishes. Again, the control unit is unaware of the circuit change.

(b) When the superconducting magnet is operating at a current of I amps, the stored energy, E is given by

$$E = \tfrac{1}{2}LI^2 \quad \text{joules}$$

if L is in henries. If the magnet quenches, because of a current surge or a lack of liquid helium, this $\tfrac{1}{2}LI^2$ must dissipate itself. This it can do quite safely through the diode, the control unit being unaffected by the quench. The diode, by virtue of its non-linear characteristic, provides efficient damping of the ringing which tends to occur as the magnetic field collapses. Were the diode not present, the surge voltage produced at the superconducting magnet terminals by the magnet quench could be of the order of kilovolts, and would certainly destroy the

Evacuated
interspace

Liquid nitrogen
jacket

Liquid helium
reservoir

Position of
superconducting
magnet

Figure 2.
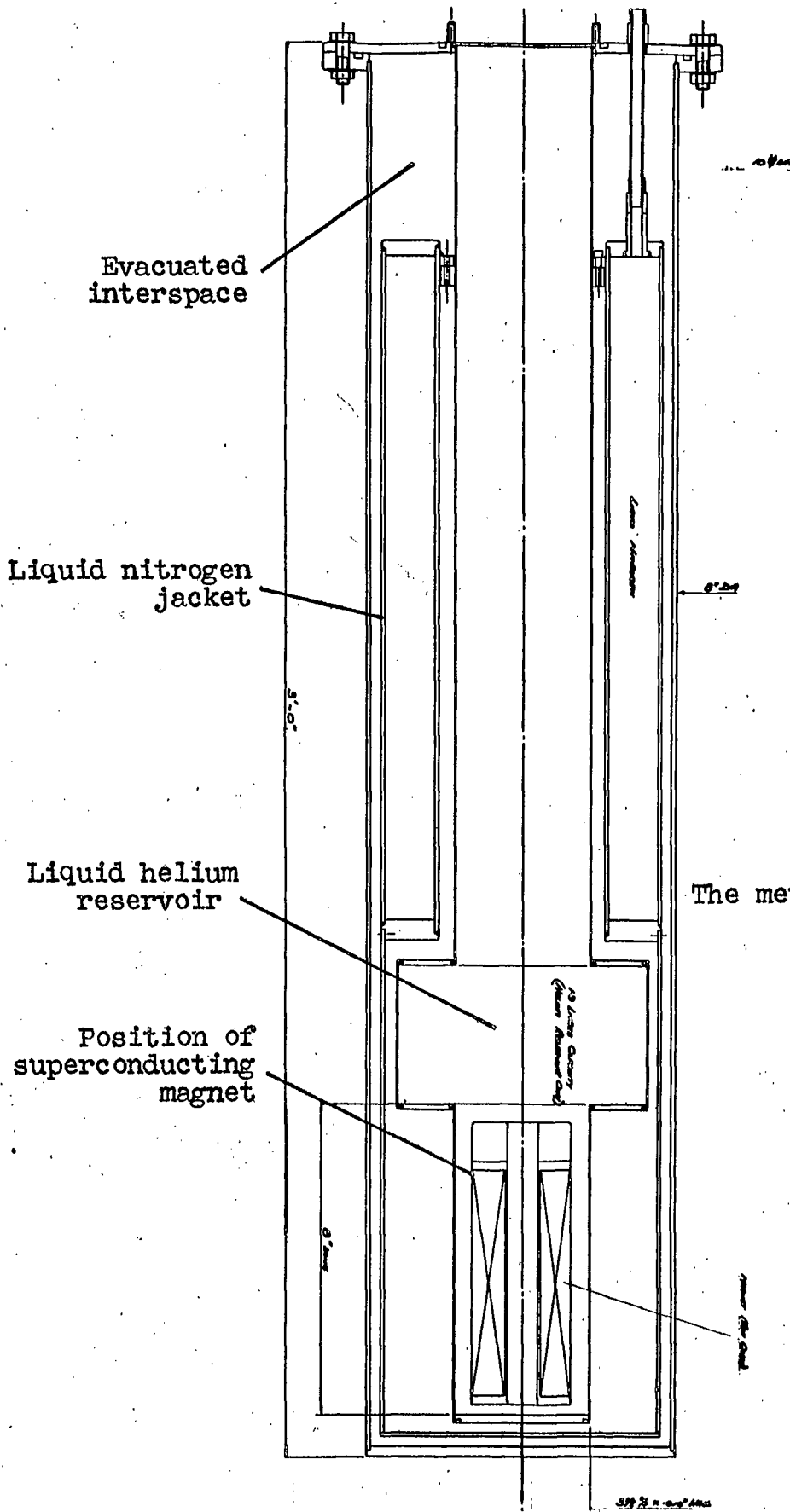
The metal cryostat

control unit. Because of this, the diode is tested before each
helium run.

2.2 The metal cryostat

All the initial tests were carried
out using a cryostat comprising two double-walled Pyrex dewar
vessels, the inner filled with liquid helium and containing the
magnet and the outer filled with liquid nitrogen. While this
system proved reasonably satisfactory for some half-dozen runs,
it later became unreliable and much time and money was spent on
re-annealing the helium dewar and stopcock, all to no avail.
Because of this difficulty it was decided to obtain a metal
cryostat. The cryostat was designed jointly with Oxford Instruments,
Ltd., and was built and supplied within eight weeks. The
construction of the cryostat is shown in figure 2.

2.3 The magnet mounting assembly and modulation coil

Because of the low ceiling of the
laboratory in which the equipment was to be situated, care was
necessary to ensure that there was sufficient clearance between
the top of the cryostat and the ceiling to enable the low-
temperature waveguide to be removed from the cryostat. Previous
cryostats had been mounted on the spectrometer frame, and a

Figure 3(a).

The magnet assembly

specially designed syphon had been used for the liquid helium transfer. However, it was decided that to have the greatest cooling efficiency during the transfer, the arm of the syphon must reach the bottom of the helium dewar in the cryostat. This necessitated a 40-inch clearance above the cryostat, and it was found that this was just possible with the cryostat resting on the floor of the laboratory.

The design of the top plate for the cryostat was straightforward. Four apertures were required:

(i)   waveguide mount;

(ii) syphon entry;

(iii) exit to vacuum system and gas collection system;

(iv) electrical outlet.

The syphon entry and gas exit apertures required supporting tubes to be soldered into the top plate, the syphon entry tube extending some 12 inches down into the helium dewar to provide guidance for the syphon. Electrical outlets were provided by a ceramic button with twelve electrical connections through it, mounted in the top plate by a ceramic-to-metal seal. The waveguide mounting and magnet support are of a more involved design and are shown in figure 3. The magnet support tube is a
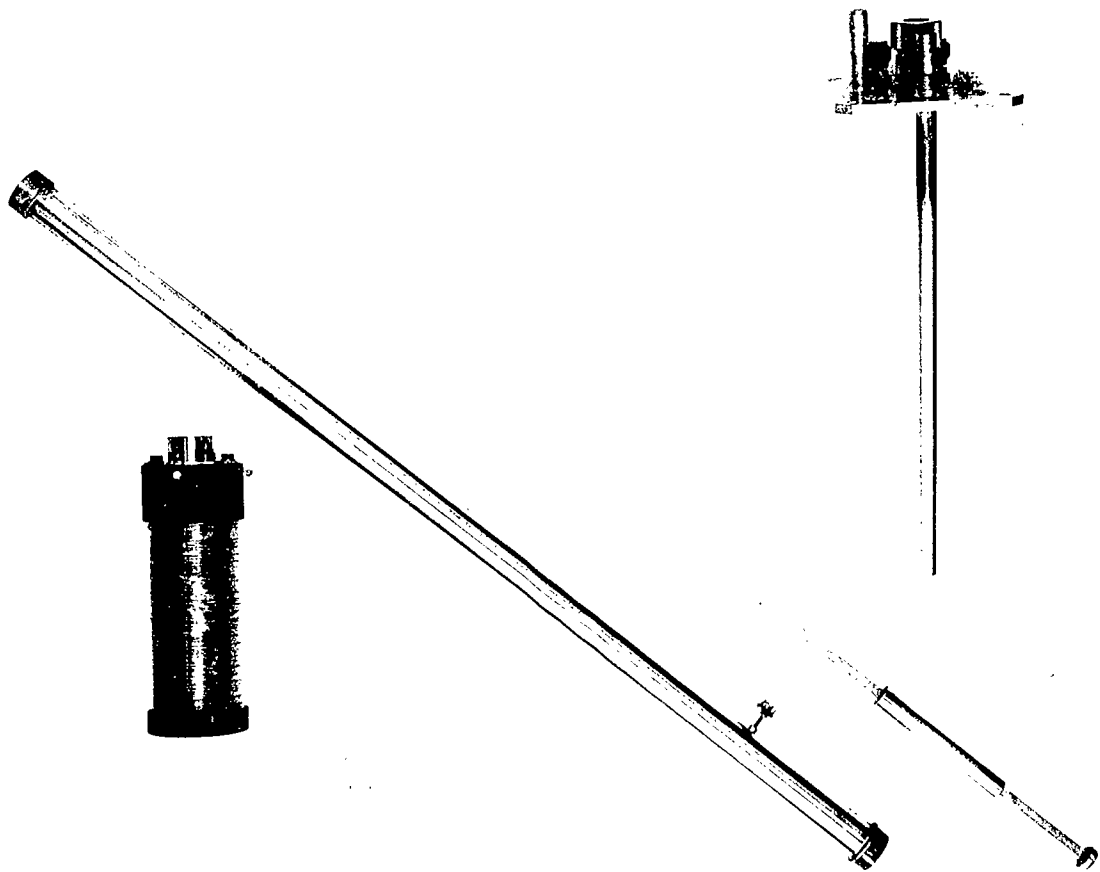
Figure 3(b).

The dismantled magnet assembly

1-in. diameter stainless steel tube with a wall thickness of 0.012 in., providing a rigid, low thermal conductivity support for the magnet.

A necessary design feature was an auxiliary modulation coil capable of producing a magnetic field scan of about 200 oersteds peak-to-peak to enable a video display of absorption signals on a cathode-ray oscilloscope. In order to minimise the ampere-turn product for the coil, the windings had to be as close to the specimen as possible, the magnetic field being coaxial with that of the superconducting magnet. A coil former was designed to be a push fit into the magnet bore, and is shown in figure 4. The coil consists of 6 layers of 22 SWG enamelled wire, the connecting wires being recessed along the main body of the tufnol former. Design calculations showed that the coil should have a self inductance of 0.9 mH, a sufficiently low figure to allow the use of modulation frequencies in excess of 30 kc/s if necessary. A winding of 6 layers at 80 turns per layer was chosen because (a) it gave a low value of self inductance, and (b) a current of 2 amps was calculated to produce a magnetic field of about 300 oersteds. The tufnol former was positioned in the magnet bore so that the centres of the two

6 layers at
80 turns per layer

Recessed
connecting wire

Tufnol former

$1\frac{1}{2}''$

$\frac{3''}{4}$

$\frac{21''}{64}$
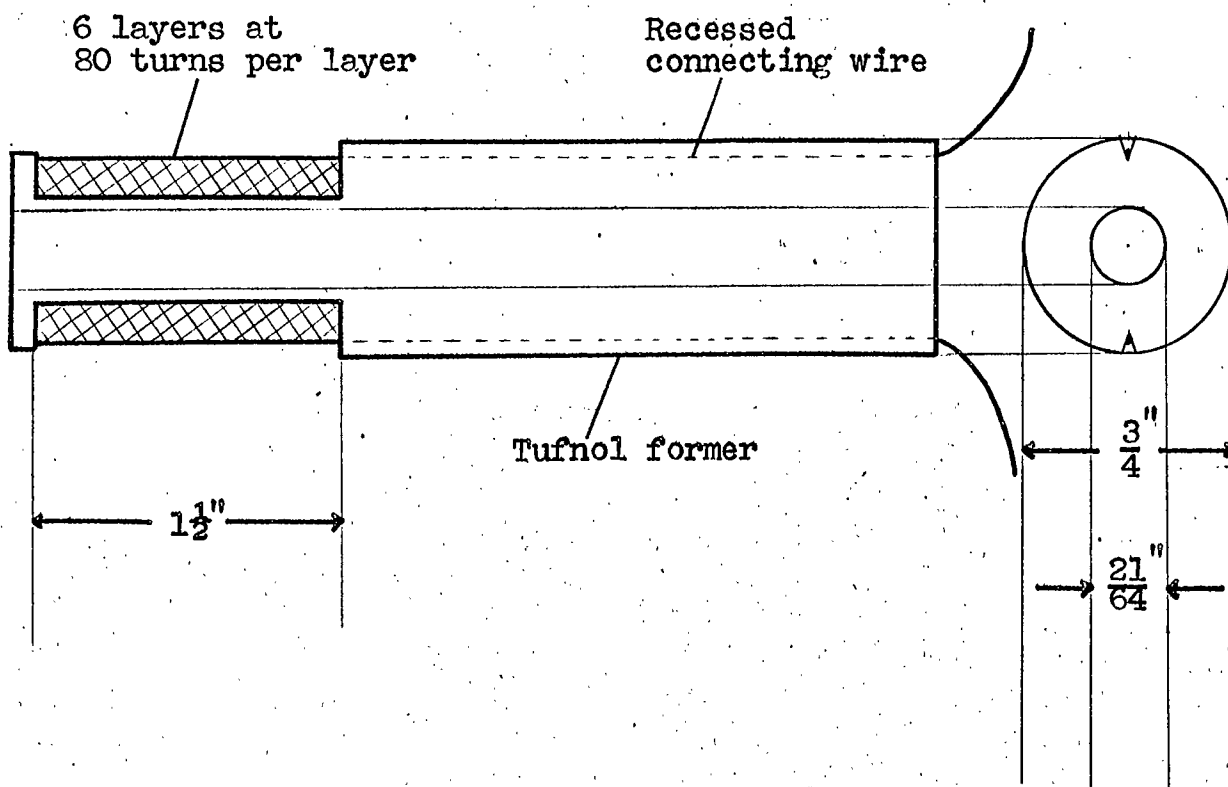
Figure 4.

The modulation coil

magnetic fields were coincident. Two terminals were mounted on

the top block.of the superconducting magnet and the wires from

the modulation coil were soldered to them inside the block. In

this way the magnet and the modulation coil is a single unit with

no floating wires.

2.4 Depth measurement of liquid helium

Knowing the level of liquid helium

in a cryostat is always useful and is often a necessity. A brief

survey follows of the most popular methods of depth measurement.

Devices for depth indication fall into two categories - those

giving an indication of the presence or absence of liquid helium

at a specific point, and those giving a continuous measurement

of depth.

The most popular "spot check"

device is a low wattage carbon resistor. This utilises the

resistance-temperature characteristic of carbon which, in the

helium temperature range, follows an inverse law. Differentiation

between gas and liquid is an important property which any depth

indicator must possess. It is a difficult differentiation to

make. If the liquid is boiling steadily, its own temperature

and that of the gas immediately above it are almost identical,

and for an exact estimation of depth to be made, the sensing

device must respond to some factor other than temperature. This

other factor is the thermal conductivity of the medium

surrounding the device. The thermal conductivity of liquid helium

is much greater than that of helium gas, and if the current

flowing through the sensing device is chosen correctly, the

following two criteria for successful operation can be fulfilled:

(a) The current through the device must be large enough to

heat up the resistor when it is in the gas so that its resistance

is appreciably different from that when it is in the liquid.

(b) This current must not be so large as to produce

excessive boiling of the liquid in contact with the device.

If a carbon resistor is used, its

physical size will be one factor in determing the sensitivity,

and the type of resistor commonly used is the 0.1 watt variety

made by Allen-Bradley. Blanplain (2) describes a carbon resistor

depth gauge and uses a Wheatstone Bridge detection system giving

an accuracy of 3 mm for the level. The basic theory of "heated

element" level detectors is developed by Maimoni (3). A very

elegant way of giving a continuous indication of depth is the

capacitor device of Meiboom and O'Brien (4). A cylindrical type

of condenser is mounted perpendicular to the liquid surface, and
any change in depth of liquid produces a change in the dielectric
constant of the medium between the plates and results in a change
of capacitance. Although simple in principle, its practical
realisation is difficult; the dielectric constant of the helium
gas is 1.0000652 and that of the liquid is 1.048. Meiboom and
O'Brien report that this change in dielectric constant produces
a maximum change of 3 pF over the 61 pF of the empty condenser.
Because of the sensitivity required, a commercial capacitance
bridge is used which has a maximum sensitivity of 3 pF full-scale
deflection and an overall stability of 0.1 pF. This principle
has also been used by Dash and Boorse (5); here the capacitance
change is used to change the frequency of a high-frequency
oscillator, the frequency shift being measured. Capacitor
detecting systems are used to operate control systems for
maintaining predetermined levels in apparatus designed by
Nechaev (6) and by Williams and Maxwell (7). The last of the
capacitor devices is a spot check system due to Kasatkin (8).
The accuracy claimed for these techniques is 1 to 2 mm. Cryostats
using glass dewars with narrow sight lines are amenable to being
fitted with the simplest of all depth indicators, a float made of

expanded polystyrene, described by Babiskin (9). For use in

opaque cryostats the float can be fitted with a balsa wood stem

protruding throgh the top plate, a method used by Rasor (10). The

provision of an exit hole for the stem precludes the use of

pressures other than atmospheric. The most sensitive depth

indicator for liquid helium employs a sensing element made of a

superconducting alloy. For continuous indication of depth the

wire is mounted perpendicular to the liquid surface and can take

the form of a single strand, a loop or a helix, depending upon

the sensitivity required and the amount of room available. A

constant current flows through the wire, its value being decided

by the considerations (a) and (b) mentioned previously. The

voltage drop across the wire is a direct measure of the length of

wire which is superconducting. Level gauges using this principle

have been described by Feldmeier and Serin (11) and by Ries and

Satterthwaite (12), the difference in the designs being the choice

of material for the sensing element. Feldmeier and Serin use

tantalum, while Ries and Satterthwaite use a fine manganin wire

coated with a 60% Sn - 40% Pb alloy. The merits of various types

of superconducting sensing element are discussed by Figgins

et al. (13); from sensitivity considerations the best materials

are vanadium and tinned constantan. The problem of heating the
wire above the liquid is overcome in a different way by Isaeva (14):
two separate wires are used - an insulated constantan wire is
used as a heater and tantalum wire is wrapped helically round it.
Superconducting "dipstick" indicators are the subject of papers
by Rovinskii (15; 16) and by Fradkov and Shal'nikov (17). An
interesting background on the heat treatment of superconductors
is given by Webber (18). For the sake of completeness, the
following indicators are included:

(i) The vibrating rubber membrane. A long tube, sealed at one
end by a rubber membrane, is lowered (open end downwards) into
the cryostat. Spontaneous oscillations of the membrane begin.
When the lower end of the tube penetrates the liquid, these
vibrations drop in frequency by 30% and in intensity by 60% (19).

(ii) Differential pressure systems. Such systems have been
described (20), (21), but they are rather cumbersome methods
compared with the electrical systems.

(iii) Semiconducting sensing elements. A sensing element of
boron-doped silicon has been used by Sauzade et al. (22). The
resistivity is heavily temperature-dependent, giving good
sensitivity.

Bearing in mind the relative merits

of each system it was decided to use a continuous-reading

superconducting depth gauge. Reference (13) advocates the use of

tinned constantan as being equally sensitive as vanadium but

having the great advantage of being able to be made in the

laboratory. The only constantan available at the time was

insulated with enamel, which had to be removed. This was

accomplished by softening the enamel in concentrated nitric acid

and removing it from the wire with a clean cloth. This method is now

not recommended; if the acid comes in contact with the wire it

cannot be tinned. The ideal way to remove the enamel from such

wires is to use a de-polymeriser such as "Stripalene 713"

manufactured by Sunbeam Anti-Corrosives Ltd. This will remove

the enamel without attacking the wire. Having cleaned the wire

and prevented the formation of kinks which, in 40 SWG wire, are

very troublesome, the wire was suspended between two vertical

pillars in such a way as to be under slight tension. A 25-watt

soldering iron with a newly-prepared bit was used to tin the wire

very evenly with Multicore Savbit Alloy solder. Measuring from

the blueprint of the metal cryostat, the top of the liquid helium

reservoir was about 11 inches from the bottom of the helium

dewar; this meant that the length of the sensing element had to

be 22 inches for a complete loop, and the wire was mounted from

the stainless steel support tube to the bottom lip of the

superconducting magnet former as the photographs of figure 3 show.

The overall change in resistance of the wire between room

temperature and $7^{\circ}K$, the critical temperature of the solder, is

only some 15 to 20,; of the room temperature value of 25 ohms. A

current of 100 mA was calculated to produce a heat dissipation

of approximately 10 mW per inch of the wire in helium gas at

$4.2^{\circ}K$. This appeared to be an average dissipation, working from

figures quoted in the literature, so a constant current power

supply was built to provide 100 mA into a load varying between

0 and 25 ohms. The circuit of the supply is shown in figure 5.

It utilises a 4.7 volt Zener diode together with a 47 ohm

reistor to provide a constant 100 mA emitter-base current.

Transistor action then maintains 100 mA in the collector load

(in this case it is the sensing element) irrespective of its

value. This level indicator had been in use in two cryostats for

over two years and there has been no trace of non-reproducibility

which might be expected from the severe temperature cycling to

which the sensing element is subjected. The accuracy of indication
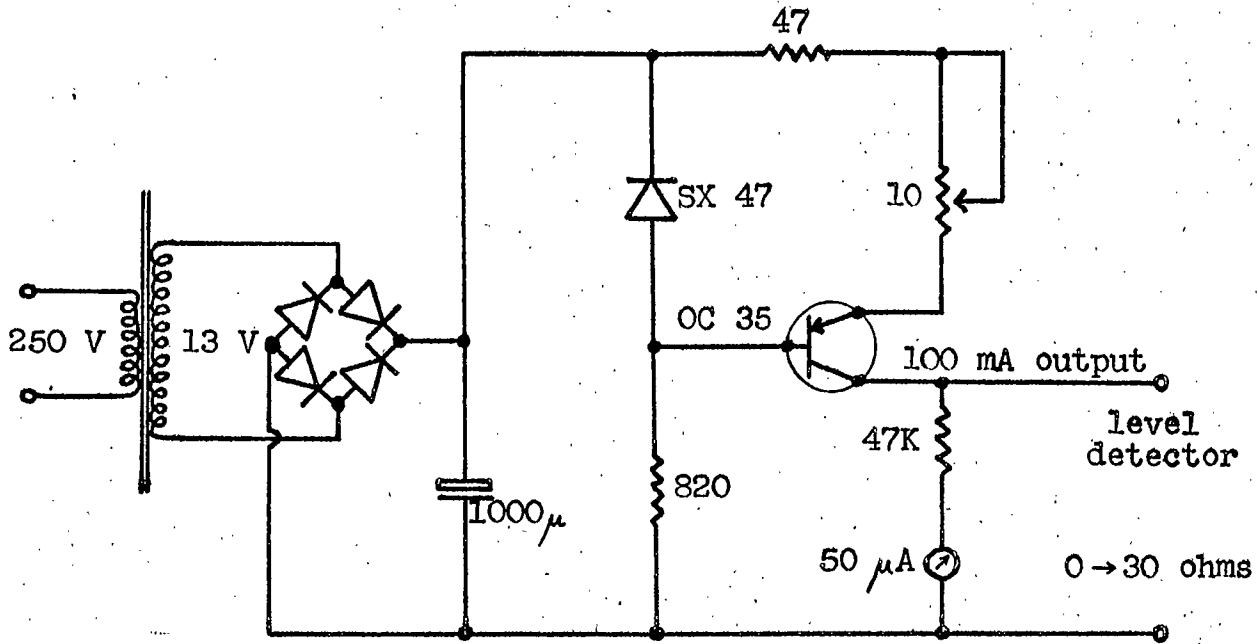
Figure 5.

Constant current circuit

of depth is within 1 mm and the differentiation between gas and liquid is very satisfactory. A large gas displacement produces a voltage drop across the wire, indicative of the cooling effect, but this voltage rises again as soon as the displacement is reduced. The rising level of helium liquid produces a steady drop in voltage across the sensing element; this voltage does not rise after liquid transfer ceases.

The onset of superconductivity is indicated by a voltmeter placed across the safety diode of figure 1. When the magnet is normal and the power supply is on, the meter reads 400 mV, the forward voltage drop of the diode. When the magnet becomes superconducting, the voltage abruptly drops to zero as the meter becomes short-circuited by the magnet. This provides a further check on the accuracy of the depth gauge.

2.5 Technique for liquid helium transfer

With the metal cryostat, the procedure for a helium transfer is as follows.

(A) Evacuate the interspace with a good backing pump to about 10^{-3} mm Hg.

(B) Fill up the screening jacket with liquid nitrogen.

(C) Wait for a few hours to enable the temperature of the

magnet assembly to reach $77^{\circ}K$. (This is optional; liquid helium

has been transferred into the helium dewar when the magnet

assembly was at room temperature. If the helium transfer is done

slowly, the extra wastage of helium liquid is very small).

(D) Transfer liquid helium by the metal syphon from the

travelling dewar. This takes about $\frac{1}{2}$ hour.

Once the transfer is completed, the helium will remain for over

9 hours without attention of any kind.

Initial testing of the system

included inducing the magnet to quench in order to check that the

quenching was completely under control. This can be done at any

value of magnetic field by producing a surge in the energising

current. Quenching under present conditions was found to be quite

safe, being evident only by:

(a)   loss of the resonance signal;

(b)   the reading on the meter across the diode;

(c)   a gentle, short boil-off of helium gas.

The boil-off is very slight, and can only correspond to a few

millilitres of liquid.

Chapter 3

Receivers for Microwave Spectroscopy

3.1 Types of receiver

Receivers used in microwave spectroscopy fall into three general categories: crystal-video; superheterodyne; synchrodyne. In the crystal-video receiver the incoming signal from the spectrometer bridge is detected by a point-contact diode and amplified by a broad-band video amplifier. The term "video" has a particular connotation in microwave spectroscopy; although derived from radar technology this adjective is used quite generally to describe the amplifier or amplifiers handling the demodulated (detected) microwave signal. The bandwidths of these amplifiers rarely exceed 10 kc/s (1). The superheterodyne receiver frequency-changes the incoming signal by direct mixing in two crystal diodes with a locally-derived oscillation, the intermediate frequency signal being amplified and later detected at high level. The synchrodyne receiver is .. very similar to the superheterodyne except that the IF used is zero frequency and the receiver is sensitive to phase and amplitude. Each type of receiver makes use of the microwave diode either as a mixer or as a detector and as a result, the performance of any such receiver is greatly dependent upon the

Crystal cartridge

Clamping screw

Waveguide aperture

Germanium slab

Tungsten whisker

Coaxial output

Locating hole
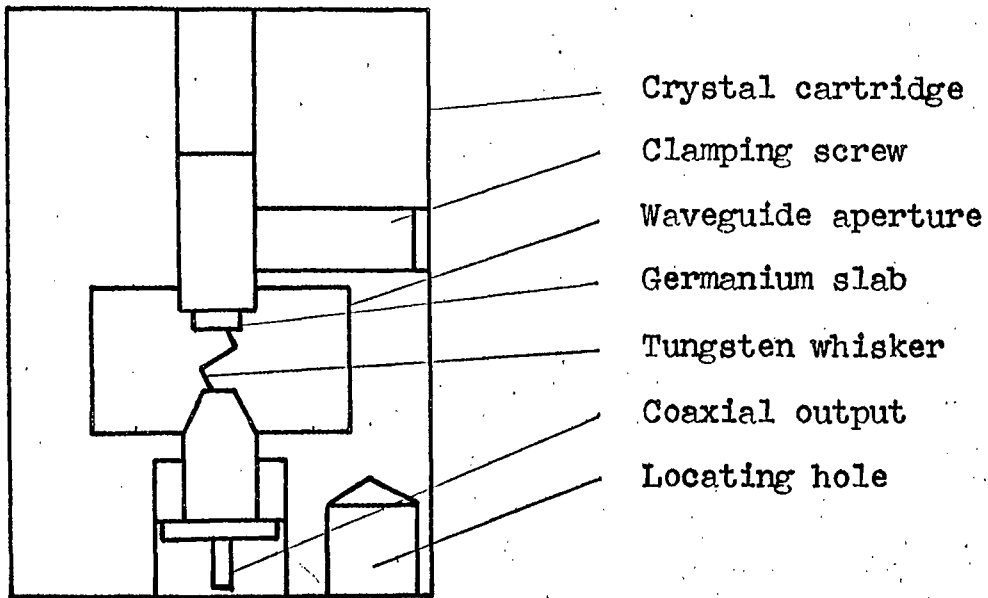
Figure 1.

Construction of a Q-band diode

quality of the diode in use.

3.2 The microwave diode

The construction of a Q-band diode is shown in figure 1. It is a point-contact device with a tungsten whisker pressing on a small slab of silicon or germanium. The area of the point of contact is about 10^{-4} cm. The slab of semiconductor is connected to one of the broad faces of the waveguide and the whisker connection is brought out to the centre pin of a coaxial socket. The electrical characteristics of these diodes are similar to those of other point-contact types and a typical curve is shown in figure 2. The shape of the characteristic gives rise to two modes of detector operation -- linear and square-law.

(a) Linear or strong-signal detection

If a large signal is incident on the detector the RF peak-to-peak voltage will be sufficient to swing the instantaneous operating point to the extremes indicated by b in figure 2. At large forward bias the characteristic becomes virtually linear; the reverse region is also linear but of a very high resistance. Thus the signal switches the detector on and off, and if the swing is large enough the distortion produced by the
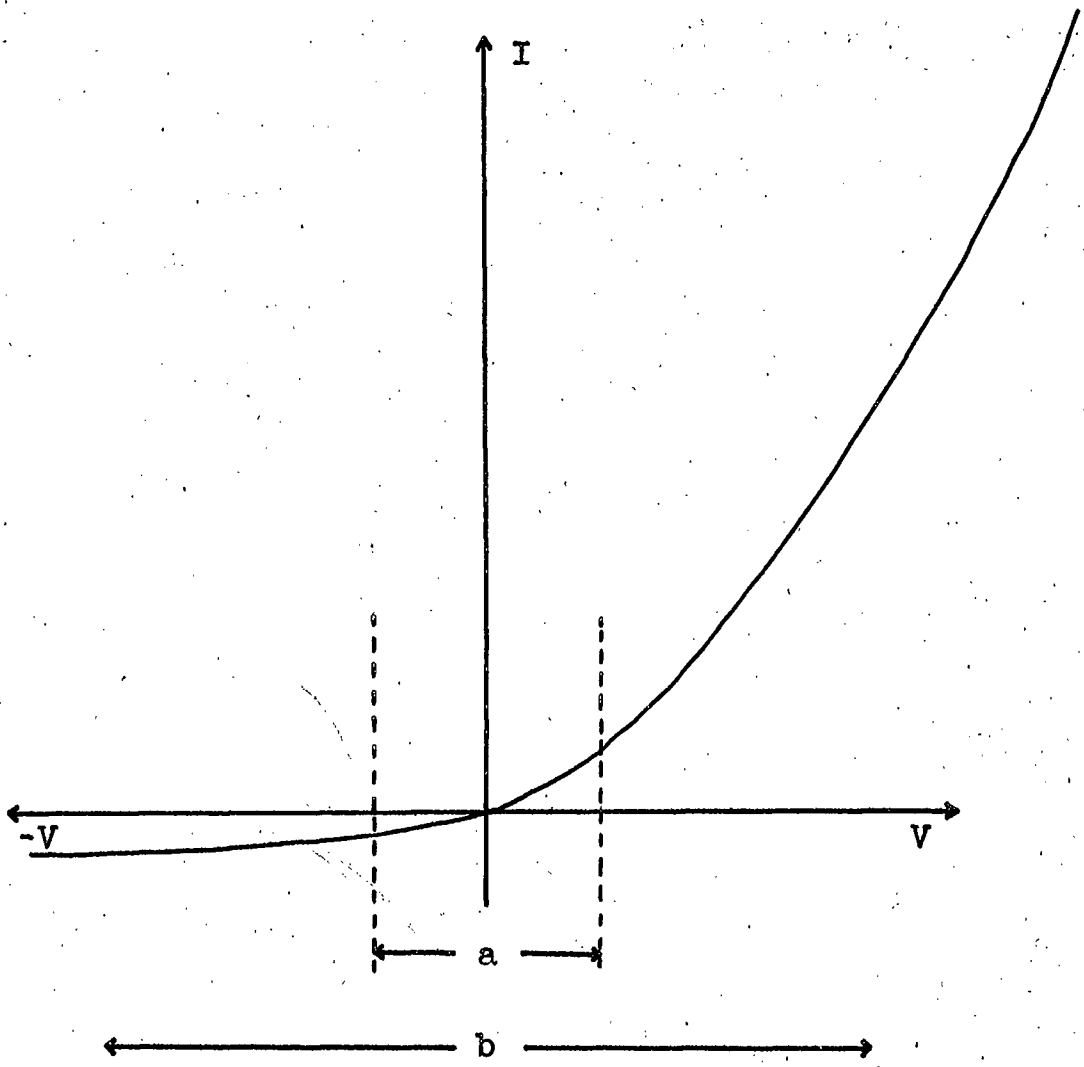
Figure 2.

Electrical characteristics of a point-contact diode

curved characteristic in the region of the origin is negligible.

(b) Square-law or weak signal detection

For a low-level incident signal, the voltage swing is small, indicated by $\underline{a}$ in figure 2. This voltage excursion uses a wholly curved portion of the characteristic and it is known that this curvature can be described mathematically by a Taylor expansion terminating in the squared term:

$$i = f(e) = f(e_o) + \frac{df}{de}(\delta e) + \frac{1}{2}\frac{d^2 f}{de^2}(\delta e)^2 \quad , \quad (1)$$

where e_o is the bias voltage determining the operating point, and δe is the small input signal voltage. The derivatives are evaluated at the operating point e_o. The diode thus functions as a square-law detector when the applied signal is sufficiently small, provided that the second derivative of the characteristic does not vanish at the operating point. The linear term is of no importance in detection, since it is symmetrical about the operating point.

It is convenient at this stage to introduce the microwave diode as a switch and as a voltage - controlled attenuator. The diode can be represented by the equivalent circuit shown in figure 3.

L   represents the whisker inductance;
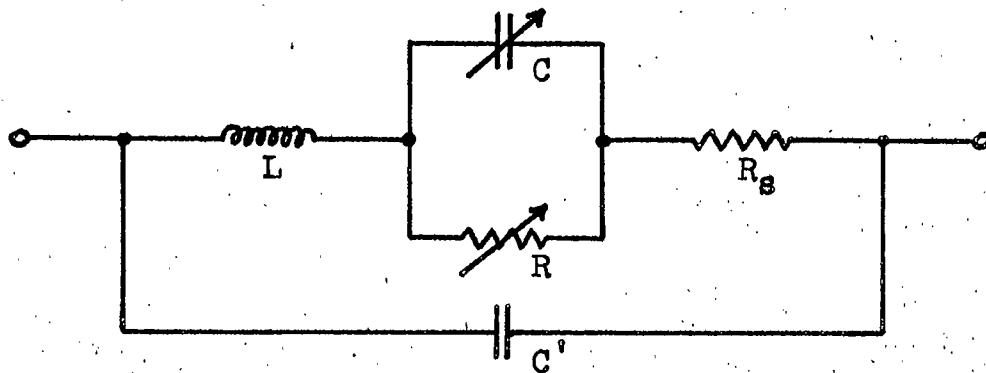
Figure 3.

Equivalent circuit of the point-contact
diode

R_s is the "spreading resistance" due to the

compression of the current flow paths in the semiconductor near

the point of contact;

C represents the barrier capacitance, a function of

bias and polarity, and accounts for the storage of charge in the

boundary layer of the semiconductor;

R represents the non-linear resistance of the

rectifying contact, and is also a function of bias and polarity.

C' accounts for the parasitic capacitances due to

the mounting of the whisker and semiconductor. It can be

compensated for by tuning the diode holder and will be neglected

in this analysis. For operation as a switch, the diode presents

one of two different impedances which are determined by the

amplitude and polarity of the applied bias. For the switch to be

ON, a forward bias is applied which results in R being small

compared to C, thereby shunting it. This produces a series R-L

circuit across the waveguide and results in a small insertion

loss. In the OFF state the applied reverse bias causes R to be

very high and effectively shunted by C. The diode can now be

represented by a series R-L-C circuit, and if the values of R

and C are correct the circuit will resonate, resulting in a low

resistance across the waveguide. The insertion loss under these
conditions is usually some 30 dB greater than the insertion loss
in the ON state.

The OFF/ON ratio is heavily
dependent upon the incident power, and at X-band the average
diode will only give 30 dB isolation for incident powers up to
1 mW. This can be increased to 50 mW but the isolation is reduced
to 12 dB maximum, this figure being attainable only after careful
choice of diode. If powers in excess of a few milliwatts are to
be switched, a diode must be chosen which has a higher forward
resistance and a larger Zener breakdown voltage than the ordinary
detector diode. The reason for this is that for successful switch
operation the peak-to-peak voltage excursion of the incident
microwave power must lie totally in the forward-bias region in
the ON state, and totally in the reverse-bias region in the OFF
state; to achieve this, a diode must have a very long voltage axis
to its characteristic, and this condition is fulfilled by a high
forward resistance and a high Zener breakdown voltage.

Switching of microwave power can be
accomplished, therefore, by switching a diode in the waveguide
from forward to reverse bias. The square-law portion of the

characteristic gives rise to a transition region in the switching

characteristic, a region where the insertion loss changes from its

minimum to its maximum value. This region is centred on the origin

of coordinates and extends for about 0.5 volt on either side of

this. This makes the microwave diode usable as an electrically-

controlled attenuator capable of amplitude-modulating the

microwave power in a waveguide. This technique is explained in

detail in Chapter 4.

Having discussed the operation of

the microwave diode, its uses will now be covered in the

description of each type of receiver.

3.3 The crystal-video receiver

As mentioned in section 3.1, a

crystal-video receiver detects the signal at the output of the

spectrometer bridge and the resulting modulation information is

amplified and fed to the display system. It is usual for the

amplifier to be a directly coupled type to enable the display of

continuous wave (CW) power levels when necessary. There is no

tuned circuit, no local oscillator to be tuned and stabilised,

and no IF amplifier. Because of these factors the receiver has a

large RF bandwidth and this, combined with its simplicity, results

in an overall loss of sensitivity of some 40 dB in comparison with a good superheterodyne receiver.

The output from the spectrometer bridge is only a few microwatts and as a result the microwave diode operates in its square-law region, where the output voltage or current is proportional to the RF power incident on the crystal diode. The sensitivity of the receiver is principally a function of the diode because at video frequencies amplifier noise is negligible compared with the Johnson noise of the diode. The term noise figure cannot be used with reference to crystal-video receivers because, together with the conversion loss, it is dependent upon the level of the incoming signal, and in order to specify a figure for the sensitivity, the "tangential signal" is usually quoted. A tangential signal is defined as that signal which is 8 dB above the RMS video noise power (2). This is not a mathematical definition; the figure of 8 dB is quoted because the strict derivation of the definition is based upon the observation of an oscilloscope display. Calculations made from this display show that the tangential signal, defined by experimental observation, is 8 dB above the RMS video noise power. At frequencies in Q-band the sensitivity of a crystal-video receiver

is about 10^{-8} watt. The wide RF bandwidth inherent in this type

of receiver is of no real importance in microwave spectroscopy,

since many experiments use a microwave source at constant

frequency and the tuning range of the klystron lies well within

the passband of the individual components. Crystal-video

receivers are prone to pulse distortion, especially if they are

required to give high gain combined with a large dynamic range.

However, if a receiver is built for a specific purpose, it is

seldom necessary for both of these requirements to be fulfilled.

3.4 The superheterodyne receiver

Invented in 1917, the

superheterodyne receiver is the most versatile and the most

widely used receiver ever introduced. The principle of operation

is the heterodyning of the incoming signal with a locally

generated CW signal, the difference-frequency being amplified by

a series of tuned stages and detected at high level. This

difference frequency is known as the "intermediate frequency" or

IF, and is usually chosen to be of much lower frequency than the

incoming signal. The versatility of the superheterodyne receiver

is illustrated by the fact that such receivers are in common

use over the frequency spectrum from 10^{4} c/s and upwards, the

advent of the laser having extended the useful range into optical frequencies. Cummins, Knable and Yeh (3) have used an optical heterodyne technique to examine diffusion broadening of Rayleigh scattered light, using a helium-neon laser and obtaining a beat frequency of 12 Mc/s. The signal stages of a superheterodyne receiver (or superhet) are independent of the working frequency and are shown in figure 4. The internal construction of these stages and the components used depend markedly upon frequency, and the further discussion on the superhet will be confined to microwave frequencies.

3.4.1 The buffer stage

The presence of the buffer stage prevents any radiation of the local oscillator carrier and acts to isolate the receiver input from the first detector.

3.4.2 The local oscillator

This is usually a low-power CW source, the frequency of which is electronically stabilised by feedback processes to remain at a fixed frequency separation from the incoming signal. The local oscillator is loosely coupled to the incoming signal by means of a balanced mixer, which also serves as a buffer stage.
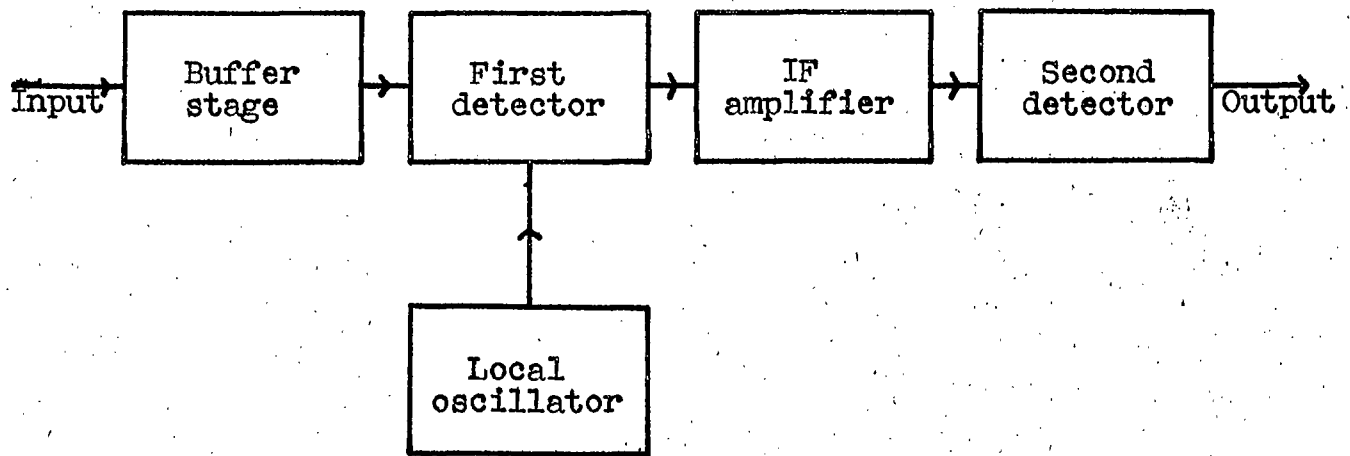
Figure 4.

Block diagram of a superheterodyne receiver

3.4.3 The first detector

The balanced mixer also provides the mixing and detecting functions of the first detector, giving an output containing, amongst other things, components at the intermediate frequency and sidebands carrying the information from the spectrometer. The other components present are discussed in Chapter 4.

3.4.4 The IF amplifier

This consists of a series of tuned stages, the response of which can be shaped almost at will by stagger-tuning the individual stages. A well-designed IF amplifier can combine high gain with wide bandwidth, a combination very rarely obtained in general amplifier circuits.

3.4.5 The second detector

Utilising either a thermionic or solid-state diode, this detector works at high level, i.e., in its linear region, and removes the modulation components from the signal ready for subsequent video amplification. Waveforms illustrating the action of superheterodyne detection are given in figure 5.

Incoming RF
signal

Local oscillator
signal

Resultant
signal

Current waveform
in mixer crystal

Input to first
IF stage

Current waveform in
second detector

Output signal
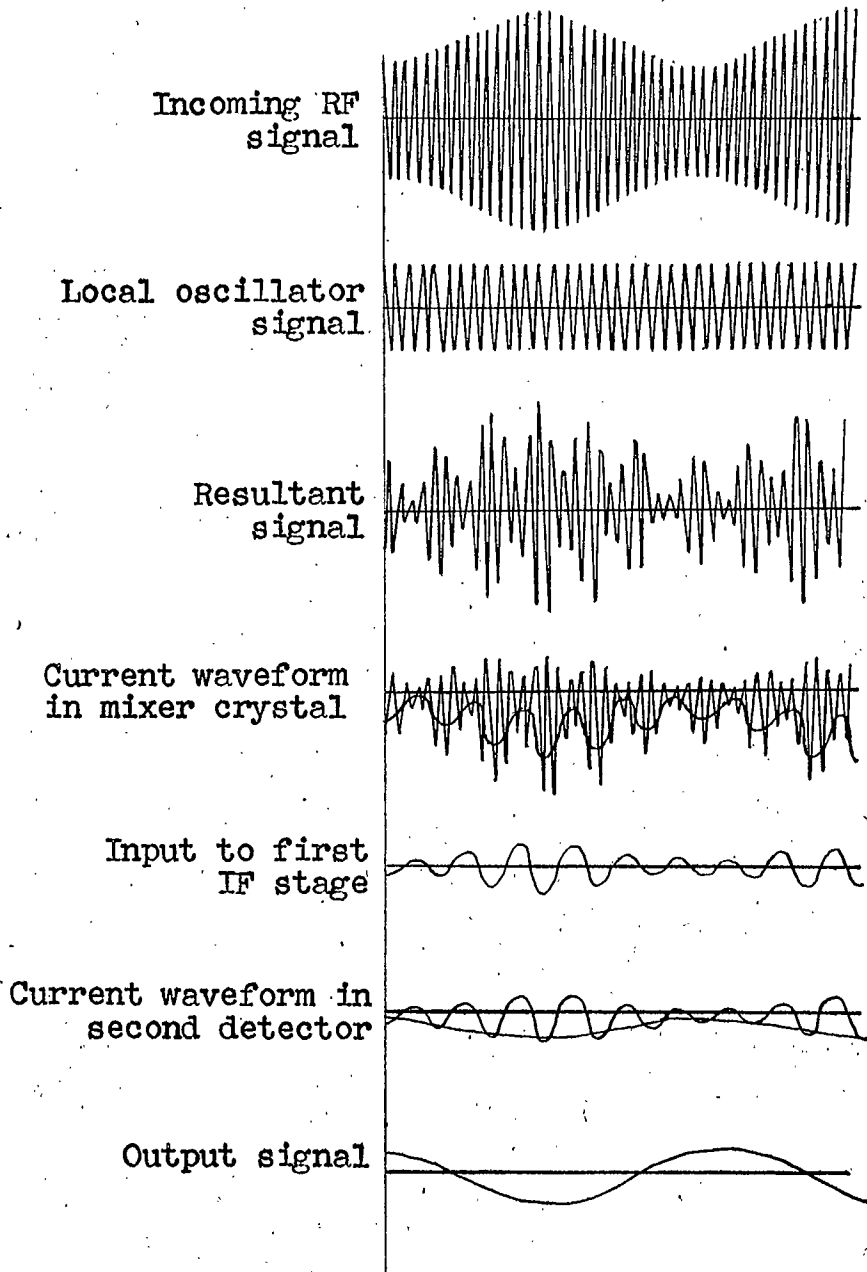
Figure 5.

Superheterodyne detection

3.5 The synchrodyne receiver

In common with both the types of receiver so far described, the synchrodyne is another device for detecting amplitude-modulated signals. It can be simply described as a superhet with an intermediate frequency of zero, and is used in spectrometers providing an output to a pen recorder. Magnetic field modulation, of amplitude much less than the line width under investigation, combined with a slow change in the DC magnetic field, produces "incremental absorption" signals which vary as the resonance line is slowly scanned. This process is illustrated in figure 6, where the incremental absorption signals are shown at various points during the scan. The amplitude of the incremental absorption depends upon the slope of the absorption characteristic, and the phase of the incremental absorption reverses when the sign of the slope of the characteristic changes. If the magnetic field modulation frequency is 160 kc/s, sidebands at $\pm$160 kc/s are produced on the microwave carrier. These sidebands vary in amplitude and phase according to the variation of the incremental absorption, the waveform of which is given in figure 7 for a complete scan of the line. Note the phase change at the peak of the resonance line.
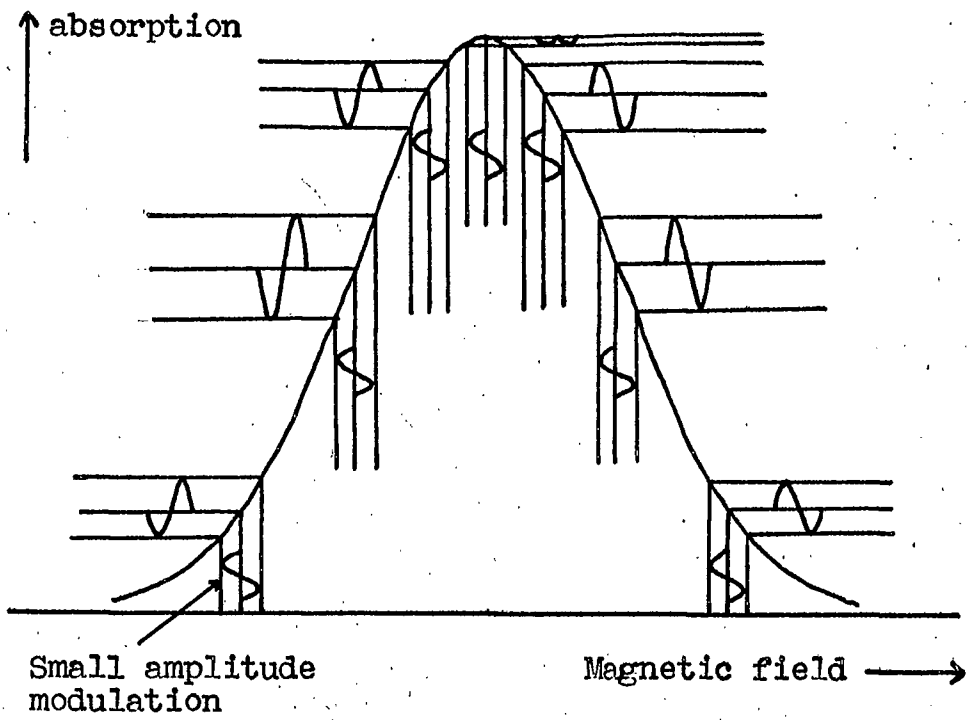
Figure 6.

Incremental absorption signals
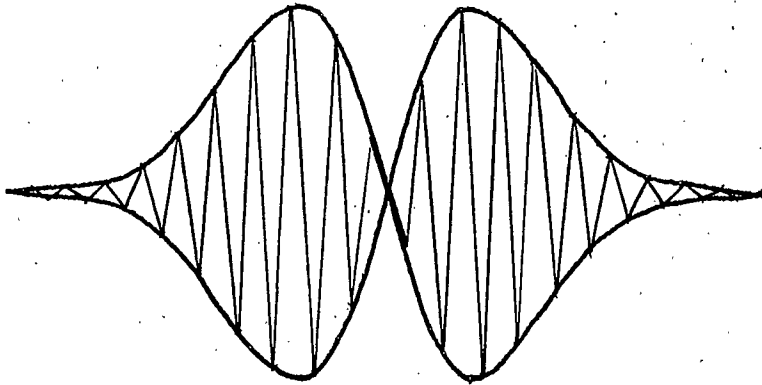
(a) Envelope of the incremental absorption signals
for a complete scan of the line
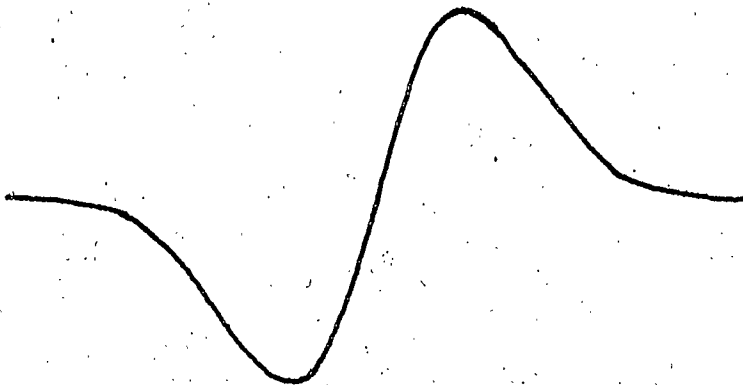
(b) Output from the phase-sensitive detector

Figure 7.

The operation of the synchrodyne receiver, or phase-sensitive

detector, is to accept the signal of figure 7 and to demodulate

it while being conscious of the phase of the input signal. Phase-

sensitive detectors are usually the sampling type; the input

signal is amplitude-sampled once, or perhaps twice, per cycle of

the modulation frequency. The sampling action is derived from a

reference source at the modulation frequency and, as a result,

when the phase of the input signal changes, the detector output

changes sign, as figure 8 shows. Phase-sensitive detection

produces, by virtue of the small-amplitude modulation, the first

derivative of the resonance line shape. There now follows a

description of the sampling operation, together with an

explanation of a typical sampling circuit.

3.5.1 Description of operation

The function of a phase-sensitive

detector is to recover from an alternating signal voltage

$$e_s(t) = E_s(t) \sin \omega t \tag{2}$$

the voltage $E_s(t)$. These waveforms are shown in figure 9.

In this case $E_s(t)$ is sinusoidal, but in the case of a

spectrometer receiver it would be the resonance information from

the paramagnetic specimen. A simple rectifier is unsuitable for

Sampling instants

↓ ↓ ↓ ↓ ↓ ↓ ↓ ↓ ↓ ↓
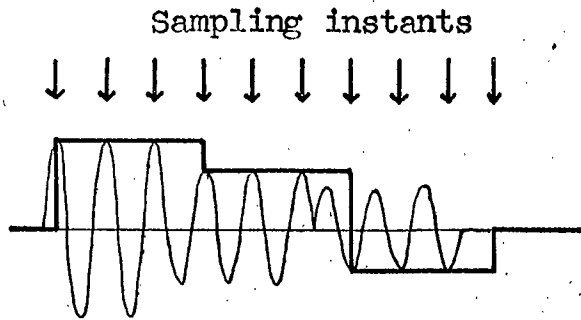
Figure 8.

An illustration of sampling action

$E_s(t)$ $E_s(t).\sin \omega t$
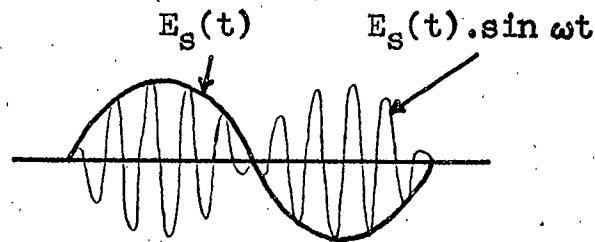
Figure 9.

Input to the phase-sensitive detector
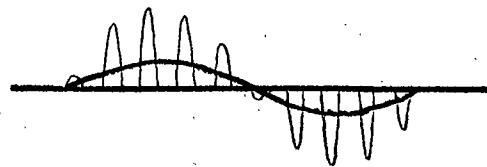
Figure 10.

Output from the phase-sensitive detector

detection because a change of sign of $E_s(t)$ appears as a change

of phase of the waveform of equation (2), as figure 9 shows. A

rectifier circuit which is sensitive to phase is required, and

it must be supplied with a reference voltage

$$e_r(t) = E_r \cdot \sin \omega t \tag{3}$$

against which to compare the phase of $e_s(t)$, and must produce an

output voltage of the correct polarity depending upon that

comparison. The signal voltage is sampled at regular intervals

of time, these intervals being controlled by the reference signal.

It is important to remember that the frequencies of the signal

and reference voltages are identical, and that the circuit

samples the instantaneous amplitude of the incoming signal, the

output changing sign when the input changes phase, as figure 10

shows.

3.5.2 Description of a typical circuit

Phase-sensitive detection is

carried out in practice by storing the result of the sampling

operation in a condenser until the next sampling instant. The

circuit is shown in figure 11. The time constants $C_1 R_1$ are

arranged to be 10 to 100 times the period of the reference

voltage, and $C_2 \ll C_1$ but C_2 must be large enough to store the
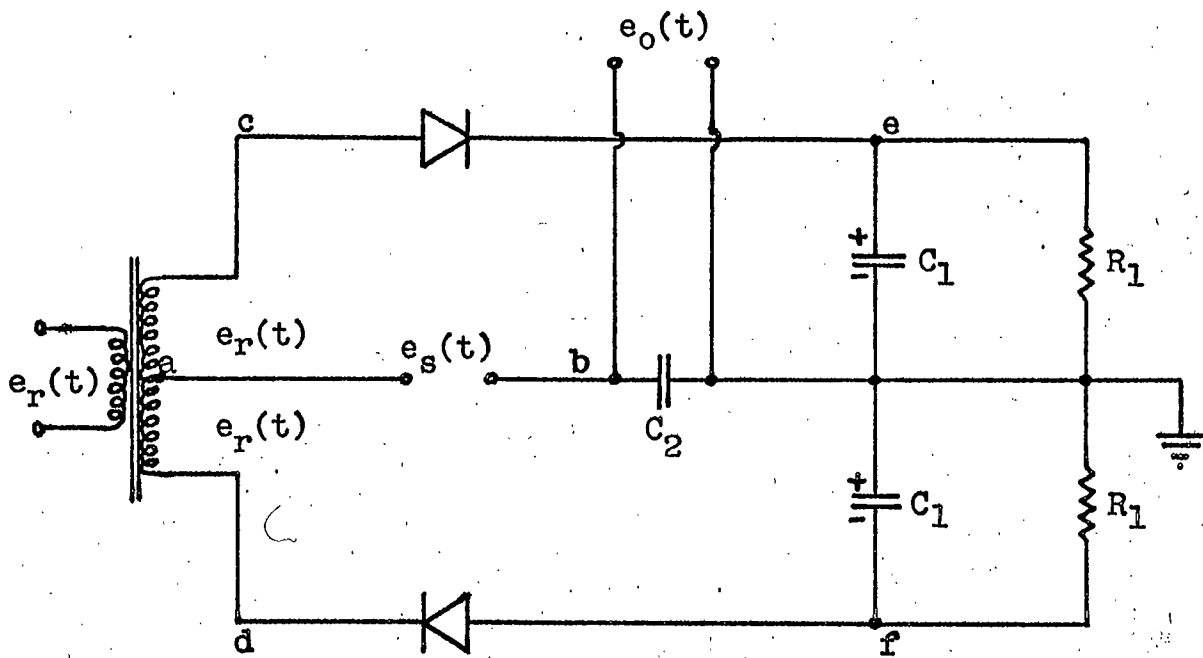
Figure 11.

A phase-sensitive detector circuit

output voltage between sampling instants despite any leakage

through the impedance of the circuit to which the output voltage

is applied.

(a) Suppose $e_s(t)$ and C_2 are removed. When $e_r(t)$ is applied

the two rectifiers will conduct in series once per cycle, and on

the condensers C_1 rectified voltages will build up which, by

symmetry, are equal and of the polarities shown. Each of these

voltages will be nearly equal to E_r of equation (3) because of

the value of $C_1 R_1$. During the conducting instants the rectifiers

have low impedance and the point $\underline{a}$ will be clamped at earth

potential. During the non-conducting periods there will be a

high impedance between $\underline{a}$ and earth, and it can attain any voltage

relative to earth provided that this voltage, added to the

instantaneous voltages developed across the two halves of the

transformer secondary, does not cause either rectifier to conduct.

(b) The signal voltage and C_2 are now replaced. During

conduction instants, $\underline{a}$ is clamped at earth so $\underline{b}$ is forced to

assume a voltage relative to earth equal to the signal voltage at

that instant. Thus a sampled voltage appears across C_2 which

receives an appropriate charge. If the conditions specified above

for non-conducting periods holds, point $\underline{a}$ is disconnected from

earth and there is no leakage path from **b** to earth, so C_2 maintains its charge and the sampled voltage until the next sampling instant. To prevent any unwanted conduction of the rectifiers between sampling instants E_r must be made greater than $E_s(t)$. The sampling instants are very brief, and for C_2 to reach its appropriate charge in such a short time, the signal source must be capable of supplying quite large current pulses.

3.6 Comparison of receivers

Of the three types considered, the crystal-video receiver is by far the simplest. It is also the least sensitive and the most noisy, since its bandwidth extends from DC to the cut-off of the video amplifier, a region where crystal noise is very great (4). Strum (5) gives a detailed account of microwave diode performance which is relevant to this, and is mentioned again in Chapter 4. Large dynamic range cannot be combined with high gain, so a compromise is necessary. The wide RF bandwidth is no asset in spectroscopy. Crystal-video receivers are uasually restricted to spectrum scanning applications for rapid identification of large intensity transitions before switching in a phase-sensitive detector. Only recently has a method been developed (6) which enables spin-lattice

relaxation to be observed on a crystal-video system.

The superhet is able to surpass the crystal-video receiver in every aspect. Its sensitivity can be expressed in units of 10^{-12} watt or less, compared with the 10^{-8} watt for the crystal-video receiver. Because the first IF stage accepts only the signals contained in a specific range of frequencies centred on, say, 45 Mc/s, the overall noise of the receiver is very low, since the crystal noise in the 30 to 60 Mc/s region is very low. Noise is further reduced by the response curve of the IF amplifier: when designed for a specific purpose, the amplifier response is shaped to accept the highest useful harmonics present in the sideband spectrum but nothing beyond these. Thus the noise bandwidth has the minimum possible value. The price paid for such good performance is an increased complexity, the provision of a local oscillator being uppermost in this respect. Because frequencies around 45 Mc/s are used as the intermediate frequency, the IF strip can be completely conventional in design and presents no problems. At microwave frequencies, local oscillators can be a big problem and for this reason systems have been evolved to generate the intermediate frequency from the incoming signal without using a separate local

oscillator klystron. Methods by which this has been achieved are described in Chapter 4.

While the superhet is such an efficient and versatile instrument, there is a large field of study in microwave spectroscopy for which it is not as ideally suited as the phase-sensitive detector. Studies of paramagnetic resonance line shapes and line widths are carried out by means of this instrument, as are most of the "static spectrum analysis" experiments, where the spin system under investigation, though slightly disturbed by the observation, is in an equilibrium state. Phase-sensitive detection gives very high sensitivity and very narrow bandwidth. The direct result of this is a very low output noise level and a relatively long response time — typically of the order of 5 seconds for a simple pen-recorder output. The experimental worker must not accept phase-sensitive detection as a universal tool for studying line shapes and intensities because the accuracy of the results obtained depends critically upon the magnetic field modulation amplitude. The smaller this amplitude is the more accurate the results will be, and it has been found (7) that for a true line shape to be obtained, the modulation amplitude must not exceed one-tenth of

the line width. Broadening of the line produced by excessive
modulation amplitude is approximately equal to the modulation
frequency. Modulation coils producing this AC magnetic field are
usually placed outside the waveguide or cavity containing the
specimen, and to avoid the metal acting as a screen to the field
modulation, care must be taken to ensure that the thickness of
the metal is less than the skin depth at the modulation frequency.

Chapter 4

The Spectrometer - 2. The Single-Klystron Superheterodyne Receiver

4.1 The need for superheterodyne reception

Two types of receiver had been in use in this laboratory - a simple crystal-video type and a much more elaborate 160 kc/s synchrodyne system. A colleague was beginning to measure spin-lattice relaxation times by the pulse saturation method (1) and the question arose as to the type of receiver which would be used. The synchrodyne was immediately ruled out because the requirement was for a receiver giving a voltage output which was directly proportional at all times to the microwave power level at the input. The choice lay between the crystal-video receiver and the superhet. For the reasons given in Chapter 3 the superhet is the better choice but it requires far greater waveguide and circuit complexity. However, sensitivity was not the prime consideration here; linearity between input and output signals was most important. The superhet is a linear receiver, the crystal-video system being linear only over a very small range of power up to about 100 μW, depending upon the characteristics of the microwave diode in use. For accurate measurements a superhet was the only choice.

4.2 Development of the single-klystron superhet

Microwave superhets fall into two categories - those using a klystron as a local oscillator, and those deriving a local oscillator signal from the monitor klystron of the spectrometer. The first type is referred to as the conventional superhet since it is a direct microwave analogue of the common radio receiver and at frequencies up to about 9 Gc/s it is the most widely used type of superhet. Some difficulty arises over the provision of a local oscillator signal which must be maintained at a constant frequency separation from the monitor klystron frequency. This separation is usually about 45 Mc/s and is such a small fraction of the incoming microwave frequency that stabilisation circuits must be used on both klystrons for efficient operation. Klystron automatic frequency control (AFC) is usually effected by a Pound stabiliser (2), the klystron being locked to the frequency of a reference cavity of high Q. Such circuitry can be easily provided up to 9 Gc/s, but for klystrons operating at 35 Gc/s and higher, the use of a Pound stabiliser becomes increasingly difficult.

To overcome the need for a local oscillator klystron it was decided to develop a single-klystron

superhet where a signal fulfilling the functions of a true local
oscillator is derived from the spectrometer klystron. The origins
of this type of superhet are not well documented; Misra (3) in
1958 used this principle in a dual-channel 9.3 Gc/s spectrometer.
This appears to be the first description of a single-klystron
superheterodyne spectrometer.

4.2.1 Requirements for a local oscillator signal

The criteria for a local oscillator
signal are that it should remain at a fixed frequency separation
from the incoming carrier and that it should be more powerful than
this signal. These are the only requirements provided that the
first detector (or mixer) has an efficiency of 100%. The effect
of a non-ideal mixer is discussed later. In microwave spectroscopy
the overall signal strength at the mixer is usually much less
than 10 μW and the percentage modulation of this signal, produced
by the paramagnetic resonance, is less than 10%. Under these
conditions the sideband power is less than 0.1 μW (4). Thus the
local oscillator power necessary to produce undistorted signals
at the intermediate frequency is very small.

4.2.2 Generation of the local oscillator signal

If a radio-frequency carrier of

frequency f_c is amplitude modulated at a frequency f_s, the

resultant signal is equivalent to three discrete frequencies,

$f_c - f_s$, f_c, $f_c + f_s$, known as the lower sideband, carrier and

upper sideband, respectively. With 100% modulation the power in

each sideband is one quarter of the power in the carrier. If f_s

were equal to the intermediate frequency of a receiver, the two

sidebands would act as a local oscillator for the carrier and the

output from the mixer would be f_s. The mathematics of mixer

operation is given in sections 4.9 and 4.10. In the case so far

considered the signal in the IF amplifier is an unmodulated

carrier of frequency f_s. Suppose the amplitude modulated wave

represented by f_c, $f_c \pm f_s$, were propagated along a waveguide to

a paramagnetic specimen under AC resonance conditions. (This term

will be used to describe the following situation: the specimen is

assumed to be resonant at a microwave frequency f_c and at a DC

magnetic field H_o; the DC field has a small-amplitude AC field

superimposed on it which is just large enough to scan the resonance

line completely). If the resonance has a frequency width less than

$2f_s$ then the two sidebands will be reflected unchanged from the

specimen. The reflected carrier, however, will be amplitude-

modulated by a non-sinusoidal periodic function produced by the

AC resonance. This means that the reflected signal has more sidebands than the incident signal, and these sidebands occupy two bands of frequencies which are symmetrical about f_c and whose widths are determined by the number of Fourier components of the non-sinusoidal resonance information. The total frequency spectrum reflected from the specimen is shown in figure 1. If this spectrum is incident on the mixer input to an IF amplifier, the signal passing through the amplifier would be a carrier wave of frequency f_s amplitude-modulated by the resonance information, this spectrum being shown in figure 2. On reaching the second detector the resonance information is separated from the carrier and can be amplified, if necessary, by a broad-band video amplifier.

To operate a single-klystron superheterodyne spectrometer all that is needed is the generation of two sidebands to act as local oscillator signal. There are a number of ways of doing this, for example:

modulation of a travelling-wave tube;

modulation of a klystron amplifier;

modulation of a klystron oscillator;

use of a microwave diode as modulator.

At 35 Gc/s the microwave diode is the only practicable solution,
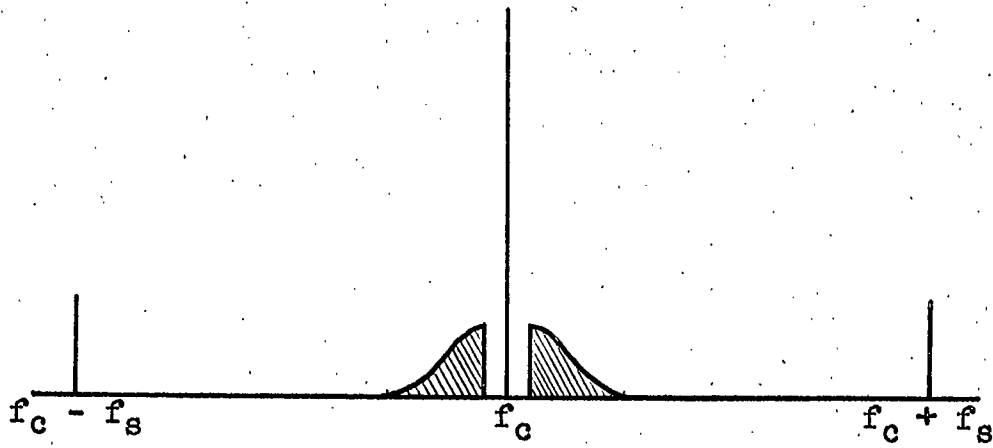
Figure 1.

Frequency spectrum incident on the mixer
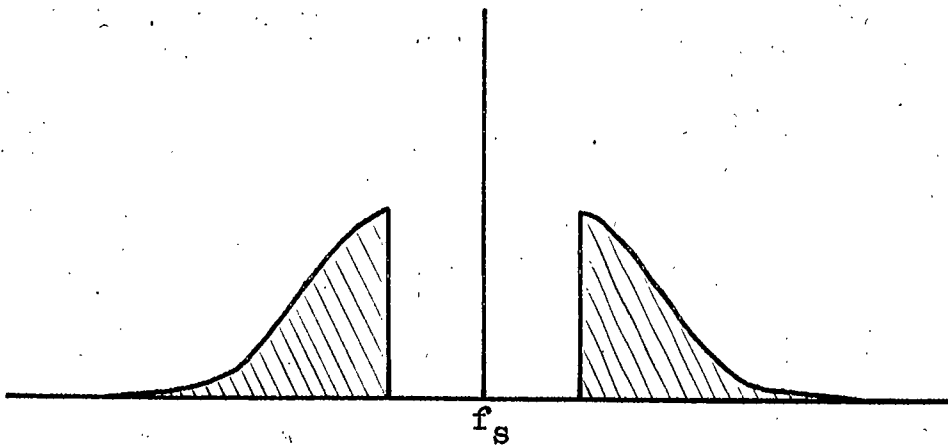
Figure 2.

Spectrum of the IF signal

travelling-wave tubes being very expensive at this frequency.
A superheterodyne spectrometer utilising a transmission crystal
modulator was the subject of a paper by myself, D.R. Mason and
J.S. Thorp, published in the Journal of Scientific Instruments in
1965 (5). A brief description follows based upon the ideas already
introduced in this chapter.

4.3 Practical details of the receiver

Figure 3 shows the overall design
of the spectrometer and receiver. The transmission crystal
modulator consists of a microwave diode mounted perpendicular to
the broad faces of the waveguide and driven at 45 Mc/s from the
output of an Advance RF signal generator delivering 1 volt RMS at
an impedance of 75 ohms. Other source impedances were tried but the
75 ohm value appeared to be the optimum. For the sake of clarity
it will be assumed that the only frequencies propagated in the
waveguide following the modulator are the 35 Gc/s carrier and the
two (35 ± 0.045) Gc/s sidebands. This is a simplification, as is
shown later, but it does not affect the principle of operation.
A 3 dB directional coupler divides the RF power into two parts:
the first is used to power the spectrometer; the second is used
as local oscillator signal, going via an attenuator to the balanced
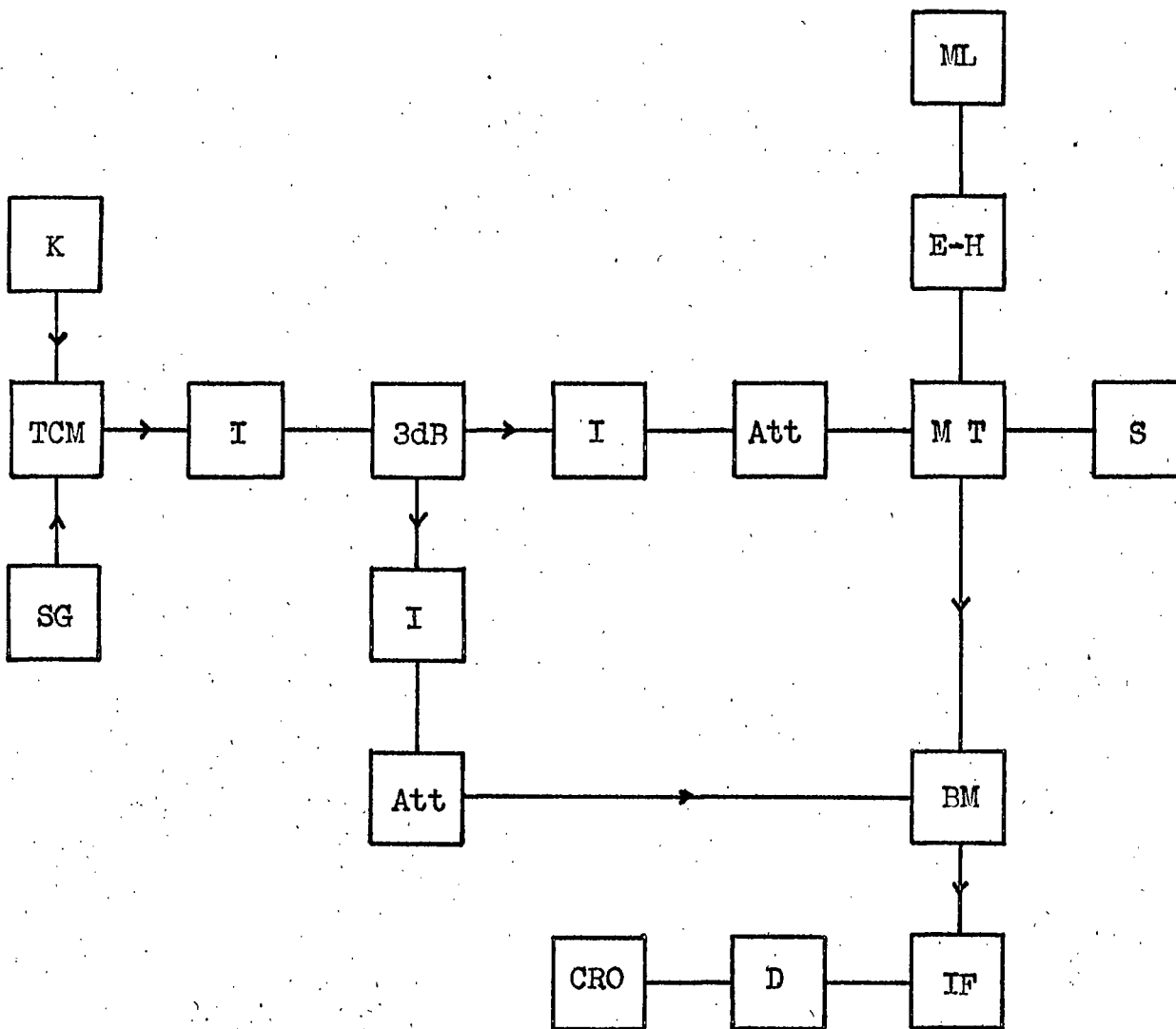
Figure 3.

The single-klystron superheterodyne spectrometer

mixer. Resonance information appears at the magic T output of
the microwave bridge and is fed directly to the balanced mixer.
The non-linearity of the diodes in the mixer produces an output
to the IF amplifier of the resonance information as sidebands
centred on a 45 Mc/s carrier in the manner discussed in section 4.2.2.
There is one marked difference from the earlier description:
power is extracted from the main waveguide run to act as local
oscillator signal instead of using the unchanged sidebands
reflected from the specimen. This is done for the following reasons:

(a) Versatility. Having a greater local oscillator power
available gives an increase in the useful range of input signal
levels which can be efficiently frequency-changed.

(b) Efficiency. The balanced mixer requires two inputs, and
the local oscillator input should be quite independent of changes
in the spectrometer. To achieve this the local oscillator power
is taken from the main waveguide run before it reaches the
spectrometer.

(c) Intermodulation. The sum and difference frequencies
generated by the local oscillator sidebands beating with their
own carrier (giving frequencies $2f_c - f_s$ and f_s, for example) are
of low intensity if the depth of modulation of f_c by f_s is small (6).

The transmission crystal modulator produces an estimated 1% modulation and hence the intermodulation product, f_s, which the superhet accepts, is of very low intensity. This intensity can be greatly increased by mixing the incoming signal to the balanced mixer with the local oscillator signal removed directly after the modulator.

Theoretically it is undesirable to have more than one frequency incident on the paramagnetic specimen; however, if the resonance linewidth is less than twice the intermediate frequency, this should not matter in practice. In the case of ruby the overall linewidth is about 90 Mc/s but the power in the (35 ± 0.045) Gc/s sidebands is so small that no traces of line broadening or splitting have been observed. If a cavity were used on the spectrometer, a loaded Q of about 1000 would be sufficient to prevent the sidebands reaching the specimen.

4.4 Spectrometer performance

This receiver has been in continous operation for $2\frac{1}{2}$ years and it has proved stable, sensitive and trouble-free. The IF amplifier which was used had been designed for conventional two-klystron operation and consisted of an 11-stage stagger-tuned circuit with a passband of 10 Mc/s centred on 45 Mc/s.

For use with this single-klystron spectrometer the stages were re-trimmed to improve the overall response without introducing instability. When this had been done the response curve had a satisfactory shape with a passband of 2.6 Mc/s centred on 44.5 Mc/s. The increase in gain and in signal-to-noise ratio fully justified the operation.

When used with the pulse saturation method for measuring spin-lattice relaxation time the superhet design has proved ideal. Operation of the complete spectrometer, shown in figure 4, has already been described (7) and is extremely simple. The only aid to frequency stability of the klystron is provided by an oil bath in which the klystron is immersed. A gating and suppression circuit was built to key off the superhet during the saturating pulses. This is a necessity in conventional superhets where a pulse of about 1 watt can damage a receiver adjusted to accept signals of 10^{-12} watt. The single-klystron receiver did not require keying off at all and the suppression circuits were found to be unnecessary. This feature is due entirely to the level of the local oscillator signal. As was stated in section 4.2.1 the local oscillator must be more powerful than the incoming signal. This ensures that the modulated wave being
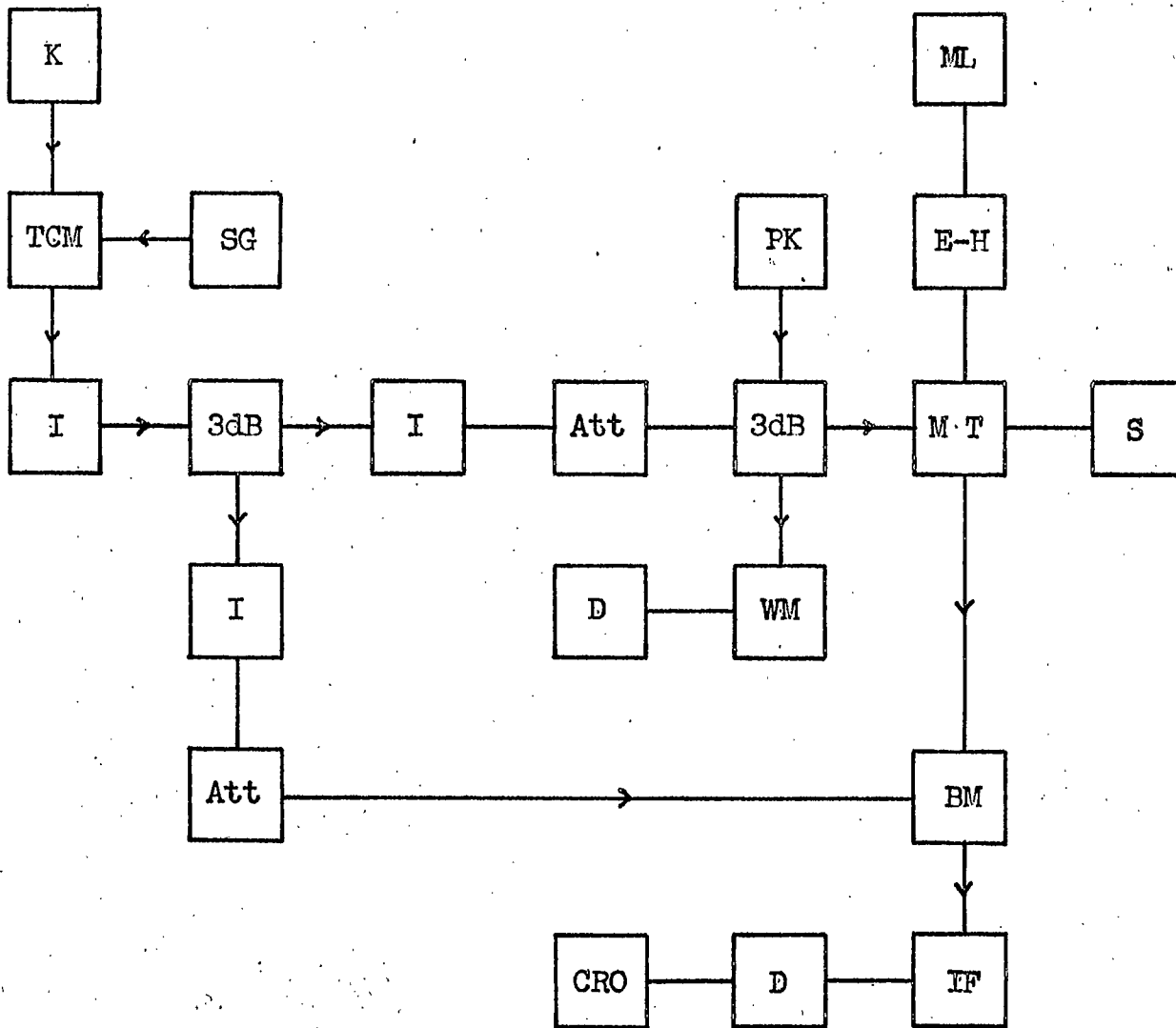
Figure 4.

The complete pulse saturation spectrometer

amplified by the IF strip is an accurate replica of the incident microwave signal. The mathematics given in sections 4.9 and 4.10 shows that the magnitude of the IF signal is directly proportional to both the incoming signal voltage and the local oscillator voltage. While being true when these voltages are of the same order, this is not a universal proportionality. For example, the mathematics would give the same magnitude of IF signal for incoming signal and local oscillator voltages of 10 and 12 as it would for 0.5 and 240, and in practice this is not true. When one voltage is very much less than the other, virtually no mixing takes place; this is mainly due to the fact that the larger component biases the mixer diodes so hard that they do not act as true mixers at all. In conventional superhets the local oscillator signal is usually many orders of magnitude larger than it is here, so that some mixing does occur during the RF pulses and the IF output is sufficient to overload the later stages of the amplifier, thus necessitating the use of an IF suppression circuit.

The stability of the intermediate frequency is independent of the stability of the monitor klystron and is determined entirely by the stability of the 45 Mc/s signal

generator. Because the local oscillator signal is derived from
the monitor klystron, the local oscillator is automatically
self-tracking, that is it follows any frequency changes of the
monitor klystron. It is interesting to compare this design with
a conventional superheterodyne spectrometer incorporating a
self-tracking local oscillator klystron, such as that described
by Holton and Blum (8).

4.5 Mixer and intermediate frequency considerations

So far only theoretical arguments
have been proposed to define a minimum acceptable local
oscillator power level, assuming a 100% efficiency for the mixer.
In practical terms, a "mixer" comprises a mounting block with a
flange for waveguide connection, and a removable crystal cartridge
as described in Chapter 3. To the experimental worker who
purchases, say, a balanced mixer, the only variable over which
he has any control is the type of mixer crystal, because the
matching and balancing of the mixer block are normally optimised
by the manufacturers.

4.5.1 Important mixer crystal parameters

(a) Noise temperature. This is defined as the ratio of the
noise power available from a given network (e.g. the mixer diode)

to that available from an equivalent resistor at room temperature. The noise temperature of a mixer crystal is never less than unity; this would imply that there was no excess noise developed in the crystal itself and the noise power available would only be the Johnson noise associated with the IF input admittance. Noise temperature varies with the intermediate frequency at which it is measured, being lower at high IF's than at low IF's. This variation is as $(\text{frequency})^{-1}$. DC bias affects the noise temperature also, a reverse bias raising the noise temperature. Because of this it is advisable to maintain low resistance DC paths for the crystal current.

(b) Conversion loss. Defined as the ratio of the input RF power to the output IF power, it is critically dependent upon aspects of the mixer block design, upon the DC bias to the crystal and upon the local oscillator power level. The effect of a small forward bias is to make the conversion loss at a reduced local oscillator power level almost as small as that at the normal level. Under these conditions the conversion loss/local oscillator drive variation is much reduced. Strum (9) gives details of the conversion loss as a function of the crystal current produced by local oscillator drive. The minimum loss is created by crystal currents

of about 0.5 mA. When the mixer is used in conjunction with an
IF amplifier, as in the spectrometer, further noise considerations
are necessary.

4.5.2   IF amplifier noise

The excess noise of an IF amplifier
using a given type of valve increases approximately linearly with
frequency (10).

The two over-riding parameters
from the preceding discussion are crystal noise and IF amplifier
noise, the first depending upon (frequency)$^{-1}$ and the second upon
frequency directly. The overall excess noise curves are given in
reference (9) and quoted by Ingram (11). Minimum noise lies in the
region from 20 to 60 Mc/s approximately. The commonest intermediate
frequencies for microwave spectroscopy are 30 and 45 Mc/s.

4.6   Criticisms of the spectrometer

Buckmaster and Dering (12) have
criticised this design in detail but from a very dubious standpoint
in certain places. Each point is covered in the following discussion.

(i) Degradation of the noise figure.

Buckmaster and Dering (referred to
as BD in this discussion) quote a figure of 13 dB as being the

ratio of the bridge balance information at zero IF to that at

45 Mc/s. Certainly this is true, but BD admit that such

synchronous demodulation at the microwave frequency (producing a

DC output) is a very insensitive detection method because of the

high flicker noise of diodes at near-zero frequencies. If

superheterodyne detection is to be used to overcome the noise

problem then this factor of -13 dB is automatically incurred,

irrespective of the type of superhet used. This figure of 13 dB

does not arise from the presence of "extraneous signals". The

balanced mixer derives its bias almost completely from the

microwave carrier component of the local oscillator signal,

i.e., at a frequency of 35 Gc/s. In a conventional superhet the

0.5 mA current bias mentioned in section 4.5.1 is derived from

the local oscillator at a frequency of 35.045 Gc/s. BD state

that this biasing, by not taking place at the true local

oscillator frequency, also degrades the noise figure. It seems

unlikely that the noise figure would be sensitive to a 0.13%

change in microwave frequency, as this statement implies. As is

shown in Chapter 3, the phase-sensitive detector or synchrodyne

demodulator can have far greater sensitivity than the superhet

because its bandwidth is extremely narrow and its response time

correspondingly slower. BD, in their quest for ultimate

sensitivity (13), (14), appear to have overlooked the fact that

a sensitive superheterodyne spectrometer specifically designed

for pulse saturation measurements is not the most sensitive

spectrometer for detecting paramagnetic resonance. This is shown

in their third paragraph where they introduce magnetic field

modulation at a frequency f and suggest that a noise figure

improvement of 13 dB could be obtained by using synchronous

demodulation at the microwave frequency followed by amplification

and further synchronous demodulation at a frequency f. Quite so,

but the superhet is no longer usable to measure relaxation times.

(ii) Inherent instability.

The sidebands in the reflected signal

from the microwave bridge do mix with the carrier present in the

local oscillator signal to give an unmodulated output at the

intermediate frequency but adverse effects due to this are overcome

by careful adjustment of the microwave bridge and local oscillator

level. A suppressed-carrier local oscillator system has since

been developed to overcome this problem and is described in

section 4.12. BD again reveal their misunderstanding of the system

in this same paragraph when they explain that the effect of a

swamping carrier in the IF amplifier can be removed by
unbalancing the synchronous demodulator following the amplifier.
This shows direct confusion between the system we describe and
the hypothetical double-synchronous-demodulation system which
they introduce in their third paragraph.

It is interesting to note that most
superhet spectrometers use a balanced mixer and 45 Mc/s IF
amplifier, and if some form of synchrodyne receiver is to be used
as well (in conjunction with small-amplitude magnetic field
modulation at a frequency f), the synchronous demodulator at f is
connected to the output from the superhet second detector.
According to paragraphs two and three of BD a noise figure
degradation of at least 13 dB will be incurred. The most recent
paper on this particular type of dual-purpose spectrometer is by
Patankar (15), who also presents some semi-quantitative information
on noise in single-klystron systems, showing that his system's
sensitivity is very close to the theoretical value given by
Feher (16) and attributes the discrepancy to the poor noise
figures of the mixer crystals, and not to two successive stages
of frequency changing incurring 13 dB of noise figure degradation.

A short letter by myself, D.R. Mason

and J.S. Thorp was published (17) to point out some of the
fallacies in the argument of Buckmaster and Dering.

4.7 Possibilities of extending the principle to
70 Gc/s

The attractions of a single-klystron
system lie in the low powers needed, the extremely high IF
stability, and the need for only one klystron instead of two.
The principle becomes increasingly attractive as the microwave
frequency is increased. A single-klystron superhet spectrometer
has been designed and operated at 70 Gc/s, the only microwave
source being a 30 mW reflex klystron operating at 35 Gc/s. This
design is described in Chapter 6.

4.8 Survey of superheterodyne spectrometers

Though descriptions of the major
superhet spectrometers were thought to be superfluous to this
chapter, references (19) to (32) are included in order to collate
the sources of some very interesting superhet designs, developed
since England and Schneider (18) described the first in 1950.

4.9 Low-level conversion theory for point-contact
diodes

Having discussed the action of the

superhet it is now useful to see how the microwave diode works
in its various roles. The simplest operation it performs is that
of low-level detection (demodulation) of an amplitude modulated
RF wave.

It is well known that the
characteristic of a point-contact diode can be represented, over
a small range near the origin, by a Taylor series ending at the
squared term:

$$I = I_o + \left[\frac{dI}{dE}\right]_o (E - E_o) + \frac{1}{2}\left[\frac{d^2I}{dE^2}\right]_o (E - E_o)^2 \quad . \quad (1)$$

At the moment the magnitudes of the coefficients are unimportant
and the equation is thus simplified to:

$$I = I_o + K_1(E - E_o) + K_2(E - E_o)^2 \quad . \quad (2)$$

Suppose an amplitude modulated wave given by:

$$E = E_o + C(1 + k.\sin \omega_s t).\sin \omega_c t \quad (3)$$

is incident on the diode. E_o and I_o specify the DC operating
point. C is the carrier amplitude and ω_c its angular frequency;
k is the modulation factor and ω_s the modulation angular
frequency. Equation (3) can be expanded into:

$$E - E_o = C(\sin \omega_c t + (k/2).\cos(\omega_c - \omega_s)t - (k/2).\cos(\omega_c + \omega_s)t), (4)$$

which shows the equivalence to a carrier and two symmetrical

sidebands. Equation (4) is now substituted into equation (2) and,

using the common trigonometrical identities, becomes:

$$I = I_o + K_1 C(\sin \omega_c t + (k/2).\cos(\omega_c - \omega_s)t - (k/2).\cos(\omega_c + \omega_s)t)$$

$$+ K_2 C^2 \left[\begin{array}{l} 1/2 + (k^2/4) - (1/2 + k^2/4).\cos 2\omega_c t \\[2ex] -(k^2/4).\cos 2\omega_s t \\[2ex] +(k^2/8)(\cos(2\omega_c + 2\omega_s)t + \cos(2\omega_c - 2\omega_s)t) \\[2ex] +(k/2)(\sin(2\omega_c - \omega_s)t + \sin(2\omega_c + \omega_s)t) \\[2ex] +k.\sin \omega_s t \end{array} \right]. \quad (5)$$

It is the squared term in equation (2) which is responsible for

the actual conversion operation. Three frequencies are incident;

squaring these individually produces the harmonic terms in

$2\omega_c$, $(2\omega_c \pm 2\omega_s)$. It is the cross-product terms produced in

squaring which give rise to the other terms, and this is the true

conversion process. The following distinction is stressed here

as it occurs frequently in the mathematical analyses:

harmonic generation is produced by the incident frequencies

being raised to a power n, n being the harmonic number;

conversion and mixing are results of the cross-product terms between the input frequencies.

Thus, by making the input to the amplifier following the diode frequency-selective, any one of the terms in equation (5) can be amplified, the other terms being filtered out. For operation as a simple detector for the amplitude modulated RF input, the signal output from the diode would be

$$K_2 c^2 k. \sin \omega_s t.$$

4.10 Amplitude modulation using a microwave diode

A statement can usually be found in a microwave textbook to the effect that if three frequencies and a non-linear element are given, any two of these frequencies can be combined to give the third frequency (33). Mathematically this is easy to confirm, but exactly how it happens in practice is often a very complex problem. Chapter 3 has already shown the basic principle by which a microwave diode could act as a voltage-controlled attenuator (modulator) and has shown that the modulation efficiency is only good for very low incident power. However, the transmission crystal modulator of section 4.3 operates with the full klystron power incident on it; the modulation efficiency is very low but does not increase if the klystron power is reduced,

so that the process of modulation must be different under 45 Mc/s
drive from that at DC.

A microwave diode, under self-bias
conditions due to a microwave field, assumes a reverse bias so
that the instantaneous operating point lies for some 90% of the
time in the reverse region of the characteristic (34). Thus it
is reasonable to assume that it is the reverse characteristic
which is dominant in the modulation process. The DC characteristic
of the diode used in the modulator is shown in figure 5.
Measurements made on the reverse portion showed that its shape
was almost a true exponential function, and its equation was
derived, postulating an arbitrary operating point of
(-5 volts, -9.6 mA), and is given by:

$$I = 9.6 \times 10^{-3} . \exp\left[-\frac{(5 - V)}{1.47} \right] \qquad . \quad (6)$$

This can be simplified to:

$$I = I_p . \exp(-q(V_p - V)), \qquad (7)$$

where $I_p = 9.6$ mA, $V_p = 5$ volts and $q = 0.68$ (volt)$^{-1}$.
Using the series expansion for an exponential function, this becomes:

$$I = I_p(1 - q(V_p - V)+(q^2/2)(V_p - V)^2 - (q^3/6)(V_p - V)^3 \ldots). \quad (8)$$
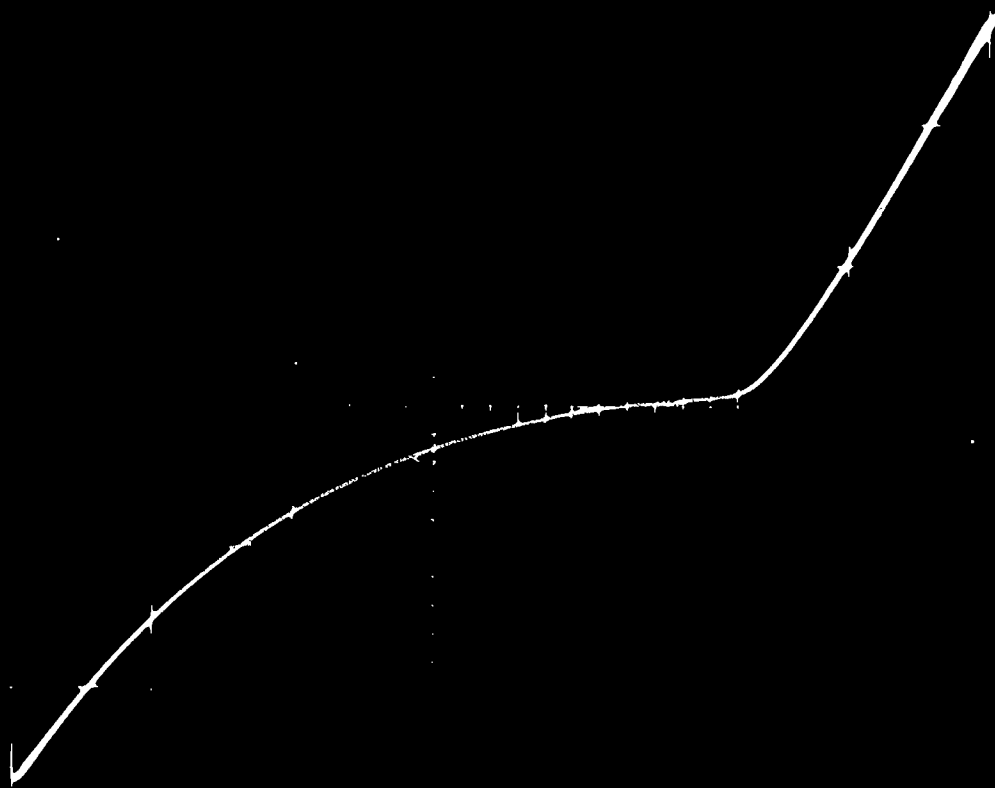
Figure 5.

Characteristics of the modulator diode

X axis: 1 volt per division

Y axis: 4 mA per division

The diode is subject to two sinusoidal frequencies, $V_c \sin \omega_c t$ as the microwave field and $V_s \sin \omega_s t$ as the 45 Mc/s modulation signal. The resultant signal is therefore:

$$V = V_p + V_c \sin \omega_c t + V_s \sin \omega_s t \qquad . \quad (9)$$

This voltage is time-symmetrical about V_p, so that $(V - V_p)$ of equation (9) can be substituted fo $(V_p - V)$ of equation (8) without any changes of sign. As yet, no assumptions can be made as to where the expansion can be truncated. (Observations in Chapter 6 show that it cannot be truncated below the fourth power term). Substituting equation (9) into equation (8) gives, after simplification and rearrangement, the equation (10) shown on the next page. Only the asterisked frequencies are propagated down the waveguide. The terms used for operation of the single-klystron superhet are A and E; the terms H are just detectable – the terms I are not. As a result, the spectrometer and superhet are virtually unaffected by the many modulation products of the transmission crystal modulator. Harmonic terms of ω_c are dealt with in Chapter 6.

This treatment is not a variant of the usual high-level conversion mathematics (35) which assumes

$$I = I_p \begin{bmatrix} 1+q^2V_c^2/4+q^2V_s^2/4+q^4V_c^4/64+q^4V_c^2V_s^2/16+q^2V_s^4/64 \\[2mm] -(qV_c+q^3V_c^3/8+q^3V_cV_s^2/4)\cdot\sin\,\omega_c t \qquad\qquad * \\[2mm] -(q^2V_c^2/4+q^4V_c^4/48+q^4V_c^2V_s^2/16\cdot\cos\,2\omega_c t \qquad * \\[2mm] +(q^3V_c^3/24)\cdot\sin\,3\omega_c t \qquad\qquad * \\[2mm] +(q^4V_c^4/192)\cdot\cos\,4\omega_c t \qquad\qquad * \\[2mm] -(qV_s+q^3V_s^3/8+q^3V_c^2V_s/4)\cdot\sin\,\omega_s t \\[2mm] -(q^2V_s^2/4+q^4V_s^4/48+q^4V_c^2V_s^2/16)\cdot\cos\,2\omega_s t \\[2mm] +(q^3V_s^3/24)\cdot\sin\,3\omega_s t \\[2mm] +(q^4V_s^4/192)\cdot\cos\,4\omega_s t \\[2mm] +(q^2V_cV_s/2+q^4V_c^3V_s/16+q^4V_cV_s^3/16)(\cos(\omega_c-\omega_s)t-\cos(\omega_c+\omega_s)t) \\[2mm] +(q^3V_c^2V_s/8)(\sin(2\omega_c+\omega_s)t-\sin(2\omega_c-\omega_s)t) \qquad * \\[2mm] +(q^4V_c^3V_s/48)(\cos(3\omega_c+\omega_s)t-\cos(3\omega_c-\omega_s)t) \qquad * \\[2mm] +(q^3V_cV_s^2/8)(\sin(\omega_c+2\omega_s)t+\sin(\omega_c-2\omega_s)t) \qquad * \\[2mm] +(q^4V_cV_s^3/48)(\cos(\omega_c+3\omega_s)t-\cos(\omega_c-3\omega_s)t) \qquad * \\[2mm] +(q^4V_c^2V_s^2/32)(\cos(2\omega_c+2\omega_s)t+\cos(2\omega_c-2\omega_s)t) \qquad * \end{bmatrix} \begin{matrix} \\ A \\ B \\ C \\ D \\ \\ \\ \\ \\ *E \\ F \\ G \\ H \\ I \\ J \end{matrix}$$

Equation (10)

true zero-bias operation where the forward and reverse

characteristics are equally important. This attempt to bring

the theory to fit the experimental conditions goes further than

the average textbook, but is no nearer being an exact description

of the modulation process.

Notice that the coefficients of

terms in ω_c and ω_s, $2\omega_c$ and $2\omega_s$, $\omega_c \pm 2\omega_s$ and $2\omega_c \pm \omega_s$,

etc., are all symmetrical in their constants, q's, V_c's and V_s's,

and this shows up where the interpretation fails. Because of this

symmetry it could be expected that the ratio of the amplitudes

of ω_c to $2\omega_c$ would be the same as the ratio of the amplitudes

of ω_s to $2\omega_s$ if V_c and V_s were made equal. This is not the case

by any means. Using an audio frequency analyser to examine the

voltage across the microwave diode, for a 400 c/s sine wave input,

showed a loss of 15 dB to the second harmonic and 24 dB to the

third harmonic. This contrasts with typical figures obtained

from microwave diode harmonic generators (36) of 21dB to the

second and 40 dB to the third harmonic of the microwave frequency.

The explanation of this must be that the diode presents a totally

different characteristic to the microwave frequency from that

which it presents to the modulating frequency, and no mathematical

approach can be satisfactory if both signals are applied to the
same equation for the characteristic.

No quantitative data can be given
even on the relative magnitudes of the coefficients in equation (10)
because all the detection systems available in the laboratory
utilise a microwave diode and this would mix all the components
of equation (10) still further, introducing more coefficients
due to its own particular characteristic. A microwave spectrum
analyser would be able to evaluate the conversion loss to the
various harmonics of ω_c and perhaps give some indication of the
diode characteristic as seen by the microwave field.

4.11   The balanced mixer and its performance in
this superhet

Superheterodyne receivers use
balanced mixers because (a) the local oscillator can be very
loosely coupled to the signal;

(b) no local oscillator power is radiated
into the signal arm, and

(c) local oscillator noise is balanced
out. These points are explained in Chapter 3 and in section 4.12.

When a balanced mixer is operated

under optimum conditions (section 4.5) the local oscillator

signal is large and the mixer diodes are switched from ON to OFF

by this. The diode resistance, plotted as a function of time,

becomes a square wave of frequency equal to the local oscillator

frequency and thus contains only odd harmonics of the fundamental

(37) and can be written:

$$P(t) = h_0 + h_1 (\cos \omega t - (1/3).\cos 3\omega t + (1/5).\cos 5\omega t \ldots) \quad . \quad (11)$$

The local oscillator signal in the single-klystron receiver has

most of its power at the signal frequency ω_c and if the

frequencies ω_c, $\omega_c \pm \omega_s$ are applied to a switched mixer acting

at ω_c, there is an output at ω_s, ω_c, $2\omega_c$, and sum and

difference frequencies but no distortion terms, i.e. no harmonics

of ω_s. This contrasts with the low-level conversion case of

equation (5) where a term in $2\omega_s$ appears and is down by a factor

of only $k/4$ on the fundamental.

It would be simple to accept the

normal switching idea for the operation of the balanced mixer

here and not consider the fact that the mixer crystals could be

working in their square-law region. There are two ways of testing

which method is operating: (a) if mixer output signals are

present at $2\omega_s$ then the square-law action must be operative;

(b) if the carrier is suppressed
from the local oscillator signal and no change for the worse is
observed, again the square-law action must be operative. Both of
these tests have been tried; both give the same result. The
modulator was driven at 22.5 Mc/s and an output from the mixer
at 45 Mc/s was just visible above the noise. This could be
produced by distortion in a square-law mixer or by mixing of the
terms H and A (equation (10)) in a linear switching mixer.
However, suppression of the local oscillator carrier effected no
change in performance and this proved that the mixer was operating
in its square-law or low-level conversion state.

4.12   An improvement to the design

The carrier was removed in test (b)
above by careful adjustment of a high-Q wavemeter cavity. A more
elegant method of carrier suppression which also gives more
efficient 45 Mc/s modulation uses a balanced modulator. This
consists (38) essentially of a balanced mixer used in reverse.
The two reversed polarity crystals in the terminated H-plane arms
are driven in parallel from the same 45 Mc/s signal generator.
The microwave carrier enters at the H-plane input and is reflected,
modulated, from the terminations. The two waves approaching the

T-junction are thus:

$$V_1 = K(\sin\omega_c t + (k/2).\cos(\omega_c - \omega_s)t - (k/2).\cos(\omega_c + \omega_s)t)$$

and
$$V_2 = K(\sin\omega_c t - (k/2).\cos(\omega_c - \omega_s)t + (k/2).\cos(\omega_c + \omega_s)t) ,$$

the sideband terms being of different polarity because of the

reversed pair of diodes. At the T-junction the in-phase carrier

components add and leave by the H-plane arm while the out-of-phase

sideband terms add and leave by the E-plane arm. The output

signal is thus:

$$V = Kk.\cos(\omega_c - \omega_s)t - Kk.\cos(\omega_c + \omega_s)t .$$

The transmission crystal modulator

was removed and the balanced modulator inserted into the local

oscillator waveguide immediately after the attenuator. The

improvement in performance is probably due to the increased

sideband power at (35 ± 0.045) Gc/s. Carrier suppression appears

to be about 40 dB and is dependent upon good matching of the

modulator crystals and upon the proximity of the working frequency

to the design frequency of the modulator block.

Because of good isolation of the

H and E-plane inputs to the balanced mixer the coupling of the

local oscillator to the signal is very loose and virtually none

of the local oscillator power can escape from the other input.
Thus the mixer acts as a buffer stage between the spectrometer
and the local oscillator signal. Noise, present in the local
oscillator signal, will reach the crystals in antiphase and beat
with the true local oscillator frequency which is also in
antiphase, producing in-phase IF noise, (39). Because the crystals
are of reversed polarity, these IF noise signals cancel out. This
applies equally to linear and to square-law balanced mixers.

Chapter 5

35 Gc/s Relaxation Time Measurements at Microwatt Power Levels

In Chapter 1 the importance of
relaxation time in electron spin resonance generally, and in
maser materials in particular, was outlined. The commonest
techniques for measuring relaxation time were introduced, together
with details of the microwave frequency used, the power required
and the material investigated by each method. (In the following
discussion the ultrasonic method of Dobrov and Browne (1) will
not be considered since it introduces sound waves as the energy
source that induces electron spin transitions. Only those methods
which use a microwave field to induce the transitions will be
considered). The outstanding feature of these methods (2), (3),
(4), (5), (6), is the microwave power requirement. In each case
this power must be sufficient to saturate the spin system; at
frequencies up to 35 Gc/s this is no problem, but above this the few
valves giving enough power are extremely expensive, and as a result
no direct measurements of spin-lattice relaxation time have been
made above 35 Gc/s. The pulse saturation method of Davis et al. (4)
has become accepted as the standard technique for the measurement
of T_1, but it has the disadvantage of needing three klystrons
in its conventional form and two klystrons if a single-klystron

superhet receiver (7) is used. In the pulse saturation method,
the spin system is completely saturated by a pulse of microwave
energy and the recovery of the system to a state of virtual
thermal equilibrium is observed by the increase in absorption
of a very small microwave signal at the same frequency as the
pulse and derived from a reflex klystron, normally referred to
as the "monitor" klystron.

A method has been developed which
maintains the important advantages of pulse saturation (Chapter 1)
but requires the use of only one low-power reflex klystron. The
basis of the method lies in the simple relaxation theory for a
two-level spin system.

5.1 Theory

Symbols used:

N_1 : population of level 1 at thermal equilibrium;

N_2 : population of level 2 at thermal equilibrium;

n_1 : instantaneous population of level 1;

n_2 : instantaneous population of level 2;

Δn : instantaneous population difference; $(\Delta n = n_1 - n_2)$;

T_1 : spin-lattice relaxation time;

w_{12} : relaxation transition probability from level 1 to 2;

W_{12} : stimulated transition probability from level 1 to 2;

ΔN : population difference at thermal equilibrium; $(\Delta N = N_1 - N_2)$.

This notation is that of Siegman (8).

For a two-level system in thermal equilibrium only the relaxation processes are active, and the following rate equations, describing the rates of change of the populations n_1 and n_2, can be written:

$$dn_1/dt = -w_{12} \cdot n_1 + w_{21} \cdot n_2 \quad ,$$
$$ \tag{1}$$
$$dn_2/dt = w_{12} \cdot n_1 - w_{21} \cdot n_2 \quad .$$

In thermal equilibrium, $n_1 = N_1$ and $n_2 = N_2$, therefore by definition:

$$dn_1/dt = dn_2/dt = 0 \quad . \tag{2}$$

By taking the equations (1) and subtracting the second from the first, a single rate equation for the population difference Δn can be written:

$$d\Delta n/dt = dn_1/dt - dn_2/dt = 2(w_{21} \cdot n_2 - w_{12} \cdot n_1)$$

$$= (w_{21} - w_{12})N - (w_{12} + w_{21})\Delta n \quad , \tag{3}$$

The exponential nature of the relaxation process is easier to recognise if equation (3) is rewritten as:

$$\frac{d\Delta n}{dt} = -\frac{(\Delta n - \Delta N)}{T_1} \quad , \tag{4}$$

where T_1 is defined as:

$$T_1 = (w_{12} + w_{21})^{-1} \quad . \tag{5}$$

The solution of equation (4) is:

$$\Delta n(t) = \Delta N + (\Delta n_o - \Delta N) \cdot \exp(-t/T_1) \quad , \tag{6}$$

where Δn_o is the value of Δn at time $t = 0$.

If a microwave signal at the resonance frequency is applied to the system, transitions in both directions will be stimulated by it. The relaxation processes will continue, but a new pair of rate equations must be written:

$$dn_1/dt = -w_{12} \cdot n_1 + w_{21} \cdot n_2 - W_{12} \cdot n_1 + W_{21} \cdot n_2 \qquad ,$$

$$dn_2/dt = w_{12} \cdot n_1 - w_{21} \cdot n_2 + W_{12} \cdot n_1 - W_{21} \cdot n_2 \qquad ,$$

(7)

thus accounting for the stimulated and the relaxation transitions. The important things about the stimulated transition probabilities W_{12} and W_{21} are: (a) they are equal;

(b) they are directly proportional to the incident microwave power.

Subtraction of the equations (7), as before, gives a single rate equation:

$$\frac{d\Delta n}{dt} = -\frac{\Delta n - \Delta N}{T_1} - 2W_{12} \cdot \Delta n \qquad . \qquad (8)$$

This equation can be rearranged into the form:

$$\frac{d\Delta n}{dt} = -\frac{\Delta n - (1 + 2W_{12} \cdot T_1)^{-1} \cdot \Delta N}{(1/T_1 + 2W_{12})^{-1}} \qquad . \qquad (9)$$

By comparison of this equation with equation (4) it can be seen

that the solution of equation (9) is exponential in form and of time constant C given by:

$$C = (1/T_1 + 2W_{12})^{-1} \qquad . \qquad (10)$$

The magnitude of W_{12} at resonance is determined by the incident microwave power level, so that C becomes power-dependent when W_{12} is comparable with $1/T_1$. If the experimental conditions can be arranged such that the microwave power is large enough to produce an accurately measurable power absorption but yet is small enough for W_{12} to be very small compared with $1/T_1$, equation (10) can be simplified to:

$$C = T_1 \qquad . \qquad (11)$$

The accuracy to which a measured value of C gives T_1 depends upon how small W_{12} is compared with $1/T_1$, and an exact determination of the result should be given by measuring C as a function of power and extrapolating to give the value of C at zero power. However, this was not found to be necessary, as is explained later.

Equation (9) is the basis for the new method described here; the manner in which the spin system responds to a low-power microwave pulse is given by this equation provided that the spin-spin relaxation time is very much less

than T_1. This contrasts with the pulse saturation method where it is the recovery of the spin system from a saturating pulse which is observed. This new method will be referred to in the succeeding descriptions as the pulse response technique. A paper describing the technique and its uses, written by myself and J.S. Thorp, is to be published in the British Journal of Applied Physics (9). The spin systems to which this method has been applied have not been of the simple two-level type which this theory covers. However, the examination of multi-level systems by this method involves the same modifications as in the pulse saturation method, i.e., for an n-level spin system there are n - 1 rate equations, leading in turn to n - 1 relaxation times (10). For the 4 level system of the Cr^{3+} ion there are thus three possible relaxation times but in practice the time-constants and the amplitudes of the signals corresponding to these relaxations are such that only the true spin-lattice relaxation is visible. Mason (11) has observed two exponential signals on various occasions using the pulse saturation method; the true spin-lattice relaxation is always the longest time-constant present, and this is the main reason for taking the measurements for T_1 from the "tail" of the displayed curve. In this way all the faster relaxation processes have died

ML

E–H

K   I   3dB   Att   M·T   D

PG

TS   D   DA   DCA

S

PWM   CRO
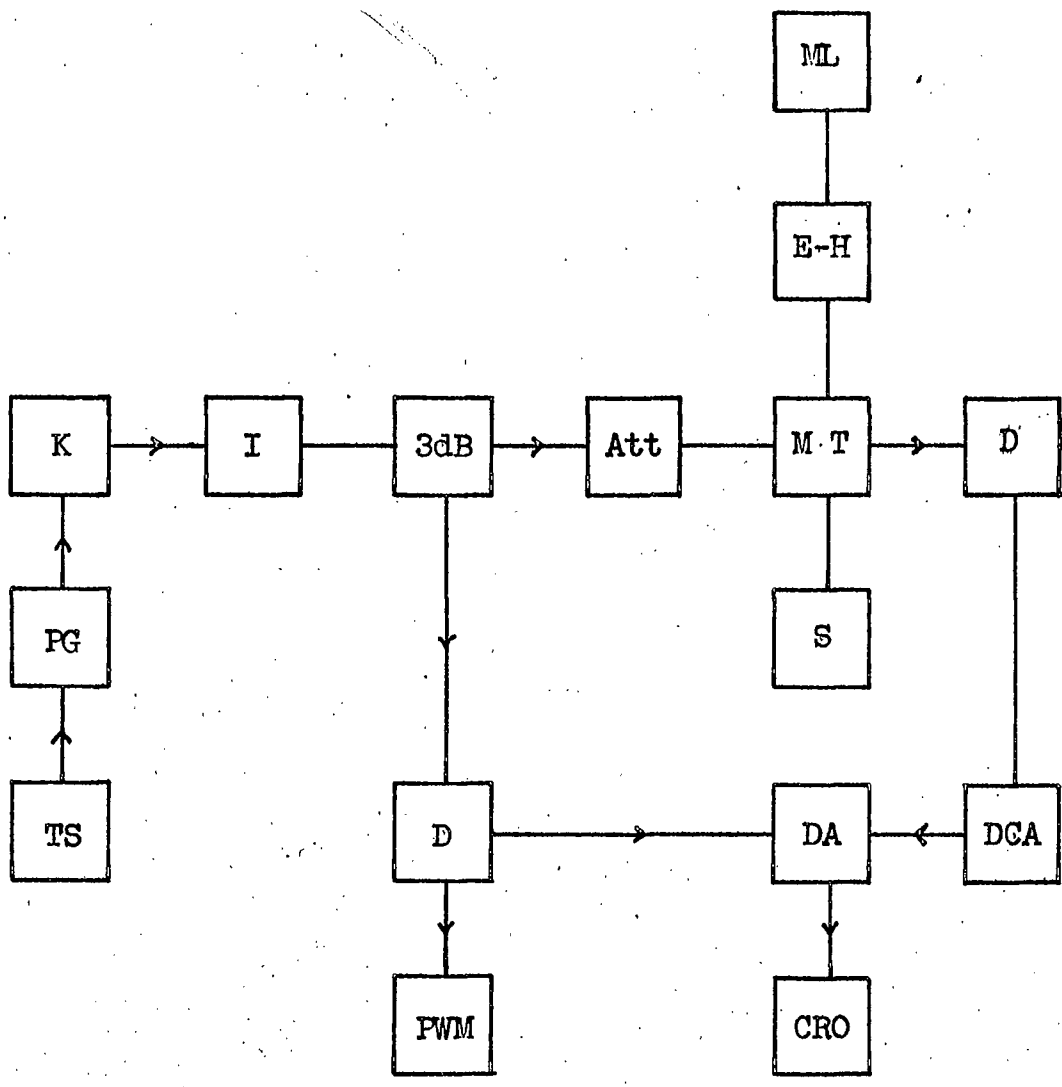
Figure 1.

The pulse response spectrometer

away, leaving only the true spin-lattice relaxation.

5.2 The experimental method

At 35 Gc/s a conventional bridge
spectrometer with crystal-video detection was used. The specimen
was mounted on the short-circuit termination of the waveguide,
positioned at the centre of a superconducting solenoid. The
use of the short-circuit termination (which is not an essential
feature of the method) placed less stringent requirements on
the frequency stability of the klystron. Figure 1 shows the
component layout. The reflex klystron (Elliott type 8RK19) is
grid-modulated to produce RF pulses with a mark-space ratio of
about 1 : 9 and a peak pulse power of about 3 mW. Frequency
deviation during the pulse does not exceed 5 Mc/s and an
amplitude sag of less than 10% could be achieved at pulse lengths
below 80 msec. A calibrated attenuator reduces the power at the
specimen to about 10 μW.

Figure 2 shows the waveforms
obtained from the crystal-video receiver after the microwave
bridge was balanced to select the absorption signal. The upper
trace is the pulse waveform off resonance. The lower trace,
obtained with the magnetic field on resonance, shows the power

Figure 2.

Receiver output display

Upper trace : off magnetic resonance.

Lower trace : on magnetic resonance.

0.2% Cr ruby at 4.2°K. Horizontal scale 2 msec per division

absorption decreasing with time. All the present measurements

have been made on ruby and sapphire specimens. The power dependence

of C (section 5.1) has been observed but it was found unnecessary

to plot C against power and extrapolate to zero power because

there was an appreciable range (up to about 300 μW) over which C

was independent of power and over which the amplitude of the

response signal was large. The pulse length must be much greater

than the time constant under investigation to ensure maximum

signal amplitude and to display the baseline, an important feature

in the interpretation of the curve. The interval between the

pulses is made sufficiently large to enable the spin system to

regain thermal equilibrium before the arrival of the next pulse.

Graphs of the natural logarithm of the absorption against time,

derived from photographs of the oscilloscope traces, yielded the

values of T_1.

5.3 Results

Measurements have been made on

different transitions in a selection of ruby and sapphire specimens

the relaxation behaviour of which had been previously examined by

the pulse saturation technique (11), (12). Figure 3 shows three

of the semi-logarithmic graphs obtained by the pulse response
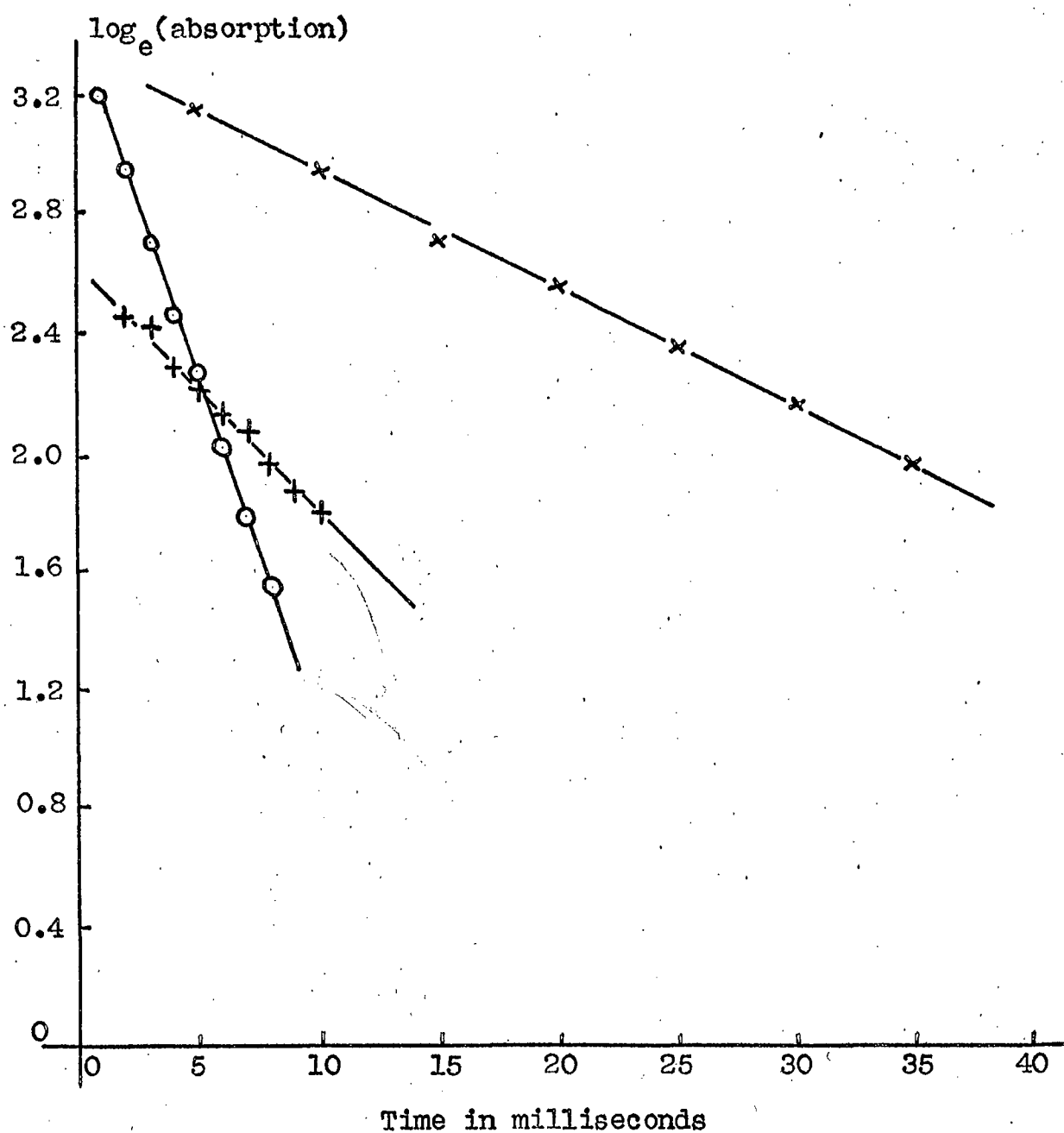
Figure 3.

Relaxation data derived from pulse response
traces

+ : -3/2 to -1/2 transition, 0.2% Cr ruby. $T_1 = 12.0$ msec.
✗ : -1/2 to +1/2 transition, 0.052% Cr ruby. $T_1 = 24.5$ msec.
O : -1/2 to +1/2 transition, 0.2% Cr ruby. $T_1 = 3.5$ msec.

method and their linearity shows that an exponential decay was
being observed. A comparison of the pulse response and pulse
saturation data is made in figure 4. Over a range of relaxation
times from 1 msec to 35 msec the agreement between the two methods
is within the experimental error of about 15%. The energy level
nomenclature follows the notation of Schultz - du Bois (13).

5.4 Important points of experimental technique

In order to make effective pulse
response measurements several experimental parameters require
close control. The most important of these are frequency deviation
and amplitude sag during the RF pulse, bridge balancing and the
choice of receiver. These are considered below.

5.4.1 The pulsed klystron

During the RF pulse the klystron
frequency must remain constant to within a fraction of the
linewidth of the transition under investigation. Grid modulation
generally produces some frequency deviation and the characteristics
of two different makes of klystron were investigated to find the
magnitude of any frequency deviation present. The first was a
35 Gc/s reflex klystron type R5146 (E.M.I.) used in conjunction
with a power supply type WE 80 (Microwave Instruments). The

Sample	Ion and transition	Relaxation time at 35.5 Gc/s. (msec)	
		Pulse response	Pulse saturation
H1	Fe^{3+} 1/2 to -1/2	1.1	0.95
	Cr^{3+} 1/2 to -1/2	5.9	5.7
G2A	Cr^{3+} 1/2 to -1/2	20.0	22.0
337A	Cr^{3+} 1/2 to -1/2	24.5	24.0
L2	Cr^{3+} -1/2 to -3/2 1/2 to -1/2 3/2 to 1/2	25.3 35.0 19.1	28.4 37.3 17.6
354	Cr^{3+} -1/2 to -3/2 1/2 to -1/2 3/2 to 1/2	12.0 3.5 7.8	15.0 4.0 6.8
S1	Fe^{3+} -1/2 to -3/2 1/2 to -1/2	3.7 2.2	2.0 1.9

Figure 4.

Comparison of the relaxation time results obtained from the same specimens by the pulse response and the pulse saturation techniques. All measurements taken at a polar angle of 90° and at a temperature of $4.2^{\circ}K$.
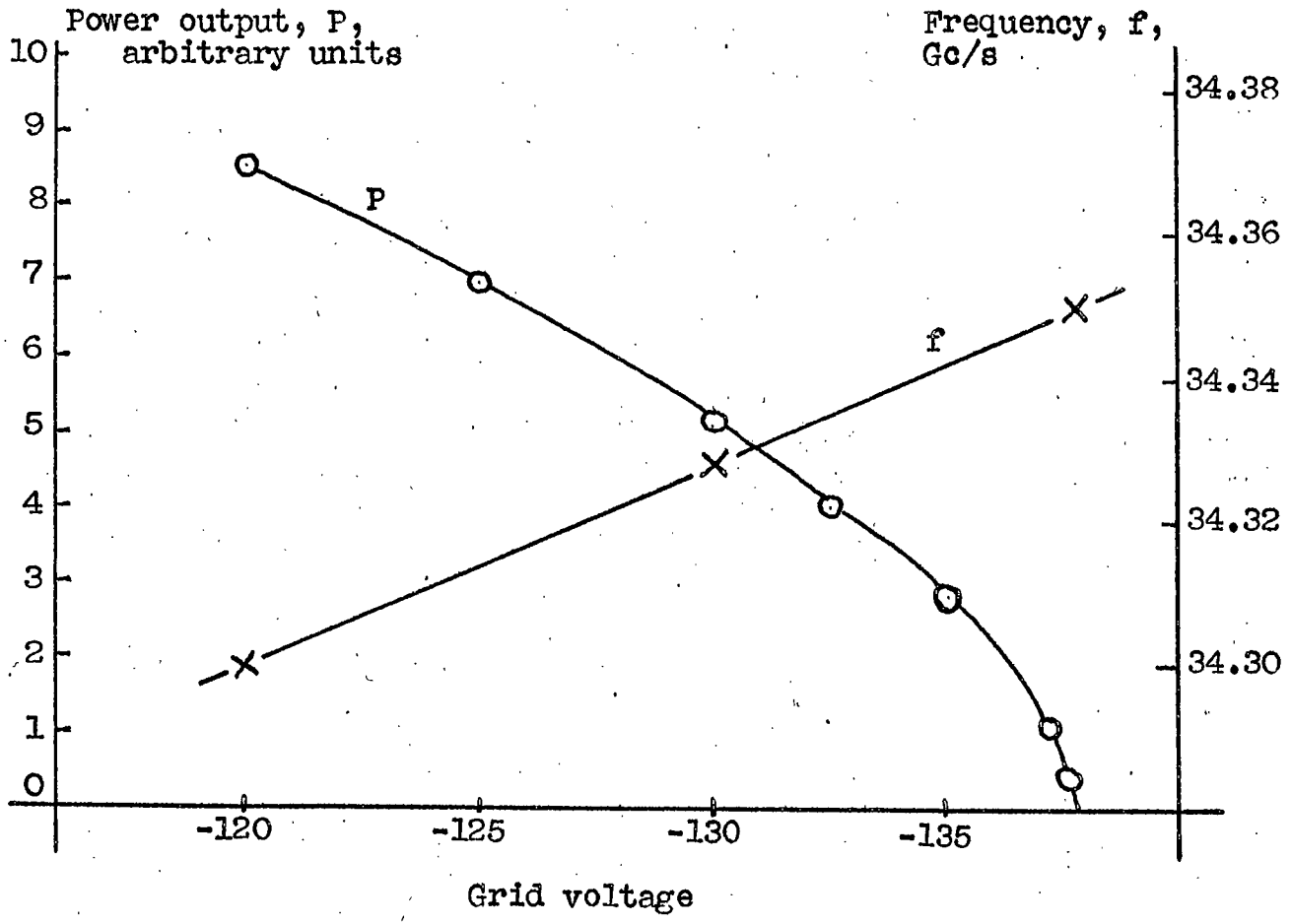
Figure 5.

R5146 klystron grid characteristics
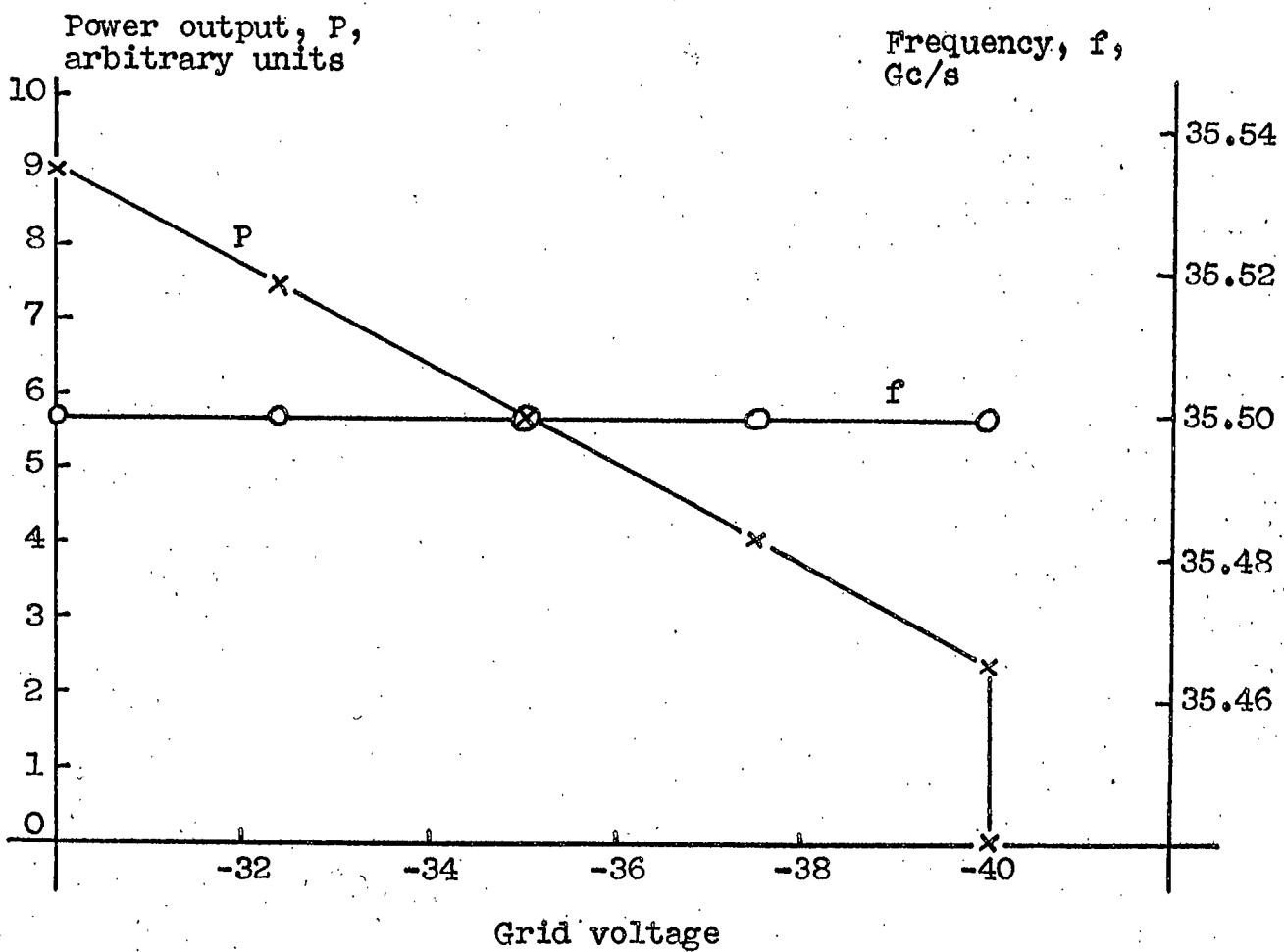
Figure 6.

8RK19 klystron grid characteristics

strongest CW operating mode was selected and, with the reflector

voltage constant, the RF power output and frequency were measured

as functions of the grid-to-cathode voltage, the results being

shown in figure 5. The power rises gradually from zero and its

variation becomes linear as the normal CW operating point at

-120 volts is reached; the frequency falls linearly by some 50 Mc/s.

This procedure was repeated with a second klystron, type 8RK19

(Elliott), again used with the WE 80 power supply. These

characteristics are shown in figure 6. Oscillation begins suddenly

at a grid voltage of -40 volts. The power then rises linearly to

the CW operating point at -30 volts, the frequency remaining

constant. The threshold value of the power output, measured on a

thermistor bridge, was 3 mW. For a closer examination of the

threshold the power output was displayed on an oscilloscope

while the timebase sawtooth voltage was applied to the klystron

grid. This gave a characteristic identical to figure 6 and showed

that the switching time of the 8RK19, at -40 volts, was $0.3\ \mu sec$,

independent of the slope of the input sawtooth. Voltage pulses

with a risetime of 10 nsec were then applied to the grid. The RF

pulse risetime remained at $0.3\ \mu sec$, showing that the switching

was initiated only by the level of the input signal. Under pulse

conditions no frequency deviation was detectable and the

characteristics of the wavemeter used suggested that any deviation

present was much less than 5 Mc/s.

The marked variation in the

performance of the two klystrons appears to arise from differences

in their mechanical construction and electron-optical properties (14).

With the 8RK19 the grid pulse necessary to produce 3 mw of RF

pulse power was about 8 volts. Larger volatge pulses produced

larger RF powers, but with fractionally greater frequency deviation.

The input pulses were obtained from a commercial pulse generator

(Solartron type GO 1101) and in order to maintain a 10% duty

cycle when using pulse lengths of about 80 msec, a separate

transistor multivibrator was constructed having two preset

periods, one of 120 msec and the other of 720 msec. The first was

used for initial adjustments because it produced a more acceptable

trace for prolonged viewing, and the second was used for the

actual measurement. This multivibrator was used to trigger the

pulse generator. With RF pulse lengths in excess of 80 msec

amplitude sag during the pulse became very large; this arises

from the resistance-capacitance coupling between the modulation

input socket on the power supply and the klystron grid. However,

the 80 msec upper limit of pulse length was quite adequate for

the present measurements in which relaxation times up to 35 msec

have been observed. For materials with longer relaxation times a

greater RF pulse length would be necessary.

5.4.2 Bridge balancing

In both the conventional pulse

saturation and the pulse response technique the accuracy of

relaxation time measurement depends upon the accuracy to which

the microwave bridge can be balanced. This is usually carried out

by means of a slide-screw tuner, a phase shifter-attenuator

combination or, as in the present work, an E - H tuner. The

experimental procedure for balancing in the pulse response method

is identical to that used in other methods. An important feature,

however, is that any unbalance is immediately visible. The klystron

operates in its pulsed mode and the pulses reflected from the

specimen assembly are displayed on the oscilloscope. The bridge is

balanced by adjusting the E and H pistons using the method

suggested by Cullen (15). At the balance point the pulses disappear

completely from the display. A small amplitude unbalance is then

introduced to select the absorption component on resonance. As

this unbalance is introduced the pulse reappears on the display,

but it always has a curved top. This indicates that phase
unbalance has also been introduced. The E - H tuner is designed
to reduce to a minimum the interaction between phase and amplitude
adjustments; this slight interaction becomes noticeable in the
pulse response method. The pulse curvature can be removed by a
very small adjustment of the phase piston of the E - H tuner. Thus
the pulse response method allows very accurate bridge balancing
and equally accurate compensation for the interaction between the
phase and amplitude adjustments.

5.4.3 RF sag compensation

Since the pulse response measurement
is of the change of absorption with time it is important that the
RF amplitude should be constant throughout the pulse. With the
circuitry used here, a little pulse sag arose because of the
resistance-capacitance coupling to the klystron grid. This was
compensated in the display by using a differential amplifier,
shown in figure 1. The RF pulse, which is displayed on the pulse
waveform monitor, is fed to one input of the differential
amplifier and the crystal-video receiver output to the other.
Off resonance the amplifier accepts pulses of the same shape at
both inputs and if the reference pulse is adjusted to be the same

amplitude as the receiver output pulse, the two pulses cancel exactly and the display is a straight line. The start and finish of the pulse are indicated by switching transients which are usually quite small. Although any magnitude of sag can be compensated in this way the differential amplifier technique is not recommended for sags exceeding about 5% because the RF amplitude variation affects the relaxation processes, the results of which cannot be removed by simple algebraic subtraction.

5.4.4 The crystal-video receiver

For relaxation studies on ruby at liquid helium temperatures a crystal-video receiver is well suited for the pulse response technique; high sensitivity is not of prime importance and the signals are at least 10 dB above peak noise with specimen volumes of about 0.1 cm^3. The technique does not require a receiver with a large dynamic range so that relatively large gain can be combined with good pulse handling capability. The receiver is always working well within its specification and tests made on its pulse performance showed no detectable traces of overshoot, ringing or sag. If greater sensitivity should be required, a superheterodyne receiver could be used.

5.4.5 Alternative pulsing systems

Grid modulation of the klystron is only suitable as a method for obtaining RF pulses if the linewidth of the transition under observation is several times the magnitude of the frequency deviation during the pulse. In the present experiments the linewidths are about 90 Mc/s overall and the frequency deviation is less than 5 Mc/s; grid modulation, therefore, is quite satisfactory. For materials having small linewidths it is preferable to operate the klystron in the CW mode and use an alternative method of producing RF pulses. The switching properties of microwave diodes are well known (16), (17), and are outlined in Chapter 3 and Chapter 4. The most important parameter of the diode in this context is the dependence of the ON/OFF ratio upon the incident RF power. A 30 dB ratio is possible for powers below about 1 mW. This ought to be a sufficient isolation for use in the pulse response method if the diode is placed between the attenuator and the hybrid T. A solenoid-operated ferrite switch (18) could be used but would require a large switching current and, because of its self inductance, would have a much slower switching time than both the diode and the klystron.

An alternative approach to the problem

is to run the klystron in the CW mode and to pulse the magnetic

field from well below resonance to exactly on resonance, using a

small, low-inductance auxiliary coil. Switching time limitations

and current ringing are possible disadvantages of this method but

for studying narrow resonances the coil inductance and the driving

current could probably be kept sufficiently small for magnetic

field pulsing to be preferable to klystron pulsing. Magnetic field

pulsing has been attempted on the present spectrometer but the

coupling between the auxiliary coil and the superconducting

solenoid was tight enough for the switching currents in the

auxiliary coil to induce current surges in the solenoid which were

large enough to drive it normal. However, the method should be

feasible with conventional electromagnets where the coupling

between the auxiliary coil and the field windings can be very

loose and where there are no problems of superconductivity quenching.

5.4.6 Direct coupling to the klystron grid

For those measurements where klystron

pulsing is the best method it is probably worth the extra trouble

to provide some form of direct coupling to the klystron grid in

order to be able to produce any length of RF pulse without any

sag. The obvious way to do this is to build into the klystron
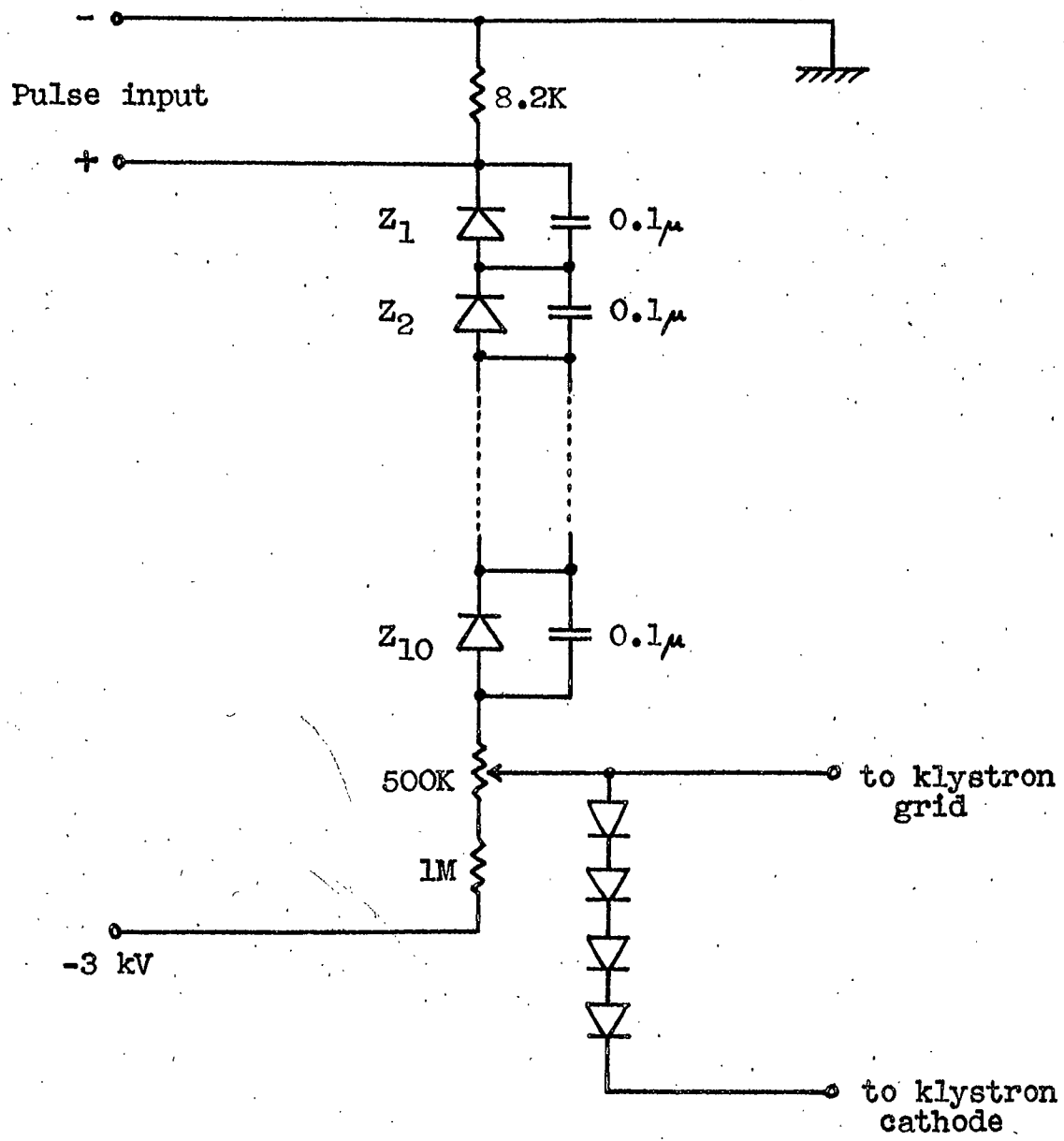
Figure 7.

Zener diode circuit

power supply a transistor monostable circuit having a wide range

of pulse lengths. The output of the circuit would need to supply

the 8 volt pulses necessary to operate the valve, and would be

connected directly between the cathode and the grid. The circuit

would be most conveniently operated by small batteries mounted,

with the circuit, inside the power supply unit. Good overall

insulation would be necessary because the entire circuit would be

floating at -2 kV, but this should not be difficult. The coarse

and fine pulse length potentiometer shafts would be brought out

to the front panel by means of extension rods made of tufnol or

bakelite. The only signal required by the monostable circuit

would be a triggering pulse supplied from an external source.

A coaxial socket mounted on the klystron power supply would be

needed for this purpose, the DC blocking condenser between this

and the monostable input being at least 2.5 kV working.

Another method of achieving direct

coupling to the klystron grid has been suggested (19). This is a

very elegant method and uses Zener diodes; the basic circuit is

shown in figure 7. The 2 kV potential on the grid is bridged to

earth by a chain of ten 200-volt Zener diodes. The pulse input

is at the earthy end of the chain, across the 8.2 K. ohm resistor.

If a negative pulse (with respect to earth) is applied at the
input the current down the chain is increased but, because all
the diodes are reverse biased to Zener breakdown, the voltage at
the klystron grid is unaffected. If a positive pulse is applied
at the input it travels along the chain virtually unattenuated
and reaches the klystron grid. Thus, although the Zener chain is
used to step down the voltage on the grid, it will act as a direct
coupling to the grid for positive signals originating at the
earthy end of the chain. The bleeder current through the diodes
is about 1 mA and the bypass condensers counteract the poor
high-frequency response of the Zener diodes. The condensers are
all of the same value and are chosen to give a good pulse shape
at the grid. Some minor modifications to the klystron power
supply would be necessary, including the disconnection of the
existing grid supply and the fitting of the protection diodes to
prevent the grid becoming positive with respect to the cathode.
The grid supply is then derived from the 3 kV power pack feeding
the Zener chain, the potentiometer giving control of the grid bias.

5.5 Discussion

The results given above show that
when the pulse response method can be used as an alternative to

the conventional pulse saturation technique comparable accuracies
can be obtained. There are three salient features of the new
method which influence its range of applicability: microwave
powers in the microwatt region are adequate because the response
of the spin system to a small disturbance is being observed;
resulting from this there is no need for receiver suppression
(section 4.4) during the pulse; the nature of the optimum RF pulse
required is determined by the linewidth and relaxation time of
the transition being studied.

In the centimetric wavelength region
the pulse saturation method is well established and a number of
valves giving sufficient power for saturation are readily available.
The pulse response method offers a simpler alternative, its
advantage lying in its potential for short time resolution. In
the pulse saturation method the receiver is normally suppressed
during the pulse and this leads to a dead time (often of about
10 μsec) at the beginning of the exponential recovery to
equilibrium; large inaccuracies can thus arise in the measurement
of relaxation times of the same order as the dead time. In the
centimetric region, however, a number of RF switching diodes are
available and can be used with the pulse response technique.

Several of these have nanosecond risetimes and, if used in
conjunction with a CW frequency-stabilised klystron, should enable
very short RF pulses of constant amplitude and frequency to be
obtained. This should facilitate studies of short relaxation times,
for example in the resolution of fast exponentials in cross-
relaxation and in direct measurements on fast-relaxing centres.
The power level required in the pulse response technique is well
below the dissipation limit of the switching diodes and the
control of RF pulse shape available should also enable measurements
to be made on materials having a very narrow linewidth.

At millimetric wavelengths the
situation is rather different in that diode switches are not
readily available at or above 35 Gc/s. Voltage modulation (either
of a klystron or of a backward-wave oscillator) appears to be the
only method for producing RF pulses and this limits the range of
materials which can be examined to those having overall linewidths
of at least 30 Mc/s and relaxation times greater than about 0.5 msec
at 4.2°K. As Chapter 7 shows, the low power requirement of the
pulse response method enables harmonic generation to be used to
extend the measurement range to the shorter millimetric wavelengths
where the few valves available which give sufficient power for

pulse saturation are extremely costly. This technique should
enable studies on the frequency and magnetic field dependence
of relaxation time to be made over a large range, as Chapter 7
shows. The use of a superconducting magnet can, however, create
some cryostat design problems if measurements are required at
temperatures above $4.2^{O}K$.

Chapter 6

The 70 Gc/s Single-Klystron Superheterodyne Spectrometer

Because of the very low power level requirement for

a local oscillator signal in the 35 Gc/s single-klystron superhet

it was decided to try and operate a 70 Gc/s superhet working on

the same general principle. Power could be derived by harmonic

generation from 35 Gc/s and a 70 Gc/s diode could be used as a

sideband generator either in a reflection or a transmission mode.

The harmonic generator available for this work was manufactured

by Microwave Instruments Ltd., and consisted of a microwave diode

in a transmission mount followed by a 35 to 70 Gc/s taper acting

as a high-pass filter.

6.1   The harmonic generator

There are four main types of

microwave harmonic generator, each type being characterised by

the nature of the non-linear element used. The first and commonest

type is the microwave diode (1), the non-linearity of which is

described in Chapter 4. The second type uses a discharge in an

inert gas at pressures up to about 40 mm of mercury (2), (3), (4).

The third type uses a high-pressure mercury arc over a small gap

between a tungsten wire and a mercury pool cathode (5), (6).

Extensions of this method using solid platinum and calcium as

```
┌──────────────┐      ┌──────────────┐      ┌──────────────┐
│  35 Gc/s     │ ───> │   Isolator   │ ───> │   Phase      │
│  Klystron    │      │              │      │   Shifter    │
└──────────────┘      └──────────────┘      └──────────────┘
                                                    │
                                                    v
                      ┌──────────────┐      ┌──────────────┐
                      │   Diode      │ <─── │   Mixer      │
                      │   Load       │      │   Diode      │
                      │              │ ───> │              │
                      └──────────────┘      └──────────────┘
                                                    │
                                                    v
                                            ┌──────────────┐
                                            │    Taper     │
                                            └──────────────┘
                                                    │
                                                    v
                                              70 Gc/s
                                              output
```
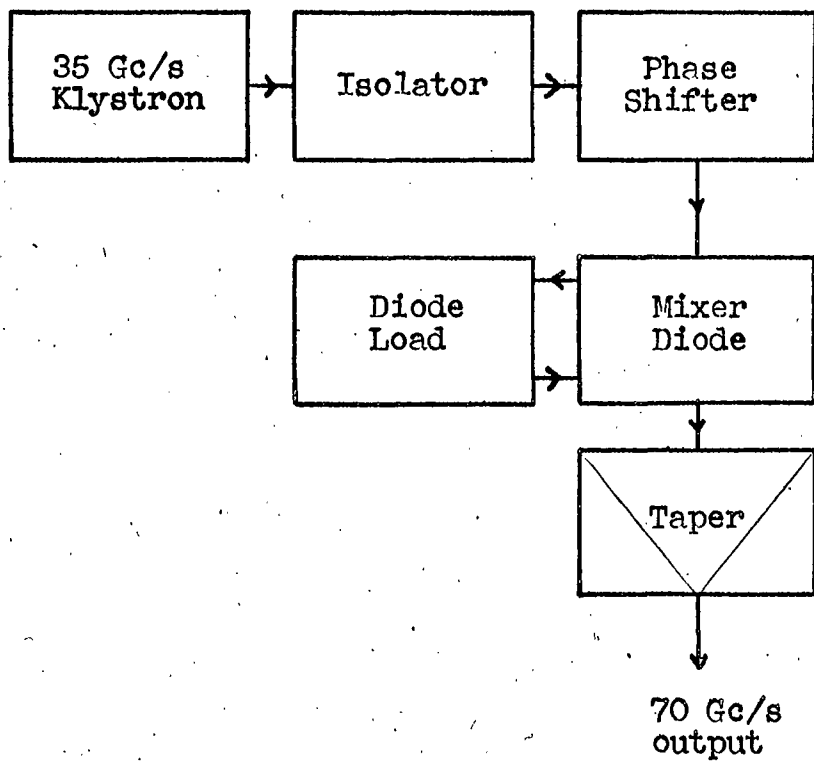
Figure 1.

Apparatus for harmonic generation

cathode have also been successful (7), (8). Ferrites have also

been used as mixers and harmonic generators. These are considered

briefly in section 6.6.

The microwave diode harmonic generator

only will be considered in detail as it is the type which is used

in the present work. If the diode is connected to a load

resistance, current flows through the circuit due to the presence

of the microwave field. Using the same sort of analysis as that

which led to equation (10) in Chapter 4 it can be shown that

harmonics of the microwave frequency are generated, their intensity

depending upon the curvature of the diode characteristic. The

apparatus used to produce 70 Gc/s power from a 35 Gc/s reflex

klystron is shown in figure 1. The phase shifter acts as a

matching device between the klystron and the diode and has been

found to be very effective in increasing the efficiency of second

harmonic generation. The fundamental frequency is not propagated

more than a few millimetres in the higher frequency waveguide; it

forms an evanescent mode and is heavily attenuated.

6.2   Sideband generation

It was originally intended to

generate the 45 Mc/s sidebands by using a 70 Gc/s diode in a

Figure 2.

The 70 Gc/s superheterodyne spectrometer
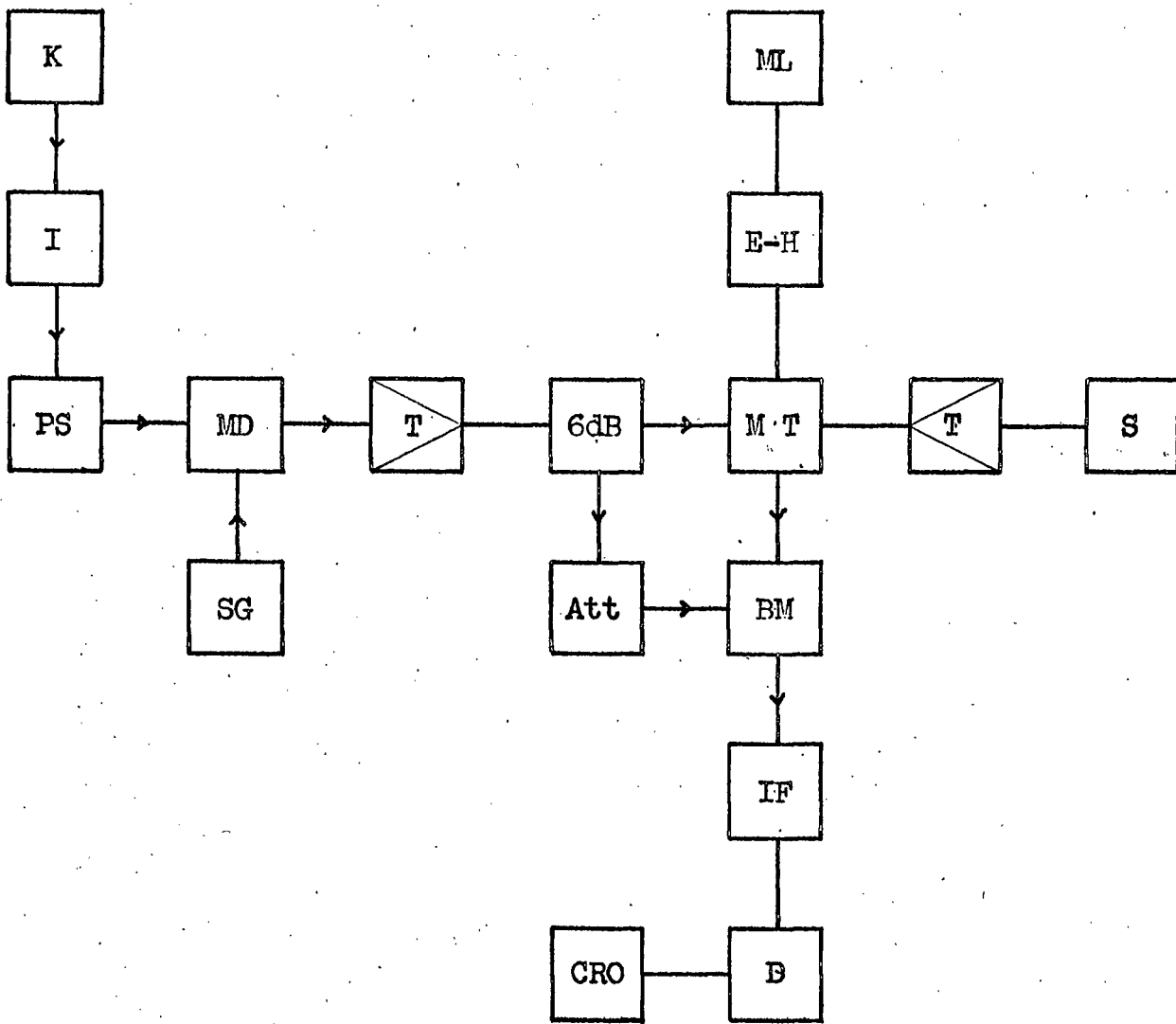
similar way to the transmission crystal modulator in the 35 Gc/s

version. However, examination of equation (10) in Chapter 4 shows

that the frequencies $2\omega_c$, $2\omega_c + \omega_s$, $2\omega_c - \omega_s$ are generated by the

modulator, and as these are the frequencies required for 70 Gc/s

operation, it was decided to build a complete 70 Gc/s

superheterodyne spectrometer using a single 35 Gc/s reflex

klystron and the transmission crystal modulator. Figure 2 shows

the component layout. The load resistance of the diode is replaced

by the 45 Mc/s modulation source. This must alter the conversion

efficiency to the second harmonic since it had been found with

the apparatus of figure 1 that the second harmonic power could be

varied over a range of some 3 dB by altering the load resistor,

maximum power being produced with a 100 ohm load. This observation

is in agreement with that of Anderson (9). Open-circuiting the

diode reduced the harmonic power by about 1.5 dB; this would

appear to be in direct disagreement with the mathematical proof

by Page (10) that harmonic generation is impossible unless there

is some DC dissipation. The operation of this diode under

conditions of infinite external load must be attributable to

some leakage paths in the diode cartridge or mounting block.

Connecting the RF signal generator to the diode produced a
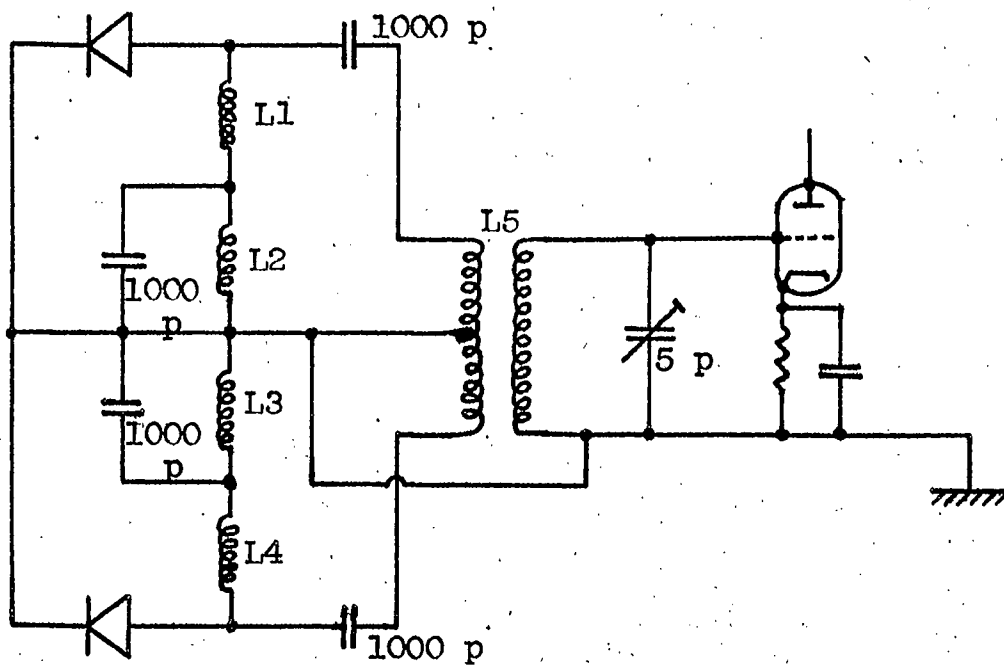
Figure 3.

Input circuit to IF strip

2.5 dB drop relative to the harmonic power with the 100 ohm load.
Attempts were made to effect an improved impedance match between
the signal generator and the diode, but the figure of 2.5 dB
could not be reduced.

6.3 The balanced mixer

No 70 Gc/s balanced mixers are
available in this country so a "laboratory equivalent" was
assembled, using a matched magic T and two tunable crystal
detectors. To tune the detectors each was put in turn on one of
the H-plane arms of the T, the opposite arm being terminated in
a matched load and 70 Gc/s power at the working frequency fed to
the junction through the third H-plane arm. Having tuned each
detector, the tuner adjustment was locked.

The crystals in the detector
mounts are of the same polarity so that in order to add the IF
signals which are in antiphase at the crystals, a push-pull input
transformer had to designed to feed the grid of the first valve
of the IF amplifier. This input circuit is shown in figure 3.
The inductances to provide the low resistance DC path for the
crystal currents (section 4.5.1) are as follows:

L_1 and L_4 - 45 turns of 40 SWG wire on a 0.25 inch diameter

paxolin former. The number of turns is adjusted to give self-resonance at 45 Mc/s.

L_2 and L_3 - 80 turns of 46 SWG wire on a 0.25 inch diameter paxolin former. The number of turns is adjusted to give self-resonance at 45 Mc/s.

L_5 primary - 6 turns of 24 SWG wire on a 0.875 inch diameter polystyrene former. The winding is centre-tapped.

L_5 secondary is wound on the primary winding and is 9 turns of 24 SWG wire. L_5 is tuned to 45 Mc/s under operating conditions by means of the 5 pF trimmer.

6.4 The IF amplifier

This is identical in design to the amplifier used on the 35 Gc/s version. It is a completely conventional design, the first two stages being a cascode circuit.

6.5 Operation

Using the equipment shown in figure 2, tests were carried out while feeding a 45 Mc/s carrier, 30% amplitude modulated at 400 c/s, into the transmission crystal modulator. A rather noisy 400 c/s signal was immediately obtained at the superhet output. The 70 Gc/s output was then maximised by adjustment of the phase shifter and by trying different

high-quality tungsten-germanium diodes as modulators. A variation of some 6 dB in harmonic power was produced by adjusting the position of the diode cartridge inside the mounting block. Maximum output was never achieved with the cartridge seated properly in the mount. A Mullard GEM 9 diode was found to give the highest harmonic power.

There was some pick-up of 45 Mc/s signal by the superhet due to slight radiation from the modulator; this was some 20 dB down on the maximum "true" signal and could be reduced to zero by careful orientation of the IF amplifier. All the components of the spectrometer functioned normally. Removing the local oscillator supply by means of the attenuator killed the IF signals completely, showing that true superheterodyne action was being observed. The 400 c/s component was removed from the modulator signal and the klystron was grid-modulated by a 1000 c/s square wave. This produced complete ON/OFF switching of the klystron (see Chapter 5). Very good signals were obtained at the superhet output and again were correctly dependent upon bridge balance and local oscillator level. However, the best signal-to-noise ratio which could be produced on this signal was about 10 dB with the microwave bridge almost completely unbalanced.

This figure of 10 dB thus represented the highest ratio possible.
This was verified by a trial run at liquid helium temperature
with a good ruby specimen. No absorption lines were visible; the
noise level was too high. Largest outputs from the superhet were
obtained with no attenuation in the local oscillator signal; this
indicated that the power level of this signal was not yet large
enough for efficient mixer operation. Note that a 6 dB
directional coupler is used to extract the local oscillator
power, compared with a 3 dB coupler on the 35 Gc/s spectrometer.
The effect of this is to increase the spectrometer signal and to
reduce the local oscillator power. No 3 dB couplers are yet
available at 70 Gc/s. The next requirement therefore, was for
greater local oscillator power to be achieved by more efficient
45 Mc/s sideband generation, and raising the question of diode
characteristics again. It was decided to find out how much power
was present at the second harmonic sidebands of the modulation
frequency, that is at the frequencies $2\omega_c \pm 2\omega_s$ (equation (10),
Chapter 4). To do this the drive frequency to the transmission
crystal modulator was reduced to 22.5 Mc/s, the rest of the
system remaining unaltered. Under these conditions the superhet
output signals were at least 6 dB up on the best of the previous

signals. This result is very interesting; subharmonic mixing, as it is called, is well known (11) but it has always been thought much less efficient than fundamental mixing. This may be a special case, because the frequencies involved in true subharmonic mixing are ω_c and $\omega_c \pm 2 \omega_s$. The presence of these frequencies in the 35 Gc/s signals has been observed in section 4.10, but the intensity of the harmonic sidebands $\omega_c \pm 2 \omega_s$ is very low. The observed phenomenon of the intensity of the $2 \omega_s$ mixer product being greater than the ω_s product could be explained if the sideband production and the harmonic generation took place separately and in that order, but in that case the resultant signal would be a 70 Gc/s carrier amplitude modulated at 90 Mc/s and having no 45 Mc/s component. This does not agree with observation and thus cannot be a valid analogy. To investigate this anomaly further the 45 Mc/s input to the modulator was replaced by a 400 c/s signal of the same amplitude and the signal obtained from a 70 Gc/s crystal detector following the modulator was fed into an oscilloscope and into a Marconi audio frequency analyser. The audio output signal from the detector was predominantly an 800 c/s oscillation; this could be seen from the oscilloscope display. The frequency analyser showed

that the component at 800 c/s was nearly 3 dB above the fundamental 400 c/s component. The third and fourth harmonics were both 30 dB down on the fundamental. Experimental observations such as these can never be explained by mathematical analyses involving the use of a power series for the diode characteristic because such series (when used in this context) will always be convergent and the second harmonic intensity will never be greater than that of the fundamental. At present, the problem remains unsolved. Hall and Schumacher (12) have used simultaneous harmonic and sideband generation from 9 to 18 Gc/s with 63 Mc/s sidebands using a mixer crystal but do not report any experiments on subharmonic mixing.

Using the present system with 22.5 Mc/s modulator drive has proved successful in that 70 Gc/s resonances have been observed, as figure 4 shows, but the dominant feature of the design which appears to be preventing more amplification from being obtained is the lack of local oscillator power. An interesting feature of this subharmonic mixing principle is that there are no problems whatsoever over stray modulator radiation being picked up by the superhet.
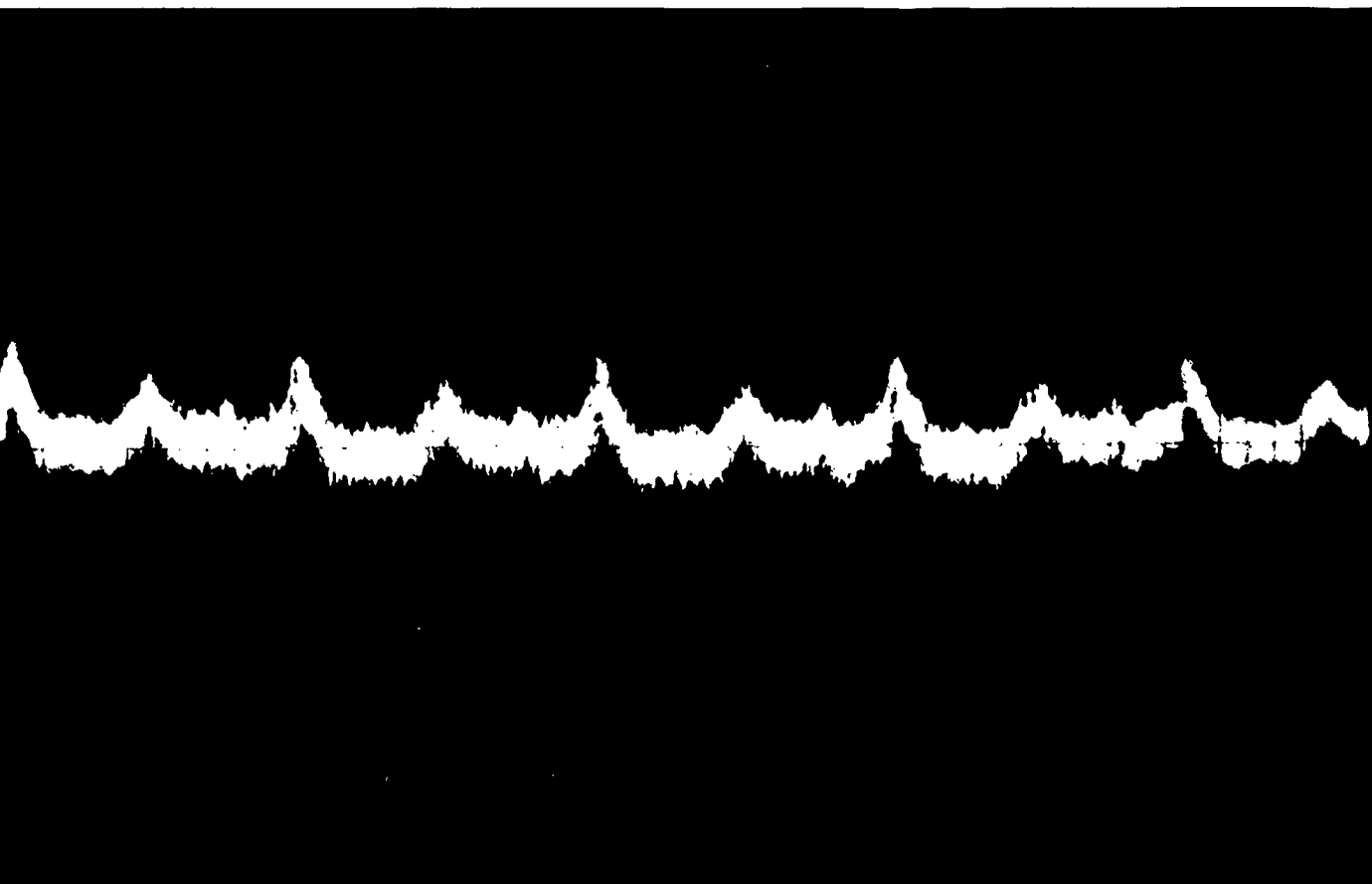
Figure 4.

An absorption signal as seen with the 70 Gc/s superhet

6.6 Frequency doubling in ferrites

The fourth type of harmonic generator utilises a ferrite as the non-linear element. Mention of this particular type has been left until now because it appears that ferrite frequency doublers can attain the maximum possible harmonic conversion efficiency. Page (10), in his mathematical treatment of the generation of harmonics, showed that the n'th harmonic cannot be generated with an efficiency exceeding $1/n^2$. Thus the maximum conversion efficiency to the second harmonic is -6 dB and to the third is -9.5 dB. Bearing these figures in mind, it is interesting to compare the conversion efficiencies of the various types of harmonic generator. In the list given below, the measured efficiency is given after the harmonic number followed by the maximum efficiency, given in brackets.

(a) Diode; 2nd harmonic: -21 dB, (-6 dB), fundamental 35 Gc/s.

(b) Discharge; 3rd harmonic: -35 dB, (-9.5 dB), fundamental 3 Gc/s.

(c) Arc; 9th harmonic: -90 dB, (-19dB), fundamental 35 Gc/s.

(d) Ferrite; 2nd harmonic: -6 dB, (-6 dB), fundamental 9 Gc/s.

Types (b) and (d) require fundamental input powers of several kilowatts; type (c) requires

several watts, and type (a) operates below about 500 milliwatts.
Ferrite harmonic generators are described by Ayres et al. (14),
Douthett et al. (15), Jepsen (16), and Melchor et al. (17).
Reference (17) describes the device giving a -6 dB conversion
efficiency to the second harmonic.

6.7 Suggestions for further work

Subharmonic mixing appears to be a
very attractive proposition for this design and there seems to
be no reason why the system should not operate as successfully
as its 35 Gc/s counterpart if a 3 dB coupler could be used to
extract the local oscillator power. One way of investigating this
problem would be to reverse the two output connections from the
6 dB coupler so that more microwave power goes into the local
oscillator arm than goes into the spectrometer arm.

It is suggested that the design
be further investigated with the aim of reducing the conversion
loss of the balanced mixer crystals to the intermediate frequency
by applying an external DC bias to the mixer diodes (13). This
could be done by disconnecting the earthy ends of L_2 and L_3 and
connecting them to a voltage supply sufficient to produce about
0.5 mA forward bias to each diode. This may help to offset the
adverse effects of low local oscillator power.

Chapter 7

The Pulse Response Method at 70 Gc/s

7.1 Introduction

The pulse response method has been used with great success at 70 Gc/s, microwave power being derived from the Elliott 35 Gc/s reflex klystron by harmonic generation. The spectrometer is shown in figure 1. The harmonic generator is a GEM 9 mixer crystal, positioned in the mount as described in section 6.5 and working into an external load resistance of 100 ohms. The manufacturers of the harmonic generator quote a conversion loss of 27 dB to the second harmonic; thus, using the 3 mW of available pulse power at 35 Gc/s will give 6 μW of pulse power at 70 Gc/s. The spectrometer uses 70 Gc/s components throughout: the harmonic generator, waveguide tapers, magic T and detector were supplied by Microwave Instruments, Ltd., the E - H tuner, waveguide bends and matched load were supplied by Mid-Century Microwavegear, Ltd. 35 Gc/s stainless steel waveguide was retained in the cryostat and was fed with 70 Gc/s power via a section of waveguide taper.

7.2 Operation

The operation of the spectrometer was identical to the operation of the lower-frequency version
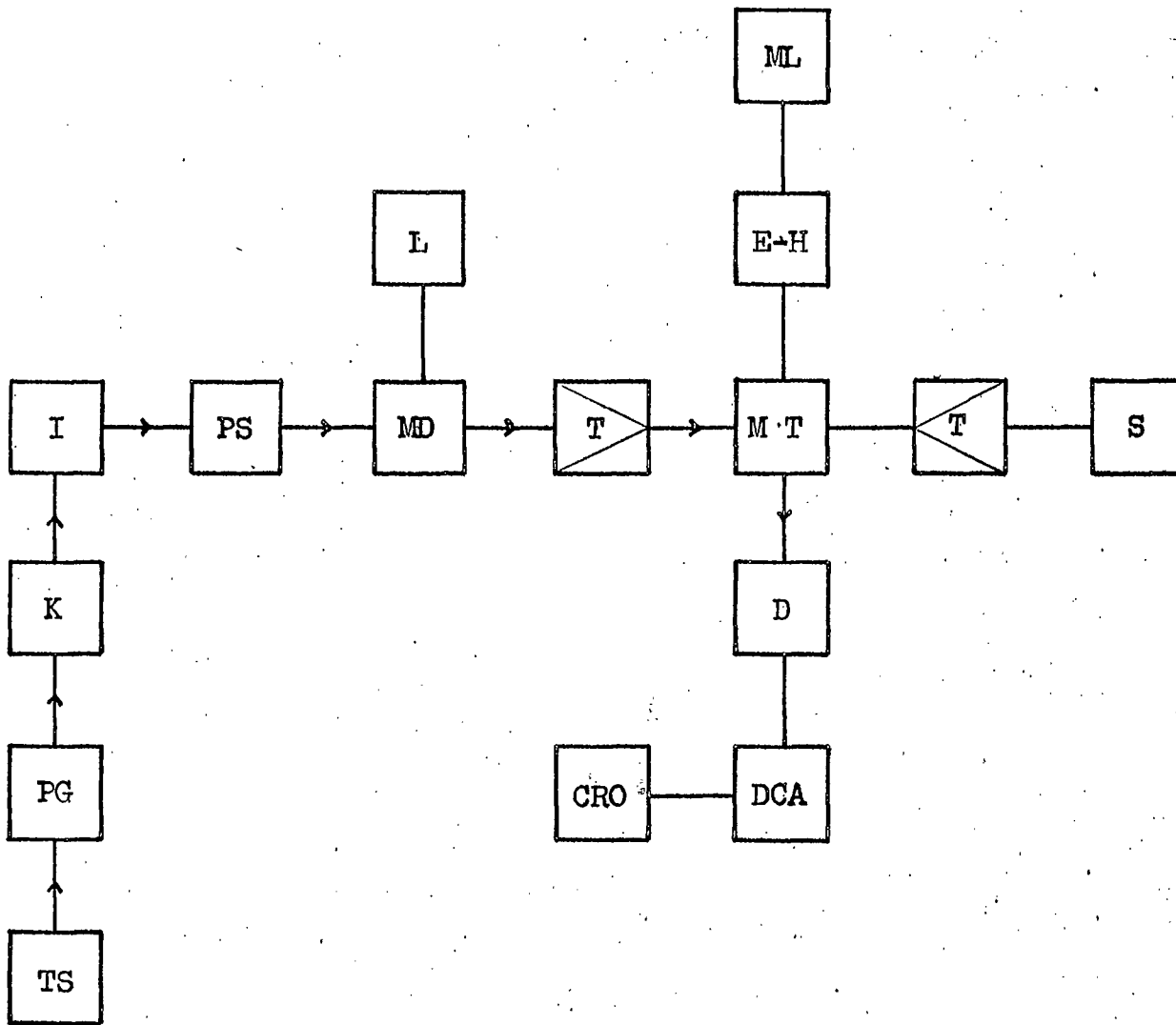
Figure 1.

The 70 Gc/s pulse response spectrometer

described in Chapter 5. Signals from the crystal-video receiver were quite large and with very little noise. Figure 2 shows a typical display of an absorption line, in this case a split line, the two components just overlapping. Pulse response traces were obtained very easily and were not too noisy. If a source power of 6 μW is assumed, the maximum possible power at the specimen is 2 μW and the maximum possible power at the detector is less than 1 μW. However, pulse response traces such as that shown in figure 3 were obtained.

7.3 Results

The pulse response technique has been used on many specimens and transitions which have already been examined at 35 Gc/s using both the pulse response (1) and the pulse saturation (2) technique. A complete table of all results is given in figure 4. It duplicates some of the information given in Chapter 5, but direct comparison of results at the two frequencies is very interesting. The pulse saturation results were obtained by Mason (3) and by Kirkby (4). The energy level nomenclature is again that of Schultz - du Bois (5). Relaxation time measurements were made on those specimens and transitions which had been investigated at 35 Gc/s purely for the sake of

Figure 2.

70 Gc/s absorption line display

assembling as complete a list of parameters for each specimen
as possible.

7.4 Discussion of results

(a) The ruby specimens G2A, 337A,
and L2 are good quality, i.e., they contain negligible quantities
of paramagnetic ions other than Cr^{3+}. The results for each
transition are much smaller at 70 Gc/s than they are at 35 Gc/s.
Excluding for the moment the +(1/2) to -(1/2) transition in
specimen L2, the relaxation times at the higher frequency are
smaller by factors ranging from 7.5 to 6.1. This corresponds to
a frequency dependence range of $f^{-2.9}$ to $f^{-2.6}$, and since magnetic
field and frequency are linearly related, the magnetic field
dependence of relaxation time lies between $H^{-2.9}$ and $H^{-2.6}$.
This is a markedly slower dependence than that predicted by
Van Vleck (6) of H^{-4}, and lies between the values of H^{-2} for a
non-Kramers salt (7) and H^{-4} for a Kramers salt (7). Donoho (8)
has given a theoretical treatment of the dependence of relaxation
time on polar angle and on magnetic field. In order to obtain a
true magnetic field dependence by experiment it is advisable to
use very dilute specimens (about 0.02%) and to take measurements
at a polar angle of 0° where there is least mixing of the spin
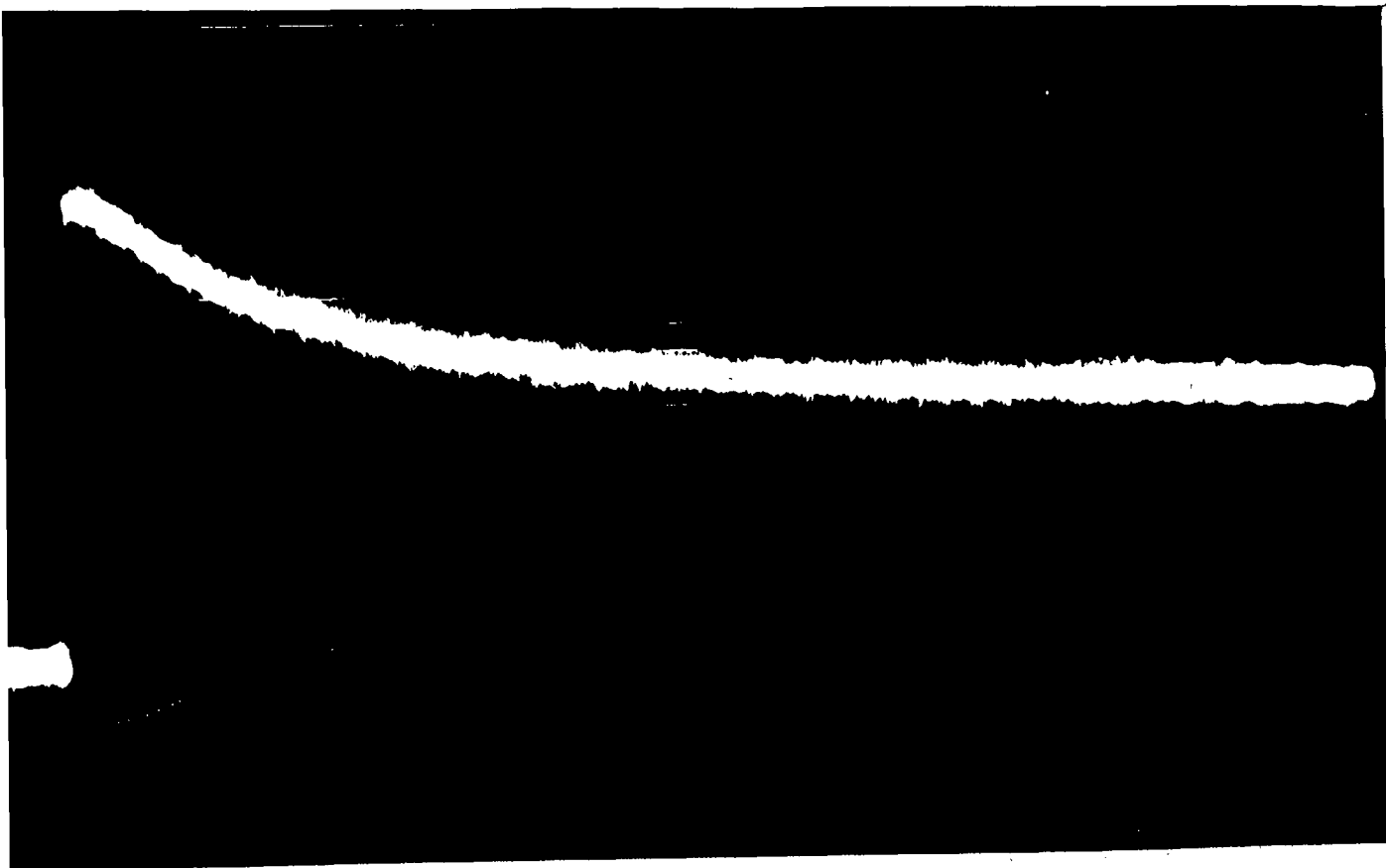
Figure 3.

A 70 Gc/s pulse response trace

-1/2 to +1/2 transition, 0.052% Cr ruby at 4.2°K. T_1 = 3.2 msec.

Sample	Ion and transition	Relaxation time at 35.5 Gc/s. (msec)		Relaxation time at 71 Gc/s. (msec)
		Pulse response	Pulse saturation	Pulse response
H1	Fe^{3+} 1/2 to -1/2	1.1	0.95	4.3
	Cr^{3+} 1/2 to -1/2	5.9	5.0	5.7
G2A	Cr^{3+} 1/2 to -1/2	20.0	22.0	3.0
337A	Cr^{3+} 1/2 to -1/2	24.5	24.0	3.2
L2	Cr^{3+} -1/2 to -3/2	25.3	28.4	4.2
	1/2 to -1/2	35.0	37.3	12.5
	3/2 to 1/2	19.1	17.6	2.9
354	Cr^{3+} -1/2 to -3/2	12.0	15.0	-
	1/2 to -1/2	3.5	4.0	3.1
	3/2 to 1/2	7.8	6.8	-
S1	Fe^{3+} -1/2 to -3/2	3.7	2.0	-
	1/2 to -1/2	2.2	1.9	-

Figure 4.

Complete table of results, including the 71 Gc/s
relaxation times. All measurements taken at a polar
angle of 90° and at a temperature of 4.2°K.

states. Any cross-relaxation (9) will also mask the true field

dependence. All the transitions in the L2 specimen had a lineshape

similar to that of figure 2; the overall width of the double

line corresponds approximately to the overall width of an un-split

Cr line. The T_1 measurements on the -(1/2) to -(3/2) and on the

+(1/2) to +(3/2) transitions were made at a position in the centre

of the overall lineshape, but the measurement on the +(1/2) to

-(1/2) transition was made on the peak of the intense, narrow

component and thus explains why the result for this transition

is different from the others.

(b) Specimen 354 is a high

concentration (0.2%) ruby, and shows that the magnetic field

dependence of relaxation time is drastically modified for non-

dilute systems.

(c) Specimen H1 is doped with almost

equal quantities of Cr^{3+} and Fe^{3+}, forming a system in which there

is very strong cross-relaxation between the two paramagnetic ions,

again destroying the standard magnetic field dependences.

Pulse saturation measurements at

9.3 Gc/s on the +(1/2) to +(3/2) and on the -(1/2) to -(3/2)

transitions in specimen L2 gave T_1 values of 51.3 msec and

86.2 msec (13). These results give a frequency dependence of $f^{-0.74}$ and $f^{-0.91}$ between 9.3 Gc/s and 35.5 Gc/s. At first these figures indicate very poor agreement with the 71 Gc/s results, but a more careful consideration shows that the 9.3 Gc/s relaxation times are not inconsistent with the others. The effect of the DC magnetic field is to lift the degeneracy of the lowest orbital energy level of the Cr^{3+} ion. The degeneracy is not completely lifted, however, and each energy state is a mixture of itself with the others. As the magnetic field is increased, the degeneracy is lifted further and the mixing of states decreases. Thus, as the measuring frequency is changed from 71 Gc/s through 35.5 Gc/s to 9.3 Gc/s, the magnetic field changes from 30 kOe through 15 kOe to 5 kOe, and the energy states become increasingly mixed. The effect of this mixing is to decrease the measured relaxation time and it is this which is being observed by the reduction of the frequency dependence from $f^{-2.9}$ to $f^{-0.91}$.

It is interesting to note that the magnetic field dependence of relaxation time in a Kramers salt has been shown to agree with the Van Vleck prediction by Davids and Wagner as recently as 1964 (10). The ion used was Fe^{3+} in potassium cobalticyanide, and this is claimed to be the first

experimental verification of the Van Vleck theory.

7.5 General remarks

The increase in the measuring frequency does not create any special problems in this method; crystal-video detection is still used, and crystal noise becomes a problem only when very low concentration specimens are used. For example: under AC resonance conditions (section 4.2.2) a 0.002% Cr ruby gives signals about 10 dB above the RMS noise level (i.e. it is better than a tangential signal) but the pulse response traces are not large enough to measure. This concentration appears to be the limit of the present 70 Gc/s system, where the amplitude of the signal and of the crystal flicker noise approach equality. The only way to overcome this difficulty is to use superheterodyne detection. For reasons given in Chapter 6, superhet detection with a single-klystron system is not yet up to the performance of a crystal-video receiver but this seems almost wholly attributable to the lack of source power, resulting in loss of local oscillator power and reducing the conversion efficiency of the mixer. However, suggestions have been made to improve matters.

7.6 A note on the use of 70 Gc/s crystals

The crystal detector mount type WO 948

(manufactured by Microwave Instruments) is fitted with a non-removable point-contact diode. These diodes are precision devices and are extremely sensitive to physical shock and vibration. To give the user some form of control over the characteristics of his diodes, the position of the germanium slab has been made adjustable with respect to the tungsten whisker by means of a minute grub screw and locking screw on the crystal mount. Retraction and insertion of the slab by a fraction of a millimetre is sufficient to produce a new point of contact with the whisker. The pressure against the whisker also changes the characteristics, but is very critical because the whisker will fracture easily. This adjustment is essential; improvements of 12 dB over the initial sensitivity figures, with the two crystal mounts as delivered, were effected by this adjustment. It is unfortunate that a maximum in conversion efficiency for crystal-video operation need not coincide with a conversion efficiency maximum to IF. After adjustment the two crystals had sensitivities matched to within 2 dB for crystal-video operation, but for conversion loss to IF, one crystal was 10 dB better than the other. This could be explained by assuming that one diode had a conversion loss 10 dB better than the other, or by assuming that the conversion losses

were the same, but that the IF impedances were drastically different.
So if crystal-video operation and supernet operation are desired,
it is better to have three crystal mounts, one adjusted for
maximum DC output and the other two matched as closely as possible
for IF output.

7.7 Further work at 70 Gc/s

A method has been devised for
measuring spin-lattice relaxation time at 70 Gc/s, providing the
foundations for a thorough investigation of the magnetic field
and frequency dependence of T_1, a study which would hitherto
have necessitated a very large capital outlay for equipment alone.
At present all the specimens are cut in such a way that the only
polar angle possible with the superconducting magnet is 90°.
To enable angular variations to be made, a superconducting magnet
in the form of two parallel windings would be required, the specimen
in the waveguide being at the centre of the system, between the
two windings.

It is difficult to say whether or
not the pulse response method would be made any easier by the
use of a 70 Gc/s klystron. With the present method, the frequency
deviation of the 35 Gc/s klystron during the pulse is doubled

by the process of harmonic generation thus introducing a possible

source of error. However, in a pilot experiment carried out at

35 Gc/s, this frequency deviation was deliberately increased by

a factor of about 3 and the T_1 results still lay within 5% of

their values under the correct conditions. It is thought unlikely

that the doubled frequency variation at 70 Gc/s is causing any error.

The Elliott 70 Gc/s klystron is thought to have much poorer

modulation properties than the 8RK19 (11), resulting in slow

switching times and large power variation during the pulse. No

information is available on the frequency deviation figures.

Until more technological experience is gained in the construction

of these klystrons, it would appear that for the pulse response

method, harmonic generation from 35 Gc/s with the 8RK19 klystron

is the best solution. If the 8RK17 klystron has switching

characteristics identical to the 8RK19 (the mechanical construction

and electron optics are identical (11)) then its 250 mW output

at 35 Gc/s should produce an 18 dB gain in 70 Gc/s power (12)

if the mixer crystal used as the harmonic generator can withstand

the increased radiation. This should produce more than ample

power to operate the single-klystron superhet at this frequency.

Chapter 1.   References

(1)   C.E. Cleeton and N.H. Williams, Phys. Rev., $\underline{45}$, 234 - 7, 1934.

(2)   B. Bleaney and R.P. Penrose, Nature, $\underline{157}$, 339 - 40, 1946.

(3)   W.E. Good, Phys. Rev., $\underline{70}$, 213 - 8, 1946.

(4)   E. Zavoisky, J. Phys. USSR, $\underline{9}$, 211, 1945.

(5)   R.L. Cummerow and D. Halliday, Phys. Rev., $\underline{70}$, 433, 1946.

(6)   J.H.E. Griffiths, Nature, $\underline{158}$, 670 - 1, 1946.

(7)   F. Bloch, Phys. Rev., $\underline{70}$, 460 - 74, 1946.

(8)   F. Bloch, W.W. Hansen and M. Packard,

      Phys. Rev., $\underline{69}$, 127, 1946.

(9)   K.D. Bowers and J. Owen, Repts. Prog. Phys., $\underline{18}$, 304 - 73, 1955.

(10) J.W. Orton, Repts. Prog. Phys., $\underline{22}$, 204 - 40, 1959.

(11) A.F. Harvey,

      "Microwave Engineering" (Academic Press), 1963, p.146.

(12) J.P. Gordon, H.J. Zeiger and C.H. Townes,

      Phys. Rev., $\underline{99}$, 1264 - 74, 1955.

(13) C.J. Gorter, Physica, $\underline{3}$, 503 - 14, 1936.

(14) A.H. Eschenfelder and R.T. Weidner,

      Phys. Rev., $\underline{92}$, 869 - 73, 1953.

(15) A.M. Portis, Phys. Rev., $\underline{91}$, 1071 - 8, 1953.

(16) A.M. Portis, Phys. Rev., $\underline{104}$, 584 - 8, 1956.

(17) A.G. Redfield, Phys. Rev., $\underline{98}$, 1787 - 1809, 1955.

(18) A.L. Kipling, P.W. Smith, J. Vanier and G.A. Woonton,

  Can. J. Phys., $\underline{39}$, 1859 - 74, 1961.

(19) J.G. Theobald, Ann. Phys. (France), $\underline{7}$, 585 - 621, 1962.

(20) R.W. Damon, Rev. Mod. Phys., $\underline{25}$, 239 - 45, 1953.

(21) N. Bloembergen and S. Wang, Phys. Rev., $\underline{93}$, 72 - 83, 1954.

(22) S. Feng and N. Bloembergen, Phys. Rev., $\underline{130}$, 531 - 5, 1963.

(23) C.F. Davis, M.W.P. Strandberg and R.L. Kyhl,

  Phys. Rev., $\underline{111}$, 1268 - 72, 1958.

(24) K.D. Bowers and W.B. Mims, Phys. Rev., $\underline{115}$, 285 - 95, 1959.

(25) J.H. Pace, D.F. Sampson and J.S. Thorp,

  Proc. Phys. Soc., $\underline{76}$, 697 - 704, 1960.

(26) A.A. Manenkov and A. . Prokhorov,

  Sov. Phys., JETP, $\underline{13}$, 1129 - 31, 1961.

(27) J.G. Castle, P.F. Chester and P.E. Wagner,

  Phys. Rev., $\underline{119}$, 953 - 61, 1960.

(28) J.S. Thorp, D.F. Sampson and J.H. Pace,

  J. Electr. Contr., $\underline{10}$, 13 - 24, 1961.

(29) J.S. Thorp, J. Electr. Contr., $\underline{11}$, 439 - 44, 1961.

(30) J. Herve and J. Pescia, C.R. Acad. Sci., $\underline{251}$, 665 - 7, 1960.

(31) J. Herve and J. Pescia, C.R. Acad. Sci., $\underline{255}$, 2926 - 9, 1962.

(32) A.Bassompierre and J. Pescia,

C.R. Acad. Sci., <u>254</u>, 4439 - 41, 1962.

(33) J. Herve,

"Paramagnetic Resonance" (Academic Press), <u>2</u>, 689 - 97, 1963.

(34) W.I. Dobrov and M.E. Browne,

"Paramagnetic Resonance" (Academic Press), <u>2</u>, 447 - 55, 1963.

(35) L. Rimai, R.W. Bierig and B.D. Silverman,

Phys. Rev., <u>146</u>, 222 - 32, 1966.

(36) G. Brown, D.R. Mason and J.S. Thorp,

J. Sci. Instrum., <u>42</u>, 648 - 9, 1965.

(37) G. Brown and J.S. Thorp,

Brit. J. Appl. Phys., to be published.

Chapter 2.   References

(1) D. de Klerk,

"The Construction of High-Field Electromagnets",

(Newport Instruments), 1965, p. 76.

(2) R. Blanplain,

Bull. Roy. Soc. Sci., (Belgium), 30, 310 - 14, 1961.

(3) A. Maimoni, Rev. Sci. Instrum., 27, 1024 - 27, 1956.

(4) S. Meiboom and J.P. O'Brien,

Rev. Sci. Instrum., 34, 811 - 12, 1963.

(5) J.G. Dash and H.A. Boorse, Phys. Rev., 82, 851 - 56, 1951.

(6) Yu I. Nechaev, Instrum Exper. Tech., No. 4, 801 - 3, 1962.

(7) W.E. Williams and E. Maxwell,

Rev. Sci. Instrum., 25, 111 - 14, 1954.

(8) Ya I. Rozenberg and V.G. Kasatkin,

Instrum. Exper. Tech., No. 3, 578 - 79, 1963.

(9) J. Babiskin, Rev. Sci. Instrum., 21, 941, 1950.

(10) N.S. Rasor, Rev. Sci. Instrum., 25, 311 - 18, 1954.

(11) J.R. Feldmeier and B. Serin,

Rev. Sci. Instrum., 19, 916 - 17, 1948.

(12) R. Ries and C.B. Satterthwaite,

Rev. Sci. Instrum., 35, 762 - 63, 1964.

(13) B.F. Figgins, T.A. Shepherd and J.W. Snowman,

J. Sci. Instrum., 41, 520, 1964.

(14) R.V. Isaeva, Instrum. Exper. Tech., No.1, 201 - 2, 1962.

(15) A.E. Rovinskii, Instrum. Exper. Tech., No.2, 398 - 99, 1961.

(16) A.E. Rovinskii, Cryogenics, 2, 115, 1961.

(17) A.B. Fradkov and A.I. Shal'nikov,

Instrum. Exper. Tech., No.3, 508 - 9, 1960.

(18) R.T. Webber, Phys. Rev., 72, 1241 - 45, 1947.

(19) J. Gaffney and J.R. Clement,

Rev. Sci. Instrum., 26, 620, 1955.

(20) D.N. Lyon and J.J. Gillich,

Rev. Sci. Instrum., 36, 1164 - 66, 1965.

(21) W.L. Pope and E.F. McLaughlin,

J. Sci. Instrum., 43, 260, 1966.

(22) M. Sauzade, C. Georges, J. Pontnau and P. Lesas,

Cryogenics, 5, 42 - 3, 1965.

Chapter 3. References

(1) D.J.E. Ingram,

"Spectroscopy at Radio and Microwave Frequencies",

(Butterworth's), 1955, p. 95.

(2) S.N. Van Voorhis,

"Microwave Receivers", MIT Rad. Lab. Series,

(McGraw-Hill), $\underline{23}$, 1948, p. 456.

(3) H.Z. Cummins, N. Knable and Y. Yeh,

Phys. Rev. Letters, $\underline{12}$, 150 - 53, 1964.

(4) D.J.E. Ingram,

"Spectroscopy at Radio and Microwave Frequencies",

(Butterworth's), 1955, p. 32.

(5) P.D. Strum, Proc. I.R.E., $\underline{41}$, 875 - 79, 1953.

(6) G. Brown and J.S. Thorp, Brit. J. Appl. Phys., to be published.

(7) R. Karplus, Phys. Rev., $\underline{73}$, 1027 - 34, 1948.

Chapter 4. References

(1) C.F. Davis, M.W.P. Strandberg and R.L. Kyhl,

Phys. Rev., 111, 1268 - 72, 1958.

(2) R.V. Pound, Rev. Sci. Instrum., 17, 490, 1946.

(3) H. Misra, Rev. Sci. Instrum., 29, 590 - 4, 1958.

(4) "Admiralty Handbook of Wireless Telegraphy"

(HMSO), Vol. 2, N.16, 1938.

(5) G. Brown, D.R. Mason and J.S. Thorp,

J. Sci. Instrum., 42, 648 - 9, 1965.

(6) "Admiralty Handbook of Wireless Telegraphy"

(HMSO), Vol. 2, N.16, 1938.

(7) D.R. Mason, Ph.D Thesis, University of Durham, 1966.

(8) W.C. Holton and H. Blum, Phys. Rev., 125, 89 - 103, 1962.

(9) P.D. Strum, Proc. I.R.E., 41, 875 - 89, 1953.

(10) G.E. Valley and H. Wallman,

"Vacuum Tube Amplifiers" MIT Rad. Lab. Series, Vol.23,

(McGraw-Hill), 1948, p. 641.

(11) D.J.E. Ingram,

"Spectroscopy at Radio and Microwave Frequencies"

(Butterworth's), 1955, p. 33.

(12) H.A. Buckmaster and J.C. Dering,

   J. Sci. Instrum., 43, 404 - 5, 1966.

(13) H.A. Buckmaster and J.C. Dering,

   Can. J. Phys., 43, 1088 - 98, 1965.

(14) H.A. Buckmaster and J.C. Dering,

   J. Sci. Instrum., 43, 554 - 7, 1966.

(15) A.V. Patankar, J. Sci. Instrum., 44, 354 - 6, 1967.

(16) G. Feher, Bell Syst. Tech. J., 36, 449 - 84, 1957.

(17) G. Brown, D.R. Mason and J.S. Thorp,

   J. Sci. Instrum., 43, 405, 1966.

(18) T.S. England and E.E. Schneider, Nature, 166, 437, 1950.

(19) J.M. Hirschon and G.K. Fraenkel,

   Rev. Sci. Instrum., 26, 34 - 41, 1955.

(20) A.C. Rose-Innes, J. Sci. Instrum., 34, 276 - 8, 1957.

(21) D. Teaney, M.P. Klein and A... Portis,

   Rev. Sci. Instrum., 32, 721 - 9, 1961.

(22) A.F. Mehlkopf and J. Smidt,

   Rev. Sci. Instrum., 32, 1421, 1961.

(23) P.M. Llewellyn, P.R. Whittlestone and J.. Williams,

   J. Sci. Instrum., 39, 586 - 9, 1962.

(24) J.L. Hall and R.T. Schumacher,

   Phys. Rev., 127, 1892 - 1912, 1962.

(25) D.E. Kaplan, J. Phys. Radium, 23, Suppl. 3, 21A - 24A, 1962.

(26) J.L. Laffron, P. Servoz-Gavin and T. Uchida,

J. Phys. Radium, 23, 951 - 3, 1962.

(27) J.G. Theobald, Ann. Phys. (France), 7, 585 - 621, 1962.

(28) W.A. Gambling and T.H. Wilmshurst,

Phys. Lett., 5, 228 - 9, 1963.

(29) J.P. Goldsborough and T.R. Koehler,

Phys. Rev., 133, A135 - 40, 1964.

(30) W. Duncan and E.E. Schneider,

J. Sci. Instrum., 42, 395 - 8, 1965.

(31) H.A. Buckmaster and J.C. Dering,

Can. J. Phys., 45, 107 - 117, 1967.

(32) E.A. Faulkner and P.W. Whippey,

Proc. I.E.E., 113, 1159 - 62, 1966.

(33) G.C. Southworth,

"Principles and Applications of Waveguide Transmission"

(Van Nostrand), 1950, p. 637.

(34) M.R. Millet, I.R.E. Trans., MTT-6, 284 - 90, 1958.

(35) G.C.Southworth,

"Principles and Applications of Waveguide Transmission"

(Van Nostrand), 1950, p. 624.

(36) C.M. Johnson, D.E. Slager and D.D. King,

Rev. Sci. Instrum., 25, 213 - 7, 1954.

(37) D.G. Tucker,

"Modulators and Frequency Changers"

(Macdonald), 1953, p. 33.

(38) R.C. Mackey, I.R.E. Trans., MTT-10, 114 - 7, 1962.

(39) E.V.D. Glazier and H.R.L. Lamont,

"Services' Textbook of Radio"

(HMSO), 1958, Vol. 5, p. 222.

Chapter 5. References

(1) W.I. Dobrov and M.E. Browne,

"Paramagnetic Resonance", (Academic Press), 1963,

Vol 2, pp. 447 - 55.

(2) A.H. Eschenfelder and R.T. Weidner,

Phys. Rev., 92, 869 - 73, 1963.

(3) S. Feng and N. Bloembergen, Phys. Rev., 130, 531 - 5, 1963.

(4) C.F. Davis, M.W.P. Strandberg and R.L. Kyhl,

Phys. Rev., 111, 1268 - 72, 1958.

(5) J.G. Castle, P.F. Chester and P.E. Wagner,

Phys. Rev., 119, 953 - 61, 1960.

(6) J. Herve and J. Pescia, C.R. Acad. Sci. 251, 665 - 7, 1960.

(7) G. Brown, D.R. Mason and J.S. Thorp,

J. Sci. Instrum., 42, 648 - 9, 1965.

(8) A.E. Siegman,

"Microwave Solid-State Masers" (McGraw-Hill), 1963, p. 153.

(9) G. Brown and J.S.Thorp, Brit. J. Appl. Phys., to be published.

(10) W.J.C. Grant, Phys. Rev., 134, A1554 - 64, 1964.

(11) D.R. Mason, Ph.D Thesis, University of Durham, 1966.

(12) C.J. Kirkby, private communication.

(13) E.O. Schultz - du Bois,

Bell Syst. Tech. J., 38, 271 - 90, 1959.

(14) A.B. Cutting, (Elliott Electronic Tubes) private communication.

(15) A.L. Cullen, Electronics Letters, 1, 55 - 6, 1965.

(16) M.R. Millet, I.R.E. Trans., MTT-6, 284 - 90, 1958.

(17) R.C. Mackey, I.R.E. Trans., MTT-10, 114 - 7, 1962.

(18) C.L. Hogan, Bell Syst. Tech. J., 31, 1 - 31, 1952.

(19) J.G. Baker, (University of Manchester), private communication.

Chapter 6.   References

(1) R.S. Ohl, P.P. Budenstein and C.A. Burrus,

Rev. Sci. Instrum., 30, 765 - 74, 1959.

(2) R.M. Hill and S.J. Tetenbaum,

J. Appl. Phys., 30, 1610 - 11, 1959.

(3) N.R. Bierrum, D. Walsh and J.C. Vokes,

Nature, 186, 626, 1960.

(4) N.R. Bierrum and D. Walsh, J. Electr. Contr., 8, 81 - 90, 1960.

(5) K.D. Froome, Nature, 184, 808, 1959.

(6) K.D. Froome, Nature, 186, 959, 1960.

(7) K.D. Froome, Nature, 188, 43 - 4, 1960.

(8) K.D. Froome, Nature, 193, 1169 - 70, 1962.

(9) A.P. Anderson, Ph.D Thesis, University of London, 1959.

(10) C.H. Page, Proc. I.R.E., 46, 1738 - 40, 1958.

(11) H.C. Torrey and C.A. Whitmer,

"Crystal Rectifiers" MIT Rad. Lab. Series, Vol 15,

(McGraw-Hill), 1948, p. 114.

(12) J.L. Hall and R.T. Schumacher,

Phys. Rev., 127, 1892 - 1912, 1962.

(13) R.V. Pound,

"Microwave Mixers" MIT Rad. Lab. Series, Vol. 16,

(McGraw-Hill), 1948, p. 249.

(14) W.P. Ayres, P.H. Vartanian and J.L. Melchor,

   J. Appl. Phys., 27, 188 - 9, 1956.

(15) D.D. Douthett, I. Kaufman and A.S. Risley,

   J. Appl. Phys., 32, 1905 - 12, 1961.

(16) R.L. Jepsen, J. Appl. Phys., 32, 2627 - 30, 1961.

(17) J.L. Melchor, W.P. Ayres and P.H. Vartanian,

   Proc. I.R.E., 45, 643 - 6, 1957.

Chapter 7.   References

(1)   G. Brown and J.S. Thorp, Brit. J. Appl. Phys., to be published

(2)   C.F. Davis, M.W.P. Strandberg and R.L. Kyhl,

      Phys. Rev., 111, 1268 - 72, 1958.

(3)   D.R. Mason, Ph.D Thesis, University of Durham, 1966.

(4)   C.J. Kirkby, private communication.

(5)   E.O. Schultz - du Bois,

      Bell Syst. Tech. J., 38, 271 - 90, 1959.

(6)   J.H. Van Vleck, Phys. Rev., 57, 426 - 47, 1940.

(7)   R. Orbach, Proc. Roy. Soc., A264, 458 - 84, 1961.

(8)   P.L. Donoho, Phys. Rev., 133, A1080 - 4, 1964.

(9)   N. Bloembergen, S. Shapiro, P.S. Pershan and J.O. Artman,

      Phys. Rev., 114, 445 - 9, 1959.

(10) D.A. Davids and P.E. Wagner,

      Phys. Rev. Lett., 12, 141 - 2, 1964.

(11) A.B. Cutting, (Elliott Electronic Tubes), private communication.

(12) C.M. Johnson, D.M. Slager and D.D. King,

      Rev. Sci. Instrum., 25, 213 - 7, 1954.

(13) D.E. Dugdale, private communication.

A single-klystron superheterodyne receiver for use at millimetric wavelengths

G. BROWN, D. R. MASON and J. S. THORP

Department of Applied Physics, University of Durham

MS. received 12th April 1965, in revised form 12th May 1965

Abstract. A superheterodyne receiving system is described using a transmission crystal modulator instead of a separate klystron to generate the local oscillator signal. It has been used in paramagnetic resonance experiments at millimetric wavelengths. Instrumental line broadening is negligible and the signal-to-noise ratio is 30 dB.

1. Experimental

The measurement of relaxation times in paramagnetic materials by the pulse saturation method (Davis *et al.* 1958) involves the use of at least two klystrons. A low-power klystron supplies the continuous monitor power, and a high-power klystron operating at the same frequency provides the saturating pulses. To enable weak transitions to be observed a superheterodyne receiver is usually used to amplify the resonance signal. Superheterodyne detection requires the presence of a local oscillator signal to beat with the incoming resonance signal, producing an intermediate-frequency oscillation in the balanced mixer. In conventional microwave superheterodynes a third klystron is used as the local oscillator; but, above about 35 Gc/s, maintaining a fixed frequency separation between three independent klystrons is an acute problem.

To overcome this difficulty a microwave signal is generated containing both the monitor and local oscillator frequencies. The transmission crystal modulator is driven at 45 Mc/s, amplitude-modulating the power incident from a 35 Gc/s reflex klystron, as shown in the figure. This produces

signal was used by Pound (1946) and others in connection with frequency stabilization circuits.

The signal returning from the microwave cavity consists of a 35 Gc/s carrier amplitude-modulated by both the resonance signal and a 45 Mc/s oscillation. In the balanced mixer this meets the local oscillator signal of 35 Gc/s amplitude-modulated at 45 Mc/s. The local oscillator sidebands beat with the incoming signal to produce, after detection in the balanced mixer, a 45 Mc/s i.f. carrier amplitude-modulated by the resonance signal. This is amplified by a conventional stagger-tuned circuit, and detected for cathode-ray oscilloscope presentation of the resonance.

2. Discussion

The presence in a microwave cavity of two additional frequencies 90 Mc/s apart will have the effect of broadening or splitting an absorption line of comparable frequency width. Examination of the line shape of the $+\frac{1}{2}$ to $-\frac{1}{2}$ transition in ruby with a 160 kc/s phase-sensitive detector system showed no detectable broadening. We therefore conclude from the sensitivity of this system that the power
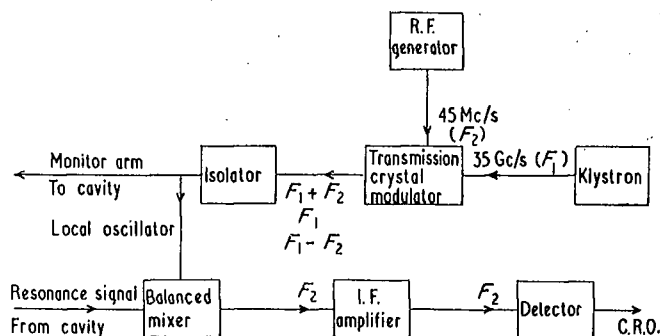
Block diagram of the receiving apparatus.

low-power sidebands at 34955 Mc/s and 35045 Mc/s. The signal is then split, half going to the local oscillator input of the balanced mixer, the other half constituting the monitor signal. The transmission crystal modulator consists of a germanium point-contact diode (GEC type VX3136) mounted in the waveguide and fed from an external signal source. The intermediate frequency of 45 Mc/s is chosen to give minimum overall noise (Strum 1953). A similar method of generating sidebands in a microwave

level of the sidebands is at least 30 dB below carrier level. Placing the transmission crystal modulator in the local oscillator arm immediately before the balanced mixer removes the possibility of instrumental broadening due to the presence of sidebands in the cavity. However, it appears from present work that the efficiency of sideband generation is proportional to the incident 35 Gc/s power level over the range 5 to 20 mw. For this reason the transmission crystal modulator is placed as near the klystron as possible. The

power in the sidebands is dependent upon the level of 45 Mc/s drive to the modulator diode. At present the maximum available drive is 1 v r.m.s., the limit of the r.f. generator in use. Experiment suggests that this drive could be usefully increased.

The insertion loss of 3 dB for the transmission crystal modulator was found to be independent of the r.f. generator output, and was almost entirely due to the modulator diode alone. Ideally it would be preferable to have a single frequency in the local oscillator arm. However, because the sideband power level is so low, the presence of F_1 serves to bias the balanced mixer crystals to the minimum noise condition.

3. Conclusion

The elimination of the local oscillator klystron simplifies the use of the microwave spectrometer for all forms of resonance experiments. The frequency separation of carrier and sidebands is constant, ensuring optimum performance of the superheterodyne at all times. The only bandwidth limitation of the present receiver is set by the highest frequency component of the resonance signal. This contrasts with the conventional superheterodyne in which the i.f. bandwidth is determined by the relative frequency instability of the monitor and local oscillator klystrons. The overall signal-to-noise ratio of the spectrometer and superheterodyne is 30 dB, which compares favourably with conventional systems.

The modification described appears to be directly applicable to spectrometers operating at higher frequencies, where frequency instability is an even greater problem.

References

DAVIS, C. F., STRANDBERG, M. W. P., and KYHL, R. L., 1958, *Phys. Rev.*, **111**, 1268–72.
POUND, R. V., 1946, *Rev. Sci. Instrum.*, **17**, 490–505.
STRUM, P. D., 1953, *Proc. Inst. Radio Engrs, N.Y.*, **41**, 875–89.

LETTERS TO THE EDITOR

A single-klystron superheterodyne receiver for use at millimetric wavelengths

Abstract. Comments are given on the design of single-klystron superheterodyne electron paramagnetic resonance spectrometers.

Recently, Brown, Mason and Thorp (1965) have described a 35 Gc/s superheterodyne spectrometer designed primarily to be used for the measurement of electron paramagnetic resonance relaxation times by the pulse saturation method but described as useful for all forms of resonance experiments. This spectrometer used a single microwave source of power for both the signal F_1 and the local oscillator $F_1 \pm F_2$ channels ensuring that the intermediate frequency F_2 is as stable as that of the modulator, eliminating the necessity for maintaining two separate frequency sources with a constant difference frequency. This was accomplished by modulating the entire output power from the klystron at 45 Mc/s before it was divided into the two channels. No attempt was made to remove the modulation sidebands from the signal power, nor to remove the carrier and one sideband from the local oscillator power. It was claimed that the presence of these unrequired sidebands did not degrade the sensitivity of the detection system although a "signal-to-noise ratio of 30 dB" was reported. It is assumed that this was intended to mean the noise figure of the system since, otherwise, it is a meaningless statement in the absence of details of the sample. The analysis of the sensitivity of this system reported in this letter corroborates this assumption.

This letter draws attention to the fact that the presence of these unrequired carriers degrades the sensitivity of the spectrometer described by Brown *et al.* by about 13–16 dB. It is well known that 35 Gc/s superheterodyne receivers can be built which have a noise figure of about 13 dB if point-contact mixer diodes of contemporary design are employed, and if the intermediate frequency is between 1 and 60 Mc/s (Blore *et al.* 1964). When the spectrometer described by Brown *et al.* (1965) is used to study relaxation times, the factor measured is the microwave bridge balance as the paramagnetic sample in the resonant cavity returns to thermal equilibrium after being saturated by a high power pulse of energy. This pulse is at the resonant frequency of the cavity and the sample is in a magnetic field which satisfies the condition for magnetic resonance. Brown *et al.* (1965) correctly conclude that the modulation sideband power does not enter the cavity to any significant extent provided that the Q of the resonant cavity exceeds about one thousand. It should be noted that when a reflection cavity is part of a microwave bridge the bridge can be balanced only at one frequency which, of necessity, must be the cavity resonant frequency. Consequently, one quarter of the sideband power incident on the bridge is reflected from the bridge and is incident on the microwave mixer where it plays a significant role in degrading the noise figure of the system as described below. Synchronous demodulation at the microwave frequency produces a d.c. output power. This is a very insensitive method of detection since the effective noise figure is very large because flicker noise in point-contact diodes is excessive at near zero sideband frequencies. Superheterodyne demodulation will minimize the noise figure of the detection

system provided that the intermediate frequency is suitably chosen. It can be shown by detailed analysis of the power spectrum incident on the microwave mixer that microwave bridge balance information at zero intermediate frequency exceeds that at F_2 by a factor of about twenty (13 dB). This is the factor by which the noise figure of this system has been degraded by the presence of the extraneous signals and is independent of whether a transmission or reflection sample cavity is employed. Effectively, the result of the extraneous sidebands is to convert a large fraction of the information power to a sideband frequency where amplification and display does not occur, leaving a small fraction of the information power at the sideband frequency where amplification and display does occur. This is due to the fact that the balanced mixer is biased for minimum noise figure with power at frequency F_1, rather than with power at either $F_1 + F_2$ or $F_1 - F_2$, and the result is equivalent to a degradation of the noise figure of the system.

If the superheterodyne configuration of Brown *et al.* (1965) is employed as a conventional electron paramagnetic resonance spectrometer with magnetic field modulation at frequency f, then the output power spectrum of the microwave mixer has components at f, $F_2 \pm f$ and F_2, as well as the various higher harmonics of these frequencies. The previous analysis is valid in this case and shows that the resonance information at f exceeds that at $F_2 \pm f$ by a factor of about twenty. It can be concluded that the noise figure of the spectrometer would be improved by about 13 dB if synchronous demodulation at the microwave frequency were followed by amplification and further synchronous demodulation at f. The improvement depends on the condition that the noise figure of the microwave mixer is the same at f as at F_2. Buckmaster and Dering (1965) have shown that 9 Gc/s point-contact mixer diodes of contemporary design have optimum noise figure when incorporated into detection systems in which the sideband frequency is as low as about 10^5–10^6 c/s. The minimum of a plot of noise figure against frequency is very broad and does not increase significantly until frequencies in excess of 60 Mc/s are reached. Similar unpublished noise figure measurements at 35 Gc/s indicate that flicker noise in point-contact diodes becomes negligible at about 1 Mc/s. It can be concluded that the simplest and most sensitive method of detecting electron paramagnetic resonance is to use a synchrodyne (homodyne) spectrometer in which the magnetic field is modulated at frequencies in the range 10^5–10^6 c/s provided that the resonance line width is such that modulation broadening does not occur. When broadening occurs, then the point-contact diodes may be replaced by backward diodes, since flicker noise in this type of diode becomes negligible at sideband frequencies above about 1 kc/s (Eng 1961).

It should also be noted that the single-klystron electron paramagnetic resonance spectrometer described by Brown *et al.* (1965) is inherently unstable because a large fraction of the

power spectrum at the intermediate frequency F_2 does not carry electron paramagnetic resonance information. The local oscillator power at $F_1 \pm F_2$ mixes with local oscillator power at F_1 producing an output signal at F_2 which is dependent on the bridge balance of the balanced mixer but, typically, would exceed any information signal power by 80 dB. The situation further degrades if a reflection cavity is employed since power at $F_1 \pm F_2$ is also present as a component of the power in the signal channel and is not attenuated by the balance of the mixer. This useless power limits the maximum gain that can be usefully employed without saturating the intermediate frequency amplifier. It will also produce a large d.c. signal at the output of the synchronous demodulator following the intermediate frequency amplifier. This quasi-signal can be removed only by deliberately unbalancing the synchronous demodulator, which will degrade the stability of the zero signal baseline. The effect is equivalent to that of detecting a small signal in the presence of a large noisy signal.

Although it has been demonstrated in this letter that a single klystron superheterodyne spectrometer of the type described by Brown *et al.* (1965) has inferior sensitivity and stability, it should not be concluded that this inferiority is an inherent feature of all single-klystron superheterodyne spectrometers. Several alternative methods of generating the local oscillator power from a fraction of the signal power

source have been described in the literature. These have been reviewed by Buckmaster and Dering (1966 to be published) who also studied the sensitivity of this type of system at 9 Gc/s, using point-contact diodes in the microwave mixer and intermediate frequencies in the range 1–100 kc/s. The additional complexity of this type of electron paramagnetic resonance spectrometer is justified whenever modulation broadening of resonance lines must be avoided, or when high sensitivity is required when studying very broad resonance lines necessitating large field modulation amplitudes which are difficult to obtain at frequencies above about 500 c/s.

Department of Physics,   H. A. Buckmaster
University of Calgary,   J. C. Dering
Calgary, Alberta,   *9th March* 1966, *in revised*
Canada   *form* 28*th March* 1966

Blore, W. E., Robillard, P. E., and Primich, R. I., 1964, *Microwave J.*, 7, 61–5.
Brown, G., Mason, D. R., and Thorp, J. S., 1965, *J. Sci. Instrum.*, 42, 648–9.
Buckmaster, H. A., and Dering, J. C., 1965, *Can. J. Phys.*, 43, 1088–98.
Eng, S. T., 1961, *I.R.E. Trans. Microw. Theory Tech.*, MTT-9, 419–25.

Abstract. Further information is given on the operation of the single-klystron superheterodyne receiver described by the authors in this journal in 1965.

A short time ago we outlined a single-klystron superheterodyne receiver for use at millimetric wavelengths (Brown *et al.* 1965). Buckmaster and Dering have shown that, in some circumstances, the use of such a system may lead to a lower sensitivity than can be obtained with other forms of electron spin resonance spectrometer. In order to avoid confusion between the two approaches we wish to emphasize the following points. When using the single-klystron superheterodyne receiver our detection system comprises a microwave bridge, balanced mixer, 45 Mc/s i.f. amplifier and cathode-ray oscilloscope. The signal reflected from the cavity and crystal assembly passes to the microwave bridge where the standing reflection is balanced out in the usual way, giving an output voltage across the detector crystals proportional to the imaginary part of the susceptibility. This system is used for two purposes: (i) for rapid identification of transitions and (ii) for the measurement of spin-lattice relaxation time. In the first case we superimpose a 50 c/s modulation on the magnetic field, the display then being the profile of the absorption line; in the second case the signal developed at the output of the second detector (usually 1–2 v in magnitude) is applied directly to the Y-amplifier input of the oscilloscope, enabling the exponential recovery from saturation to be observed. For the measurement of linewidth we use a completely separate 160 kc/s synchrodyne detection system; this does not utilize the single-klystron superheterodyne receiver.

We agree with Buckmaster and Dering that the use of a single-klystron superheterodyne receiver of the type we have

described followed by synchronous detection at 160 kc/s would result in impaired sensitivity. We do not use this method; neither do we claim that the presence of the unrequired sidebands does not degrade the sensitivity of the system. With reference to saturating the i.f. amplifier with "useless power" we would point out that if the power to the local oscillator input of the balanced mixer is of the same order as the power in the information-carrying sidebands, then the 45 Mc/s signal in the i.f. amplifier is almost 100% modulated. Any saturation produced in this amplifier is due to the magnitude of the information present, rather than to a large unmodulated carrier. The 30 dB signal-to-noise ratio which we quote refers to observations at 300°K on the $+\frac{1}{2}$ to $-\frac{1}{2}$ transition in a 0·052% chromium ruby specimen of volume 0·2 cm^3, taken at a polar angle of 90°.

If the aim is to seek the maximum spectrometer sensitivity, the single-klystron superheterodyne receiver is not as good as the synchrodyne spectrometer, but the authors of this letter are confident that experimental workers will find this particular single-klystron superheterodyne receiver preferable to the conventional two-klystron type.

Department of Applied Physics,   G. Brown
University of Durham   D. R. Mason
                                             J. S. Thorp
                                            5th April 1966

Brown, G., Mason, D. R., and Thorp, J. S., 1965, *J. Sci. Instrum.*, 42, 648–9.

The measurement of spin-lattice relaxation times at very low power levels

G. BROWN and J. S. THORP

Department of Applied Physics, University of Durham

MS. received 1st May 1967, in revised form 8th June 1967

Abstract. Spin–lattice relaxation times in ruby and sapphire have been measured at 35 and 70 Gc/s by a pulse-response technique using a grid-modulated reflex klystron, the peak pulse power at the specimen being about 10 μw. Relaxation times at $4 \cdot 2°$K covering the range from 2 msec to 24 msec have been measured at 35 Gc/s, the results in each case agreeing with those obtained from pulse-saturation measurements on the same specimens. Preliminary data are given of the relaxation in ruby at 70 Gc/s, the microwave power being obtained by harmonic generation from 35 Gc/s. The range of applicability of the method is discussed.

1. Introduction

All the resonant methods of measuring spin–lattice relaxation time (Eschenfelder and Weidner 1953, Davis *et al.* 1958, Castle *et al.* 1960, Herve and Pescia 1960, Feng and Bloembergen 1963) require a high-power source of microwave radiation to saturate, or partially saturate, the spin system. Such sources are not readily available at the shorter millimetric wavelengths and a pulse-response method has been developed to enable the spin-lattice relaxation time T_1 to be measured without the use of a high-power source. This technique uses a pulsed reflex klystron operating with a duty cycle of less than 10% delivering a peak pulse power at the paramagnetic specimen of about 10 μw. From the response of the spin system to each individual pulse the value of T_1 can be derived. The method was developed and tested at 35 Gc/s before being extended for studies at 70 Gc/s, a region in which very few relaxation measurements have been reported.

2. Theory

The effect of relaxation on the population difference in a two-level spin system has been described previously (Slichter 1963, p. 7, Siegman 1964, p. 153). It is assumed that the spin–spin relaxation time T_2 is much smaller than the spin–lattice relaxation time T_1. Then the rate equation governing the population difference on application of the microwave field is, using Siegman's notation,

$$\frac{d}{dt}(\Delta n) = -\frac{\Delta n - \Delta N}{T_1} - 2W_{12}\,\Delta n \tag{1}$$

where Δn is the instantaneous population difference, ΔN is the thermal-equilibrium population difference and W_{12} is the stimulated-transition probability. Equation (1) can be written as

$$\frac{d}{dt}(\Delta n) = -\frac{\Delta n - \Delta N(1 + 2W_{12}T_1)^{-1}}{(1/T_1 + 2W_{12})^{-1}}$$

the solution of which has a time constant τ given by

$$\tau = \frac{1}{1/T_1 + 2W_{12}}. \tag{2}$$

The magnitude of W_{12} at resonance is determined by the incident microwave power level and so τ becomes power dependent when W_{12} is comparable with $1/T_1$. In practice the

microwave power can be made sufficiently small for W_{12} to have a negligible effect on τ
but still be large enough to produce an accurately measurable power absorption. Under
these conditions, equation (2) becomes

$$\tau = T_1.$$ (3)

An exact determination of T_1 is possible by measuring τ as a function of the incident micro-
wave power and extrapolating to give the value of τ at zero power. However, in the
materials examined here this was not found to be necessary, as §3 shows. The simple
two-level system has been considered for theoretical clarity; any detailed analysis of the
pulse-response method must take into account the particular multi-level system under
investigation (Grant 1964).

3. Experimental method

At 35 Gc/s a conventional bridge spectrometer with crystal–video detection was used.
The specimen was mounted on the short-circuit termination of the waveguide, positioned at
the centre of a superconducting solenoid. The use of the short-circuit termination (which
is not an essential feature of the method) placed less stringent requirements on the frequency
stability of the klystron. Figure 1 shows the component layout. The reflex klystron
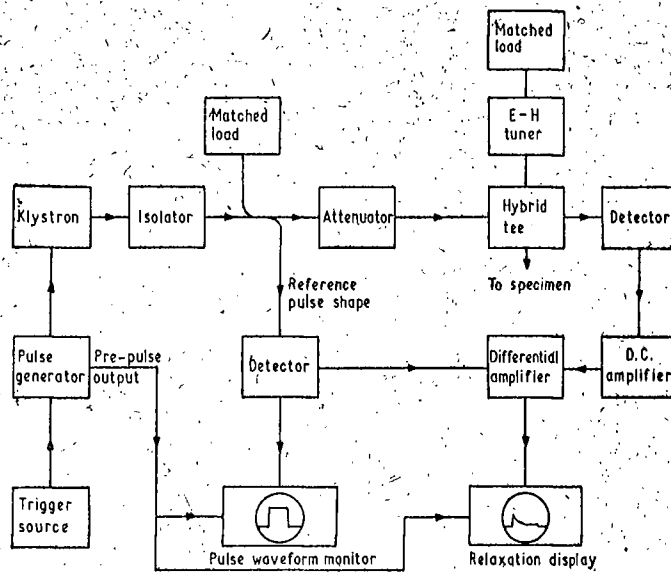

Figure 1.   Block diagram of the spectrometer.

(Elliott type 8RK19) is grid modulated to produce r.f. pulses with a mark–space ratio of
about 1 : 9 and a peak pulse power of about 3 mw. Frequency deviation during the
pulse does not exceed 5 Mc/s and an amplitude sag of less than 10% could be achieved at
pulse lengths below 80 msec. A calibrated attenuator reduces the power at the specimen
to about 10 μw.

Figure 2 shows the waveforms obtained from the crystal–video receiver after the bridge
was balanced to select the absorption signal. The upper trace is the pulse waveform off
resonance. The lower trace, obtained with the magnetic field on resonance, shows the
power absorption decreasing with time. All the present measurements have been made on
ruby and sapphire specimens. The power dependence of τ has been observed but it was
found unnecessary to plot τ against power and extrapolate to zero power because there was
an appreciable range (up to about 300 μw) over which τ was independent of power and the
size of the response signal was large. The pulse length must be much greater than the time
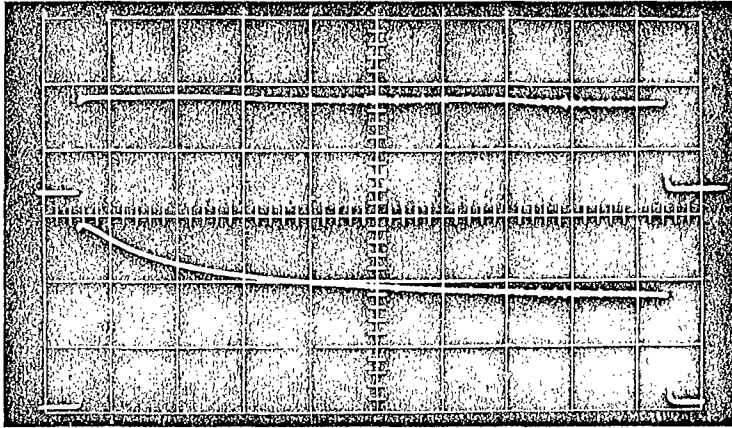
Figure 2. Receiver output display: upper trace, off magnetic resonance; lower trace, on magnetic resonance. 0·2 at. % Cr ruby at 4·2°K. Horizontal scale 2 msec per division.

constant under investigation to ensure maximum signal amplitude and to display the base-line, an important feature in the interpretation of the curve.· The interval between pulses is made sufficiently large to enable the spin system to come to thermal equilibrium before the arrival of a pulse. Graphs of the natural logarithm of the absorption against time, derived from the photographs of oscilloscope traces, yielded the values of T_1.

4. Results at 35·5 Gc/s

Measurements have been made on different transitions in a selection of ruby and sapphire specimens, the relaxation behaviour of which had previously been examined by pulse-saturation techniques (Mason 1966, C. J. Kirkby 1967, private communication). Figure 3
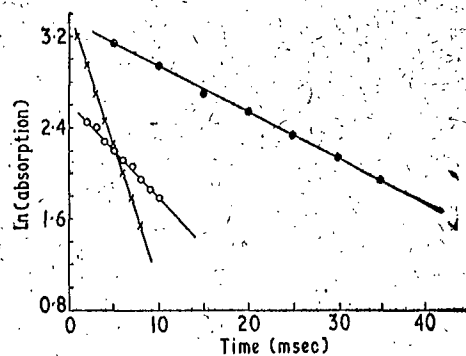

Figure 3. Relaxation data derived from pulse-response traces: open circles,· $-\frac{3}{2}$ to $-\frac{1}{2}$ transition, 0·2 at. % Cr ruby, $T_1 = 12·0$ msec; full circles, $-\frac{1}{2}$ to $+\frac{1}{2}$ transition, 0·052 at. % Cr ruby $T_1 = 24·5$ msec; crosses, $-\frac{1}{2}$ to $+\frac{1}{2}$ transition, 0·2 at. % Cr ruby, $T_1 = 3·5$ msec. All measurements taken at 35·5 Gc/s, 4·2°K, $\theta = 90°$.

shows some of the semilogarithmic graphs obtained by the pulse-response method and their linearity suggests that a single exponential decay was being observed. A comparison of the pulse-response and pulse-saturation data is made in the table. Over a range of relaxation times from 2 to 24 msec the agreement between the two methods is within the experimental error of about 15%. The energy-level nomenclature follows the notation of Schultz-du Bois (1959).

Comparative relaxation data obtained by pulse-response and
pulse saturation methods

Paramagnetic ion concentration (Al_2O_3 host)	Transition	T_1 by pulse response (msec)	T_1 by pulse saturation (msec)
0·052 at.% Cr	Cr^{3+}: $-\frac{1}{2} \to +\frac{1}{2}$	24·5	24·0
	Cr^{3+}: $-\frac{3}{2} \to -\frac{1}{2}$	12·0	15·0
0·20 at.% Cr	Cr^{3+}: $-\frac{1}{2} \to +\frac{1}{2}$	3·5	4·0
	Cr^{3+}: $+\frac{1}{2} \to +\frac{3}{2}$	7·8	6·8
0·037 at.% Cr 0·02 at.% Fe	Cr^{3+}: $-\frac{1}{2} \to +\frac{1}{2}$	5·9	5·0
0·001 at.% Fe	Fe^{3+}: $-\frac{3}{2} \to -\frac{1}{2}$	3·7	2·0
	Fe^{3+}: $-\frac{1}{2} \to +\frac{1}{2}$	2·2	1·9

All measurements taken at 35·5 Gc/s, 4·2°K, $\theta = 90°$.

5. Specific operational requirements

In order to make effective pulse-response measurements several experimental parameters require close control. The most important of these are frequency deviation and amplitude sag during the r.f. pulse, bridge balancing and the choice of receiver. These are considered below.

5.1. The pulsed klystron

During the r.f. pulse the frequency must remain constant to within a fraction of the line-width of the transition under investigation. Grid modulation generally produces some frequency deviation and the characteristics of two klystrons were investigated to find the magnitude of any frequency deviation. The first was a 35 Gc/s reflex klystron type R5146 (E.M.I.) used in conjunction with a power supply type WE 80 (Microwave Instruments). The strongest continuous-wave operating mode was selected and, with the reflector voltage constant, the r.f. power output and frequency were measured as functions of the grid-to-cathode voltage, the results being shown in figure 4. The power rises gradually from
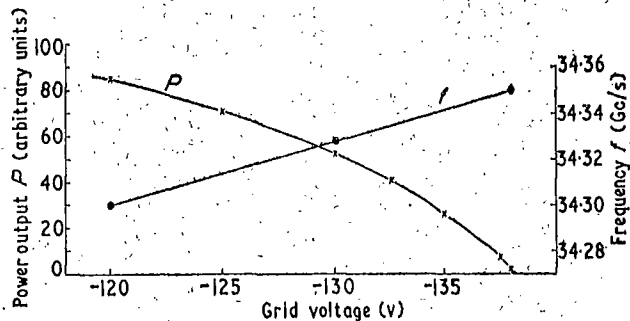

Figure 4. Grid characteristics of the klystron type R5146 taken at constant reflector voltage.

zero and its variation becomes linear as the continuous-wave operating point at −120 v is reached; the frequency falls linearly by some 50 Mc/s. This procedure was repeated with a second type of klystron, an 8RK19 (Elliott), again used with the WE 80 power supply. These characteristics are shown in figure 5. Oscillation begins suddenly at a grid voltage of −40 v. The power then rises linearly to the operating point at −30 v, the frequency remaining constant. The threshold value of power output, measured on a thermistor bridge, was 3 mw. For a closer examination of the threshold the power output was displayed on an oscilloscope while the time-base saw-tooth voltage was applied to the klystron grid. This gave a characteristic identical with figure 5 and showed that the
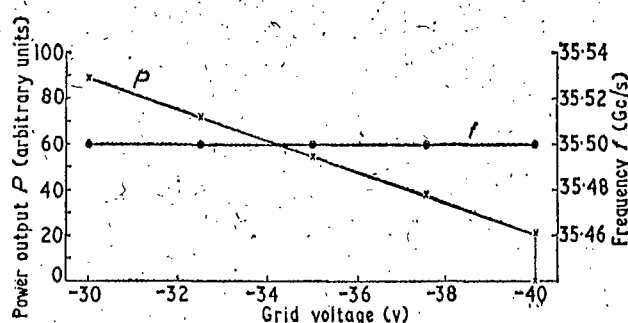
Figure 5. Grid characteristics of the klystron type 8RK19 taken at constant reflector voltage.

switching time of the 8RK19, at −40 v, was 0·3 μsec, independent of the slope of the input saw-tooth. Voltage pulses with a rise time of 10 nsec were then applied to the grid. The r.f. pulse rise time remained at 0·3 μsec, showing that the switching was initiated only by the level of the input signal. Under pulse conditions no frequency deviation was detectable and the characteristics of the wavemeter used suggested that any deviation present was less than 5 Mc/s.

The marked variation in the performance of the two klystrons appears to arise from differences in their construction and electron-optical properties. With the 8RK19 the grid pulse necessary to produce 3 mw of r.f. pulse power was about 8 v. Larger voltage pulses produced more powerful r.f. pulses, but with fractionally greater frequency deviation. The input pulses were obtained from a pulse generator (Solartron type GO 1101) and, in order to maintain a 10% duty cycle when using pulse lengths of 80 msec, a separate transistor multivibrator was used to trigger the pulse generator. The triggering period was fixed at 720 msec. With r.f. pulse lengths in excess of 80 msec amplitude, sag during the pulse became very large; this arises from the resistance–capacitance coupling between the modulation input socket on the power supply and the klystron grid. However, the 80 msec upper limit of pulse length was quite adequate for the present measurements in which relaxation times up to 24 msec have been observed. For materials with longer relaxation times a greater r.f. pulse length would be necessary.

5.2. *Bridge balancing*

In both the conventional pulse-saturation and the pulse-response techniques the accuracy of the relaxation-time measurement depends upon the accuracy to which the microwave bridge can be balanced. This is usually carried out by means of a slide-screw tuner, a phase-shifter–attenuator combination or, as in the present work, an E–H tuner. The experimental procedure for balancing in the pulse-response technique is identical with that used in other methods. An important feature, however, is that any unbalance is immediately visible. The klystron operates in its pulsed mode and the pulses reflected from the specimen assembly are displayed on the oscilloscope. The bridge is balanced by adjusting the E and H pistons using the method suggested by Cullen (1965). At the balance point the pulses disappear completely from the display. A small amplitude unbalance is then introduced to select the absorption component on resonance. As this unbalance is introduced the pulse reappears on the display, but it always has a curved top. This indicates that phase unbalance has also been introduced. The E–H tuner is designed to reduce to a minimum the interaction between phase and amplitude adjustments; this interaction becomes noticeable in the pulse-response method. The pulse curvature can be removed by a very small adjustment of the phase piston of the E–H tuner. Thus the pulse-response method allows very accurate bridge balancing and equally accurate compensation for the interaction between the phase and amplitude adjustments.

5.3. *Radio-frequency sag compensation*

Since the pulse-response measurement is of the change of absorption with time it is important that the r.f. amplitude should be constant throughout the pulse. With the circuitry used here, a little pulse sag arose because of the resistance–capacitance coupling to the klystron grid. This was compensated in the display by using a differential amplifier, shown in figure 1. The r.f. pulse, which is displayed on the pulse waveform monitor, is fed to one input of the differential amplifier and the crystal–video receiver output to the other. Off resonance the amplifier accepts pulses of the same shape at both inputs and, if the reference pulse is adjusted to be the same amplitude as the receiver output pulse, the two pulses cancel exactly and the display is a straight line. The start and finish of the pulse are indicated by switching transients which are usually quite small. Although any magnitude of sag can be compensated in this way, the differential-amplifier technique is not recommended for sags exceeding about 5% because the r.f. amplitude variation affects the relaxation processes, the results of which cannot be removed by simple algebraic subtraction.

5.4. *The crystal–video receiver*

For relaxation studies on ruby at liquid-helium temperatures a crystal–video receiver is well suited for the pulse-response technique; high sensitivity is not of prime importance and the signals are at least 10 db above noise with specimen volumes of about $0 \cdot 1$ cm^3. The technique does not require a receiver with a large dynamic range so that relatively large gain can be combined with good pulse-handling capability. The receiver is always working well within its specification and tests made on its pulse performance showed no detectable traces of overshoot, ringing or sag. If greater sensitivity should be required, a super-heterodyne receiver could be used.

5.5. *Alternative pulsing systems*

Grid modulation of the klystron is only suitable as a method for obtaining r.f. pulses if the linewidth of the transition under observation is several times the magnitude of the frequency deviation during the pulse. In the present experiments the linewidths are about 90 Mc/s overall and the frequency deviation is less than 5 Mc/s; grid modulation, therefore, is quite satisfactory. For materials having small linewidths it is preferable to operate the klystron in the continuous-wave mode and use an alternative method of producing r.f. pulses. The switching properties of microwave diodes are well known (Millet 1958, Mackey 1962); the on/off ratio is large only for incident r.f. power levels of about 1 mw and falls sharply if the incident power is increased. However, such a diode placed in the wave-guide between the attenuator and the hybrid tee would probably be successful as a r.f. pulse modulator. Microwave modulator diodes are not readily available at frequencies above 35 Gc/s. A solenoid-operated ferrite switch could be used but would require a large switching current and, because of its self-inductance, would have a much slower switching time than both the klystron and the modulator diode.

An alternative approach to the problem is to run the klystron in the continuous-wave mode and to pulse the magnetic field from well below resonance to exactly on resonance using a small, low-inductance, auxiliary coil. Switching-time limitations and current ringing are possible disadvantages of this method, but for studying narrow resonances the coil inductance and the driving current could probably be made sufficiently small for magnetic field pulsing to be preferable to klystron pulsing. Magnetic field pulsing has been attempted on the present spectrometer, but the coupling between the auxiliary coil and the superconducting solenoid was sufficiently tight for the switching currents in the auxiliary coil to induce current surges in the solenoid large enough to drive it normal. However, the method should be feasible with conventional electromagnets where the coupling between the auxiliary coil and the field windings can be very loose and where there is no problem of superconductivity quenching.

6. Results at 70 Gc/s

Some preliminary relaxation-time measurements have been made at 70 Gc/s by extending the pulse-response technique to this frequency using harmonic generation with a 35 Gc/s mixer crystal (type GEM 9) as the non-linear element. The harmonic generator was placed after the isolator in the main waveguide system and followed by a WG 22 to WG 26 taper acting as a high-pass filter. The remainder of the spectrometer used standard 70 Gc/s components and, with one exception, was similar to the 35 Gc/s spectrometer shown in figure 1. The difference was that, although the 35 Gc/s stainless-steel waveguide leading to the specimen was retained, 70 Gc/s power was fed into it from the hybrid tee via another taper. As before, crystal–video detection was used. The estimated conversion loss of 27 dв to the second harmonic indicated that the maximum pulse power available at 70 Gc/s was 6 μw; this was reduced to about 2 μw at the specimen by waveguide and component losses. Using the experimental techniques described in §§3 and 5 pulse-response traces have been obtained at 4·2°к from several specimens. One such trace is shown in figure 6; it

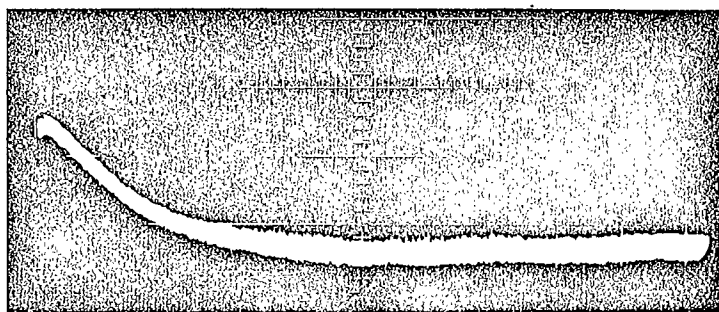Figure 6. A typical pulse-response trace taken at 71 Gc/s. 0·052 at.% Cr ruby, 4·2°к, $\theta = 90°$.

shows the response of the $-\frac{1}{2}$ to $+\frac{1}{2}$ transition in a 0·052 at.% Cr ruby specimen and gives a relaxation time of 3·2 msec at 71 Gc/s. Since the relaxation time of the same transition in the same specimen at 35·5 Gc/s was 24·5 msec (table), this preliminary result suggests that in this region the frequency dependence of the relaxation time follows an inverse cube law.

To obtain greater sensitivity and an improved signal-to-noise ratio, a single klystron superheterodyne receiver for 70 Gc/s is being tested. The design of a 35 Gc/s version of the receiver has already been described (Brown *et al.* 1965, 1966). For 70 Gc/s operation the harmonic generation and the 45 Mc/s amplitude modulation are carried out simultaneously by the one mixer crystal. The spectrometer design is changed only by the provision of a balanced mixer and its associated intermediate-frequency amplifier. The complete 70 Gc/s superheterodyne spectrometer operates from a single 35 Gc/s reflex klystron.

7. Discussion

The results given above show that when the pulse-response method can be used as an alternative to the more conventional pulse-saturation technique comparable accuracies (of about 10%) can be obtained. There are three salient features of the new method which influence its range of applicability: microwave powers in the microwatt region are adequate because the response of a spin system to a small disturbance is being observed; resulting from this there is no need for receiver suppression during the pulse; the nature of the optimum r.f. pulse required is determined by the linewidth and relaxation time of the transition being studied.

In the centimetric-wavelength region the pulse-saturation method is well established and a number of valves giving sufficient power for saturation are readily available. The pulse-response method offers a simpler alternative, its advantage lying in its potential for short-time resolution. In the pulse-saturation method the receiver is normally suppressed during the pulse and this leads to a dead time (often of about 10 μsec) at the beginning of the

exponential recovery to equilibrium; large inaccuracies can thus arise in the measurement of relaxation times of the same order as the dead time. In the centimetric region, however, a number of r.f. switching diodes are available and can be used with the pulse-response technique. Several of these have nanosecond rise times and, if used in conjunction with a continuous-wave frequency-stabilized klystron, should enable very short r.f. pulses of constant amplitude and frequency to be obtained. This should facilitate studies of short relaxation times, for example in the resolution of fast exponentials in cross-relaxation and in direct measurements of fast-relaxing centres. The power level required in the pulse-response method is well below the dissipation limit of the switching diodes and the control of r.f. pulse shape available should also enable measurements to be made on materials having a very narrow linewidth.

At millimetric wavelengths the situation is rather different in that diode switches are not readily available at or above 35 Gc/s. Voltage modulation (either of a klystron or backward wave oscillator) appears to be the only method for producing r.f. pulses and this limits the range of materials which can be examined to those having linewidths of several oersteds and relaxation times greater than 1 msec at 4·2°K. As shown in §6 the low-power requirement of the pulse-response method enables harmonic generation to be used to extend the range over which measurements can be made to the shorter millimetric wavelengths, a region where the few valves giving sufficient power for pulse saturation are extremely costly. This technique should enable studies on the frequency dependence of relaxation time in several paramagnetic materials to be made over a large frequency range. The use of superconducting magnets, however, creates some cryostat design problems if measurements are required at temperatures above 4·2°K.

Acknowledgments

References

BROWN, G., MASON, D. R., and THORP. J. S., 1965, *J. Sci. Instrum.*, **42**, 648–9.
—— 1966, *J. Sci. Instrum.*, **43**, 405.
CASTLE, J. G., CHESTER, P. F., and WAGNER, P. E., 1960, *Phys. Rev.*, **119**, 953–61.
CULLEN, A. L., 1965, *Electron. Letters*, **1**, 55–6.
DAVIS, C. F., STRANDBERG, M. W. P., and KYHL, R. L., 1958, *Phys. Rev.*, **111**, 1268–72.
ESCHENFELDER, A. H., and WEIDNER, R. T., 1953, *Phys. Rev.*, **92**, 869–73.
FENG, S., and BLOEMBERGEN, N., 1963, *Phys. Rev.*, **130**, 531–5.
GRANT, W. J. C., 1964, *Phys. Rev.*, **134**, A1554–64.
HERVÉ, J., and PESCIA, J., 1960, *C.R. Acad. Sci., Paris*, **251**, 665–7.
MACKEY, R. C., 1962, *I.R.E. Trans. Microw. Theory Tech.*, **MTT-10**, 114–7.
MASON, D. R., 1966, *Ph.D. Thesis*, University of Durham.
MILLET, M. R., 1958, *I.R.E. Trans. Microw. Theory Tech.*, **MTT-6**, 284–90.
SCHULTZ-DU BOIS, E. O., 1959, *Bell Syst. Tech. J.*, **38**, 271–90.
SIEGMAN, A. E., 1964, *Microwave Solid-State Masers* (New York: McGraw-Hill).
SLICHTER, C. P., 1963, *Principles of Magnetic Resonance* (New York: Harper and Row).